In presenting the dissertation as a partial fulfillment of the requirements for an advanced degree from the Georgia Institute of Technology, I agree that the Library of the Institute shall make it available for inspection and circulation in accordance with its regulations governing materials of this type. I agree that permission to copy from, or to publish from, this dissertation may be granted by the professor under whose direction it was written, or, in his absence, by the Dean of the Graduate Division when such copying or publication is solely for scholarly purposes and does not involve potential financial gain. It is understood that any copying from, or publication of, this dissertation which involves potential financial gain will not be allowed without written permission.

3/17/65
b

A STUDY OF THE STATIC STRESS-DEFORMATION CHARACTERISTICS OF A SAND

A THESIS

Presented to

The Faculty of the Graduate Division

by

Leonard Domaschuk

In Partial Fulfillment

of the Requirements for the Degree

Doctor of Philosophy

in the School of Civil Engineering

Georgia Institute of Technology

December, 1965

A STUDY OF THE STATIC STRESS-DEFORMATION

CHARACTERISTICS OF A SAND

Approved:

Chairman

Date approved by Chairman: Nov. 19, 1965

ACKNOWLEDGMENTS

The writer wishes to thank all those who assisted in the study and in the preparation of the thesis. Dr. N. H. Wade, the thesis advisor, deserves special thanks for his guidance and encouragement. Regents Professor G. F. Sowers and Dr. J. T. Wang served as members of the reading committee and provided invaluable assistance in the preparation of the thesis. Mr. C. Pavey, laboratory technician, aided in the construction of the experimental apparatus.

The writer wishes to acknowledge the financial assistance provided by the Ford Foundation Fellowship in Aid of Engineering Teaching.

TABLE OF CONTENTS

LIST OF TABLES

LIST OF ILLUSTRATIONS

Figure Page

Figure Page

Figure Page

GLOSSARY OF SYMBOLS

Symbol	Definition
$\sigma_1\ \sigma_2\ \sigma_3$	Principal stresses
$\sigma_z\ \sigma_\theta\ \sigma_r$	Normal stresses in cylindrical coordinates
τ	Shearing stress
σ_o	Octahedral normal stress $(\frac{1}{3}\ (\sigma_1 + \sigma_2 + \sigma_3))$
τ_o	Octahedral shear stress $(\frac{1}{3}\sqrt{(\sigma_1 - \sigma_2)^2 + (\sigma_1 - \sigma_3)^2 + (\sigma_2 - \sigma_3)^2}\ )$
$\varepsilon_1\ \varepsilon_2\ \varepsilon_3$	Principal unit strains
ε	Volumetric strain $(\Delta V/V_o)$
γ_o	Octahedral shear strain $(\frac{2}{3}\sqrt{(\varepsilon_1 - \varepsilon_2)^2 + (\varepsilon_1 - \varepsilon_3)^2 + (\varepsilon_2 - \varepsilon_3)^2}\ )$
E	Young's modulus of elasticity
ν	Poisson's ratio
K	Bulk modulus $(d\sigma_o/d\varepsilon)$
G	Shear modulus $(d\tau_o/d\gamma_o)$
K_i	Initial tangent bulk modulus
G_o	Initial tangent shear modulus
V_o	Initial volume of the sample
V_c	Volume of sample after isotropic compression
L_o	Initial height of sample
L_c	Height of sample after isotropic compression
d_o	Initial diameter of sample
d_c	Diameter of sample after isotropic compression
e_o	Initial void ratio
e_c	Void ratio after isotropic compression

Symbol	Definition
w	Deflection of a point on the surface
w_z	Deflection of a point at a depth z
a	Plate radius
r	Horizontal distance from center of plate
z	Depth below surface
p	Unit pressure on the plate
P	Total vertical load on the plate
I_w	Deflection factor
K_o	Coefficient of earth pressure at rest (σ_h/σ_v)

SUMMARY

The stress-strain behavior of soils is a complex phenomenon for which a single reliable mathematical model has not been developed. The complexity arises from the considerable variations in physical properties that a given soil will exhibit under environmental changes as well as from the variations in the physical properties of different soils. Another complicating factor is that the behavior of the soil may vary from that of an elastic solid to that of a viscous fluid depending on the soil type and the stress system. Several different mathematical models have been proposed to describe the behavior of the soil under different conditions of stress application. The models are generally extensions of existing models used to define elastic, plastic, or viscoelastic behavior.

The present investigation was concerned with the development of a mathematical model to represent the stress-strain behavior of a cohesionless soil subjected to static first loading. The theory of elasticity was used as the basis for the model. The present solutions used in the elastic analysis of soil behavior are written in terms of Young's modulus and Poisson's ratio, which are assumed to be constant for a given soil. The method used in the investigation was to use stress-dependent bulk and shear moduli to define the behavior of the soil. The justification for adopting this method was that the stress-strain relationship under first loading is non-linear, and that the bulk and shear moduli are more readily related to the stress system and better characterize the behavior

of soil.

An investigation of the variation in bulk and shear moduli with soil properties and the stress system was carried out for a micaceous, medium, uniform sand known locally as the Chattahoochee river sand.

The bulk modulus was investigated using isotropic compression tests in a triaxial cell. The results indicated that for a given initial relative density the bulk modulus could be related to the octahedral normal stress over a specified stress range by an equation of the form:

$$K = A + m\sigma_o \tag{1}$$

in which K is the bulk modulus, σ_o is the octahedral normal stress, and A and m are constants which are functions of the soil. Two such equations were used to relate the bulk modulus and the octahedral normal stress over a stress range of 0 to 100 lbs. per sq. in. The constants A and m were empirically related to the relative density of the soil.

Constant octahedral normal stress triaxial compression tests were used to investigate the variation in shear modulus with stress level and soil properties. The results of the tests indicated that the shear modulus could be related to the octahedral normal stress and the octahedral shear stress by an equation of the form:

$$G = G_o (1 - b \tau_o)^2 \tag{2}$$

in which G is the shear modulus, G_o is the initial tangent shear modulus corresponding to zero octahedral shear stress, τ_o is the

octahedral shear stress and b is a parameter that is a function of the octahedral normal stress and the relative density of the soil. The initial tangent shear modulus is also a function of the octahedral normal stress and the relative density of the soil. Equation (2) is a derivative of the two parameter rectangular hyperbolic function proposed by R. L. Kondner for relating stress and strain.

The concept of using stress-dependent bulk and shear moduli was extended to the solution of the deflection under a uniformly loaded circular area on the surface of a semi-infinite mass. The existing deflection equation based on the Boussinesq stress distribution theory and expressed in terms of Young's modulus and Poisson's ratio, was rewritten in terms of the bulk and shear moduli as indicated by equation (3):

$$w_z = pa\left[\frac{1}{2G}\sin\alpha + \frac{1 + \frac{3K - 2G}{2(3K+G)}}{3K}\ \frac{1-\cos\alpha}{\sin\alpha}\right] \qquad (3)$$

in which w_z is the deflection of a point at a depth z from the surface, p is the uniform load intensity acting on the surface, "a" is the radius of the circular area, and α is the inverse tangent of a/z. The equation is applicable only to points along the vertical axis of symmetry.

To obtain the solution for the deflection at the surface, the soil was treated as a multi-layered system with each layer having a bulk and shear modulus in accordance with the average stress system in the layer. The stress distribution in the soil was approximated by use of the Boussinesq stress distribution theory. The relationships established by the laboratory tests were used to define the bulk and shear moduli of each

of the layers of the multi-layered system. The compression of each layer was computed for a specified surface load intensity and the compressions were summed up to obtain the deflection at the surface. A computer program was developed for computing the stresses, the associated bulk and shear moduli, the compression of the layers, and the deflection at the surface for a given surface load intensity.

To assess the reliability of predicting deflections by means of equation (3), plate load tests were performed on the Chattahoochee sand. The tests were performed in an 8.33 foot diameter cylindrical pit 22 feet in depth. A 17.5 inch diameter plate was used and the sand was prepared in a dense, a medium, and a loose state.

The theoretical analysis was based on an assumed uniform boundary pressure and a stress distribution in accordance with the Boussinesq theory. The consequence of these assumptions was that the soil in a local zone below the loaded area was in a state of failure. A predetermined critical ratio of the octahedral normal stress to the octahedral shear stress, corresponding to failure conditions measured in the triaxial tests, was used as a criterion for failure. The stress distribution analysis indicated smaller ratios than could be measured in the triaxial tests. Therefore it was necessary to assign shear moduli to this zone for which there was no experimental data. Two methods of dealing with this problem were used. One method was to assign a constant shear modulus based on incipient failure conditions to the zone. The second method was to permit the shear modulus to approach zero as the ratio of the octahedral normal stress to the octahedral shear stress approached zero. The effect of assigning a constant shear modulus to the failure

zone was to linearize the load-deflection curve. The effect of using the second method was to introduce non-linearity to the load-deflection curve and also to increase the magnitude of theoretical deflections.

In view of the uncertainty with which the shear modulus could be defined for the conditions of local failure as well as the dependence of the resulting theoretical load-deflection data on this condition, no definite conclusions could be drawn regarding the reliability with which deflections could be predicted using stress dependent bulk and shear moduli.

A hypothetical case for which the condition of local failure was eliminated by the application of a surcharge indicated that the load-deflection curve was non-linear with a continuously increasing slope. This better illustrated qualitatively, the concept of using variable bulk and shear moduli to depict the behavior of the soil when subjected to static first loading.

CHAPTER I

INTRODUCTION

The nature of the response of a soil to an imposed stress system has been the subject of numerous experimental and analytical investigations. The fact that these investigations are continuing is evidence that to date a satisfactory theory has not evolved. The main basis for the analytical approaches has been the theory of elasticity, plasticity, and viscoelasticity. Since these theories are vastly different in their characterization of the response of a soil to a given stress system, the applicability of each theory must necessarily be of a very limited nature. The applicability is often governed by the magnitude of the imposed stress level relative to the ultimate strength of the soil, and by the complexity of the solution which the theory yields.

Generalizing, it may be said that the linear theory of elasticity serves as the basis for the solution of problems involving small strains, while the theory of plastic equilibrium serves as the basis for the solution of problems involving large strains. Since in many practical considerations, a soil is subjected to a wide range of stresses and strains which may be time-dependent, the viscoelastic theory would intuitively provide a more realistic basis for analysis. In this respect, several investigators (References 1 through 4) have attempted to formulate a working hypothesis, based on rheology, that would adequately describe the behavior of the soil. The concept has been extended to the solution of a limited number of practical problems (References 5 through 11). Because

of the complexity of the viscoelastic treatment of soils, and the difficulty of evaluating the parameters necessary to define the elastic and viscous components of the stress-strain relationship, the viscoelastic concept has not received wide acceptance to date as a working hypothesis.

Insofar as cohesionless soils are concerned, the stress-strain response may be categorized as being non-time dependent, and non-linear. It would therefore be desirable to develop a non-linear stress-strain theory to describe the behavior of the soil.

In examining past methods of dealing with the stress-strain response of cohesionless soils, there are, in the author's opinion, two aspects that warrant examination and possible modification. These are (1) the particular form of stress-strain data used, for which the relationship is sought, and (2) the concept of a single deformation modulus, relating stress and strain.

It may be stated that the stress-strain data obtained from triaxial compression tests are most often presented in the form of principal stress difference $(\sigma_1 - \sigma_3)$, versus axial strain. An attempt is then made to relate stress and strain. Very often the initial tangent modulus is selected for use in the linear stress strain theory which can only yield a very crude approximation of the behavior of the soil. If an attempt is made to characterize the non-linearity of the stress-strain curve, then the parameter relating stress and strain must be a function of the stress level, as denoted by the principal stress difference. The principal stress difference, however, does not in itself reflect the stress conditions in the soil, nor is there a unique relationship between a given principal stress difference and the associated strain. For example, if the magnitude

of the principal stresses is relatively high, a small principal stress difference, say 10 lbs. per sq. in., will induce a small strain. On the other hand, if the principal stresses are relatively low, the corresponding strain may be very high or failure may even occur. Thus stress difference alone has very little significance. The use of the mean or octahedral normal stress and the associated deviator stresses* provides a more meaningful concept of the state of stress. Likewise the use of axial strain is not always compatible with a stress difference when relating stress and strain components. Thus a stress-strain relationship based on principal stress difference and axial strain cannot properly describe the behavior of a soil mass.

In characterizing the behavior of most materials, two elastic constants (Young's modulus and Poisson's ratio) are used to relate stress and strain. The assumptions that permit such a simplified relationship are the assumptions of homogeneity and isotropy. If these assumptions were not valid then 36 elastic constants would be required to completely define the stress-strain relationship of the material. Eighteen constants would be required to relate the normal stresses and strains and the other 18 constants would be required to relate the shear stresses and strains. Thus basically, every component of strain is a linear combination of strains due to normal stresses and strains due to shearing stresses.

If we consider the behavior of a homogeneous isotropic elastic solid subjected to a stress system consisting of normal and shearing stresses, in general it may be said that the normal stresses will cause

---

*Throughout the text deviator stress refers to the components of the deviatoric portion of the stress tensor.

a change in the dimensions of the solid while the shearing stresses will cause a distortion of the solid. Thus the normal stresses may be associated with a change in volume of the solid while the shearing stresses are only associated with a distortion of the solid.

If on the other hand, we consider the behavior of a homogeneous isotropic soil sample subjected to an identical stress system there is a basic difference in the response of the soil. The normal stresses will bring about a change in dimensions and volume of the soil sample. However, the shearing stresses in addition to bringing about a distortion of the sample may also bring about a change in volume of the sample. The change in volume resulting from the shearing stresses may well exceed the change in volume brought about by the normal stresses.

Thus when applying the theory of elasticity to the behavior of soils, it appears advisable to separate and characterize the response of the soil to the normal stresses, and the response of the soil to the shear stresses. The implication of this is that for soils there does not necessarily exist a single unique relationship between the shear modulus and the modulus of volume expansion for all points within the mass.

In view of the preceding discussion, it was felt that an investigation of the nature of a non-linear stress-strain theory for cohesionless soils based on a modulus of volume expansion (hereinafter referred to as the bulk modulus), and a modulus of shear, might lead to a better understanding of the actual behavior of a cohesionless soil mass. Moreover, it was considered that if the respective moduli were expressed in terms of octahedral normal and shear stresses, they would be more readily identifiable in some practical soil mechanics problems.

To illustrate the practical feasibility of using such a non-linear stress-strain theory, it was decided to apply the concept to the load-deflection analysis of a distributed load acting on the surface of a semi-infinite mass. Specifically, the existing equation for the deflection under a uniformly-loaded circular area would be rewritten in terms of the bulk and shear moduli in place of Young's modulus and Poisson's ratio. The non-linearity arises from expressing the moduli as functions of the stress system rather than assigning a constant value to each.

To assess the validity of the modified equation a limited number of plate load tests would be conducted.

In accordance with the objectives stated above the investigation consisted of the following parts and their respective phases.

Part A: The investigation of the nature of a non-linear stress-strain relationship for a cohesionless soil.

This was separated into the following phases:

1. An experimental investigation of the bulk modulus of sand under varying conditions of octahedral normal stress and initial density.

2. An experimental investigation of the shear modulus of sand under varying conditions of octahedral normal stress, octahedral shear stress, and initial density.

3. The formulation of expressions for the bulk and shear moduli as functions of the properties of the soil and the stress system.

Part B. The analysis of deflection under a uniformly distributed load acting over a circular area.

This section included the following phases:

1. The development of an expression for the defection under a

uniformly-loaded circular area acting on the surface of a cohesionless soil mass in terms of variable bulk and shear moduli.

2. Plate load tests to assess the practicality and validity of the above expression.

Since each phase constituted a separate investigation, each is dealt with separately in the dissertation in the order outlined above.

Part C. Conclusions and Recommendations for the Study.

This part consists of a reiteration and integration of the conclusions pertaining to each phase along with conclusions regarding the overall study. A critical appraisal of the study as well as recommendations for further study are dealt with in this section.

PART A

THE INVESTIGATION OF THE NATURE OF A NON-LINEAR STRESS-STRAIN RELATIONSHIP FOR A COHESIONLESS SOIL

CHAPTER II

THEORETICAL CONSIDERATIONS PERTAINING TO THE STRESS-STRAIN BEHAVIOR OF COHESIONLESS SOILS

Existing Stress-Strain Theories

Generally when reference is made to a stress-strain relationship pertaining to soils, it implies a non-linear plot of axial stress, or principal stress difference, versus axial strain. Such plots have been used for the most part to define failure conditions, or an initial tangent modulus. The failure conditions have been used to define the ultimate strength of the soil in terms of an angle of shearing resistance, while the initial tangent modulus has been used in solutions based on a linear stress-strain theory. Only limited attention has been paid to characterizing the entire portion of the stress-strain plot. The following is a brief discussion of some of the investigations that were made of the stress-strain characteristics of a cohesionless soil.

Kondner et al. (12, 13) have developed a two-parameter hyperbolic function relating principal stress difference and axial strain. The two parameters incorporate the initial tangent modulus and the failure stress. The details will be given in a later section.

Wroth and Basset (14) have developed mathematical equations based on exponential functions for describing the shear stress-strain characteristics of an idealized sand. Three basic equations are used to obtain the relevant stress and strain parameters observed during a test. One equation relates the effective normal stress and the void ratio for the

particular test being performed. A second equation is an energy equation and the third is a strain equation. The mathematical expressions are used to describe the behavior of a soil sample undergoing a direct shear or triaxial compression test. The study was not extended to the solution of practical problems although the authors did express the belief that it could be extended to some boundary value problems.

Both Kondner and Wroth indicated a close correlation between the mathematical stress-strain relationship and observed data. Their approaches differ from that proposed by the author in that their equations apply only to the results of a laboratory test on a sample of soil. It was the author's intention to obtain expressions for the elastic parameters (the bulk and shear modulus) which could be used in the solution of problems which have the linear stress-strain theory as their basis.

Other stress-strain theories have been proposed but they are generally limited to a specific application. Examples of this are Rowe's (15) stress-strain theory for cohesionless soils as applied to earth pressure at rest, and Duffy and Mindlin's (16) stress-strain relations as applied to wave velocity and energy dissipation in a granular medium.

Previous Investigations of the Elastic Properties of Sand

It has been customary to represent the elastic parameters of a soil by a modulus of deformation, which is synonymous with Young's modulus, and Poisson's ratio.

The modulus of deformation as determined by triaxial compression tests has been found to be a function of the density of the soil and cell pressure.

Investigations of the modulus of elasticity by sonic methods have indicated that the wave velocity increased exponentially with confining pressure (16, 17). Since the dynamic modulus varies with the square of the wave velocity, the dynamic modulus must vary exponentially with the confining pressure.

Experimental studies of Poisson's ratio of sand have indicated that the value obtained is influenced considerably by the method used to obtain it.

Values of Poisson's ratio as determined by zero lateral strain tests as reported by Barkan (18) and Terzaghi (19) were found to be relatively constant and in the range of 0.30 to 0.35.

On the other hand, Jacobson (20) showed that Poisson's ratio as determined by triaxial compression tests varied considerably with the shearing stress. His tests indicated values of Poisson's ratio ranging from 0.1 to 0.6. This wide range of values reflects the volumetric strain that accompanies shear strain. A value in excess of 0.5 implies an expansion of volume under the imposed stress system.

Poisson's ratio based on measurements of the rate of propagation of longitudinal and shear values was found to be in the order of 0.42 to 0.47 (18) which is somewhat higher than the values obtained under static conditions.

Thus it may be categorically stated that the modulus of elasticity of sands has been found to be function of the density of the soil and some measure of the normal stress intensity. On the other hand, Poisson's ratio has been found to be relatively constant for a given sand when determined under conditions of no lateral strain but varies considerably

with shear stress when lateral strain is permitted.

Stress-Strain Relationship in Terms of Volumetric and Deviatoric Components

In tensor notation, the stress-strain behavior of a homogeneous, isotropic, elastic solid exhibiting small strains, is written as follows:

$$\sigma_{ij} = \frac{3K - 2G}{3} \varepsilon_{kk} \delta_{ij} + 2G \varepsilon_{ij} \qquad \text{(II-4a)}$$

in which σ_{ij} = stress component ($i = 1$ to 3, $j = 1$ to 3)

ε_{ij} = strain component ($i = 1$ to 3, $j = 1$ to 3)

K = bulk modulus

G = shear modulus

δ_{ij} = Kronecker delta ($\delta_{ij} = 1$ if $i = j$)

($\delta_{ij} = 0$ if $i \neq j$)

ε_{kk} = cubical dilation

Equation (II-4a) may be rewritten as:

$$\sigma_{ij} = K\varepsilon_{kk} \delta_{ij} + 2G(\varepsilon_{ij} - \frac{1}{3} \varepsilon_{kk} \delta_{ij}) \qquad \text{(II-4b)}$$

Writing equation (II-4b) in terms of volumetric components (σ_{ij}) and (ε_{ij}) and deviatoric components (s_{ij}) and (e_{ij})

$$\sigma_{ii} = 3K \varepsilon_{ii} \qquad \text{(II-5a)}$$

$$s_{ij} = 2G e_{ij} \qquad \text{(II-5b)}$$

The deviatoric components are given by:

$$s_{ij} = \sigma_{ij} - \frac{1}{3}\sigma_{kk}\delta_{ij} \qquad \text{(II-6a)}$$

$$e_{ij} = e_{ij} - \frac{1}{3}\varepsilon_{kk}\delta_{ij} \qquad \text{(II-6b)}$$

The significance of equations (II-5a) and (II-5b) is that they indicate that the moduli K and G may be determined separately by appropriate experimental tests.

The bulk modulus may be determined by tests in which only linear strains occur such as an isotropic compression test.

The shear modulus may be determined by tests in which only shear strains occur such as a pure shear test or a torsion test. As well, the shear modulus may be obtained from triaxial compression tests with the octahedral normal stress held constant. The effect of maintaining a constant octahedral normal stress is to hold the cubical dilation component constant. Consequently, as the test is performed, the changes in stresses and strains that occur are deviatoric which permits the direct determination of the shear modulus.

Thus it has been demonstrated that the stress-strain behavior of a homogeneous, isotropic, elastic solid, can be represented by a general expression in which the volumetric and deviatoric components may be separated. In this expression the bulk modulus relates the volumetric stresses and strains, and the shear modulus relates the deviatoric stresses and strains. Moreover it has been demonstrated that these two parameters G and K are readily obtainable from triaxial compression tests utilizing specific stress paths, or loading procedures.

Previous Bulk Modulus Studies

As mentioned in the preceding section, the bulk modulus is most readily obtained from isotropic compression tests. The bulk modulus is the instantaneous slope of the octahedral normal stress versus volumetric strain curve.

Isotropic compression tests have been conducted primarily on clays in conjunction with consolidated undrained triaxial compression tests and in consolidation studies of clay. Fewer isotropic compression studies have been conducted on sands. The following is a brief discussion of some of the findings regarding the bulk modulus (or what is often referred to as the modulus of isotropic compression) of sand.

Ladanyi (21) performed isotropic compression tests on a fine, uniform, well rounded quartz sand prepared at near minimum and maximum relative densities. The tests were conducted over a hydrostatic stress range of 0 to 6 kg/cm^2. The results of these tests, in qualitative terms, imply that the bulk modulus is an increasing function of the hydrostatic stress and that it is a function of the initial density of the soil. At a given hydrostatic stress, the bulk modulus is higher for the dense state than it is for the loose state.

His test results also indicated that approximately 50 per cent of the volumetric strain was recoverable.

Wroth (14) in his development of mathematical equations for the stress-strain relationship describing the shearing behavior of an idealized sand assumed that under isotropic consolidation the idealized sand followed a straight line on a semi-logarithmic plot. This differs from Terzaghi's theory of one-dimensional consolidation only in that the natural logarithm

was used in place of the common logarithm. Since no tests to confirm or disprove the relationship were reported, the validity of the equation cannot be commented on.

Clough (22) in his investigation of the shearing strength of sands at high pressures, conducted a series of isotropic compression tests on a fine micaceous sand in a dense and in a loose state up to hydrostatic pressures of 650 kg/cm^2. A qualitative analysis of his results indicated results similar to those obtained by Ladanyi in that the bulk modulus is a function of both the octahedral stress and the initial density of the sand. An assumed linear relationship between the log of hydrostatic stress and volumetric strain was found to deviate considerably from the observed values during the initial portion of the test. One important aspect of the investigation over the large pressure range was that even at the very high pressures there was no tendency for a linear relationship between hydrostatic stress and volumetric strain, which precludes the concept of a constant bulk modulus.

Wilson and Sutton (23) conducted isotropic compression tests on elastic spherical balls in a loose packing. From their study they obtained the expression

$$\varepsilon = C.\sigma^{2/3}$$

Jacobson (20) obtained a similar expression

$$\varepsilon = 0.608 \times 10^{-3} \times \sigma^{0.612}$$

The above two expressions imply that there is a linear relationship between the hydrostatic stress and the volumetric strain on a log-log plot.

From the preceding discussion of previous investigations it can only be concluded that the bulk modulus of sand is not a constant but increases with the octahedral normal stress and the initial density of the soil. No general expression has been developed that would permit the determination of the bulk modulus for a specified density and octahedral normal stress.

Previous Shear Modulus Studies

Only relatively recently has there been any attention paid to the characterization of the behavior of soils through a separation of the isotropic and deviatoric components. Moreover, much of the effort has been directed towards defining failure conditions for which a modulus of shear is not pertinent. Some of the investigations that have been carried out are cited in the following paragraphs.

Barkan (18) performed a simulated pure-shear test using a box having two metal walls with knife edges free to rotate about their supports. A horizontal force was applied to the upper part of the walls and the shearing stresses and strain were obtained for a dense soil under varying normal pressures. The results indicated that a linear relationship existed between the shearing stress and the shearing strain for a sand at a given density and subjected to a constant normal pressure. However, the modulus of shear was found to depend on the magnitude of the applied normal stresses and therefore was not a constant. Barkan also found that a significant shearing stress had to be applied before any shearing strain was registered, an observation which he attributed to a prestressing of the soil during densification. This signifies that initial

void ratio in itself is not truly an "initial" point, since the soil has undergone a stress history, much of which may be retained and which may consequently affect the future behavior of the soil. This is particularly true of sands formed in small rigid containers where pre-stress can be manifested.

Another means of determining the shear modulus is by torsion tests. Such tests were performed by Habib (24) in his investigation of the effects of the intermediate principal stress on the shearing strength of sands. However, no information was included in his report which would permit the determination of the shear modulus.

Several investigators in their study of soil dynamics determined the elastic properties of soil by the measurement of the velocities of longitudinal and shear waves transmitted through the soil. In general the results of such tests as evaluated and reported by Richart (25) indicated that the shear modulus of granular soil was not a constant but that it increased approximately with the one-third power of the confining pressure.

Another method of determining the shear modulus is to conduct a triaxial compression test with the octahedral normal stress held constant. Constant octahedral tests have been performed by such investigators as Kerisel (26), Kondner (27) and Clough (22). An examination of the results presented, revealed that, in all the above mentioned cases, the analysis and presentation of the results were of such a nature as to preclude their use for the quantitative determination of the shear modulus.

In summary, it may be categorically stated that, based on the limited available experimental evidence, the shear modulus of sands is a

function of the density of the soil, the magnitude of the effective normal stress, and possibly the magnitude of the shear stress. With regard to the last variable, Barkan's work implies that the shear modulus is independent of the shear stress while a qualitative analysis of Kondner's and Clough's work implies that the shear modulus is a function of the shear stress.

CHAPTER III

EXPERIMENTAL INVESTIGATION OF THE BULK MODULUS

Scope of the Investigation

The following factors were considered in deciding the extent to which the investigation would be carried out.

1. Range of densities to be investigated

Ideally, the densities investigated should range from 0 to 100 per cent of the relative density as defined by standard procedures.

Zero per cent relative density was impractical if not impossible to attain since a small confining pressure had to be applied to the sample to provide it with sufficient rigidity to prevent it from slumping. The loosest state was therefore chosen to correspond to that density attained by placing the sand by means of a funnel, using a zero drop in height and measuring the sample dimensions with the sample under a confining pressure of 0.5 pounds per square inch. This was found to correspond to a relative density of approximately 15 per cent.

Obtaining 100 per cent relative density involves considerable vibration of the soil in an inundated state. There is a distinct possibility of soil alteration resulting from the crushing of grains when the soil is densified in this manner. To avoid soil alteration, the densest state was chosen to correspond to that density that could be attained by moderate vibration with the sample dimensions taken under a confining pressure of 0.5 pounds per square inch. This was found to correspond to a relative density of approximately 85 per cent.

It was felt that a relative density range of 15 to 85 per cent bracketed the range of densities that one might expect to find not only in natural deposits but also in man made fills.

2. Range in hydrostatic stress

It was decided to subject the samples to a hydrostatic pressures ranging from 0.5 to 100 pounds per square inch. This range was selected on the basis of the equipment that was to be used, and the practical problem to which this concept was to be extended. It was felt that from the point of view of settlements of foundation on or near the surface of sands, an octahedral stress of 100 pounds per square inch (or 7.2 tons per square foot) was unlikely to be exceeded. Moreover, the results of Clough's tests (22) indicated that even at hydrostatic pressures of 63.3 tons per square foot, there was no linearity between stress and volumetric strain which excluded the existence of a practical limit to the bulk modulus.

3. Statistical analysis

It goes without saying that a statistical approach to the analysis of soil test results offers the best means of obtaining a good indication of the behavior of soil. Soil test results must necessarily exhibit some degree of randomness that is attributed to the physical make-up of the soil. This, along with the practical impossibility of eliminating experimental errors or inaccuracies, evinces the existence of scatter in experimental analysis.

Since an exact duplication of initial densities is difficult to achieve and impossible to define with 100 per cent confidence due to experimental inaccuracies, it was decided to perform five tests on samples

prepared at approximately the same density. The procedure was to be repeated at densities varying by approximately 10 per cent. Thus eight series of isotropic triaxial compression tests were performed to define the variation in bulk modulus with octahedral normal stress and with initial density of the soil.

Soil Investigated

The tests were performed on a micaceous, medium, uniform sand known locally as the Chattahoochee river sand. The sand is composed primarily of sub-angular quartz particles with a few per cent of mica, principally muscovite. The physical properties as determined by ASTM standard laboratory procedures are given in Table 1. The grain size distribution is given in Figure 1.

The Chattahoochee sand has been used in other research undertakings and information regarding its shear strength characteristics under normal and extremely high confining pressures can be found in references 28, 22, and 29.

Test Apparatus

The bulk modulus tests were performed on specimens 2.8 inches in diameter and 6 inches in height in a standard triaxial cell. Water was used as the cell fluid and compressed air was used to increase the cell pressure. The sand was in an air dry state (less than 0.1 per cent moisture). A volume change measuring device similar in principle to that outlined in Bishop and Henkel (20) was used to measure the volume change. Standard rubber membranes (wall thickness 0.008 to 0.013 inches) were used.

Table 1. Physical Properties of Chattahoochee River Sand

Specific Gravity	2.66
Maximum Void Ratio	1.10
Minimum Void Ratio	0.61
Coefficient of Uniformity	2.0

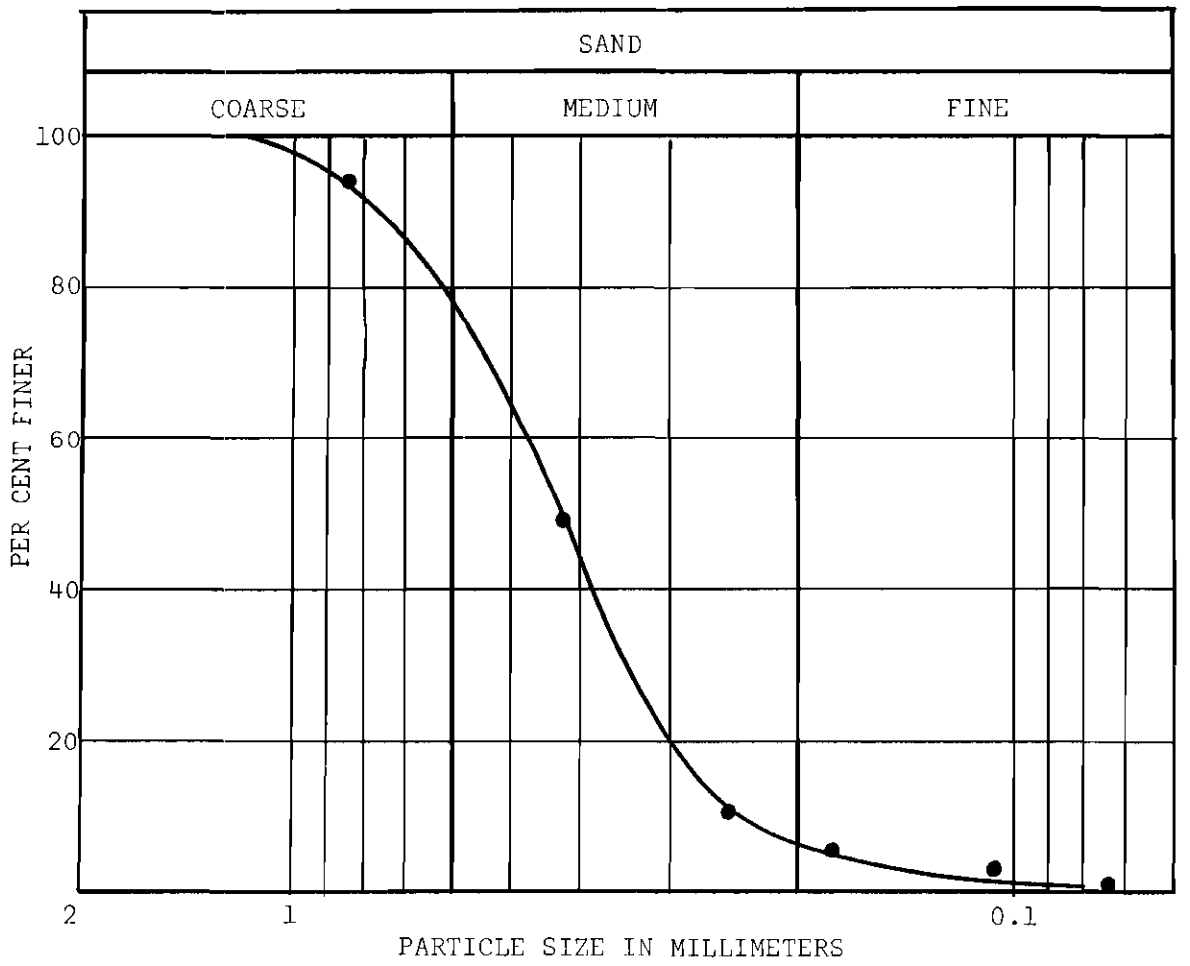

Figure 1. Grain-Size Distribution for Chattahoochee Sand.

Test Procedure

Sample Preparation

Conventional techniques and equipment were used to form the samples. The density and uniformity was controlled by permitting the sand to flow through a funnel, at a constant height of drop. The height of drop was varied to attain different densities for the different test series in accordance with a pre-established relationship between height of drop and density (29). For greater densities than could be practically achieved by this method, vibration techniques were employed. Sample dimensions were taken by means of calipers accurate to the nearest .01 mm. and a scale accurate to the nearest 0.01 inch. The dimensions were taken with the sample under a vacuum of 0.5 lbs. per sq. in. Five readings of the diameter and the height were taken for each specimen. The membrane thickness was subtracted from the measured diameter. An average membrane thickness of 0.01 inches was assumed.

After the cell had been assembled and the cell fluid added, the vacuum stress of 0.5 lbs. per sq. in. was transferred to a positive confining pressure of 0.5 lbs. per sq. in. in the cell fluid. Any future reference to initial conditions will infer a confining pressure of 0.5 lbs. per sq. in. and the corresponding dimensions and density.

Test Technique

After the confining pressure was transferred from a vacuum to a positive pressure the volume change device was connected to the cell. The test was performed by increasing the cell pressure in increments. To define the initial portion of the curve, the cell pressure was increased by raising a burrette of water to heights yielding average cell

pressures (measured relative to mid height of the sample) of 0.9, 1.3, and 2.0 lbs. per sq. in. From this point on, compressed air was used to increase the cell pressure to 3, 5, 7.5, 10, 15, 20, 25, 30, 40, 50, 60, 70, 80, 90 and 100 lbs. per sq. in.

After the application of each stress increment, sufficient elapsed time was permitted to insure isotropic compression of the sample. Generally this involved elapsed time of 7 to 12 minutes. The next stress increment was added when the volume change during a five minute interval was equal to or less than 0.1 cubic centimeters.

After completion of the isotropic compression test, the stress was reduced to 0.5 lbs. per sq. in. in decrements and volume change readings were observed.

Discussion of Test Results

The test data pertaining to the isotropic compression tests is presented in a summarized, tabular form in the Appendix (Table 4) and is reproduced in graphic form in Figures 2 through 9. Each figure represents the results of the five tests that constituted a separate series. A solid line is used to represent the average values of the five tests. The initial void ratio corresponding to each test is indicated on the figure.

To illustrate the effect of initial density on the stress-strain relationship, the average curves representing the different series were reproduced on a common plot (Figure 10).

From an inspection of Figures 2 through 10, it is apparent that the stress-strain relationship is a function of the initial void ratio and the magnitude of the octahedral normal stress. This is consistent with the findings of other investigators as outlined in the previous chapter.

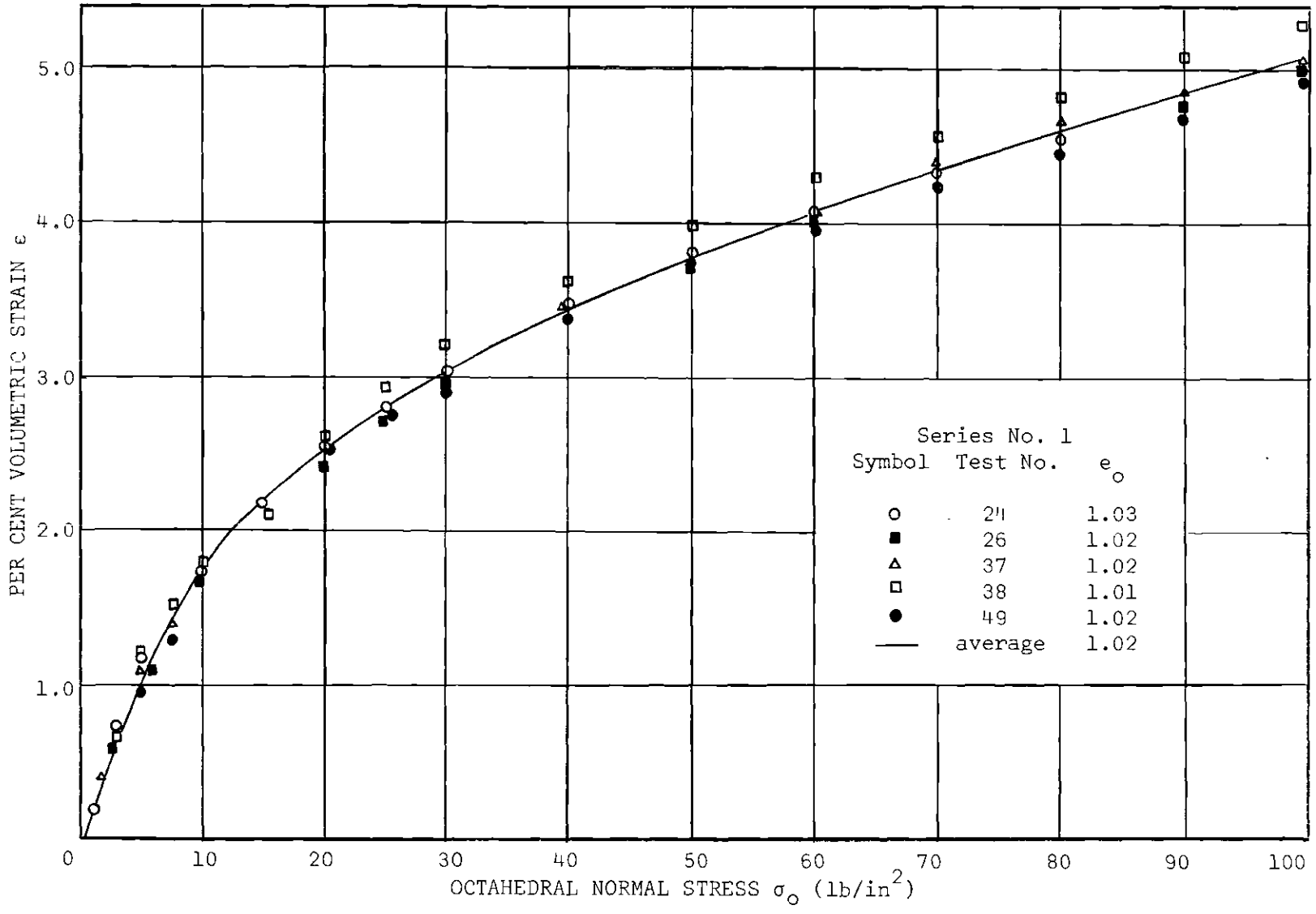

Figure 2. Volumetric Strain versus Octahedral Normal Stress: D_r = 0.18.

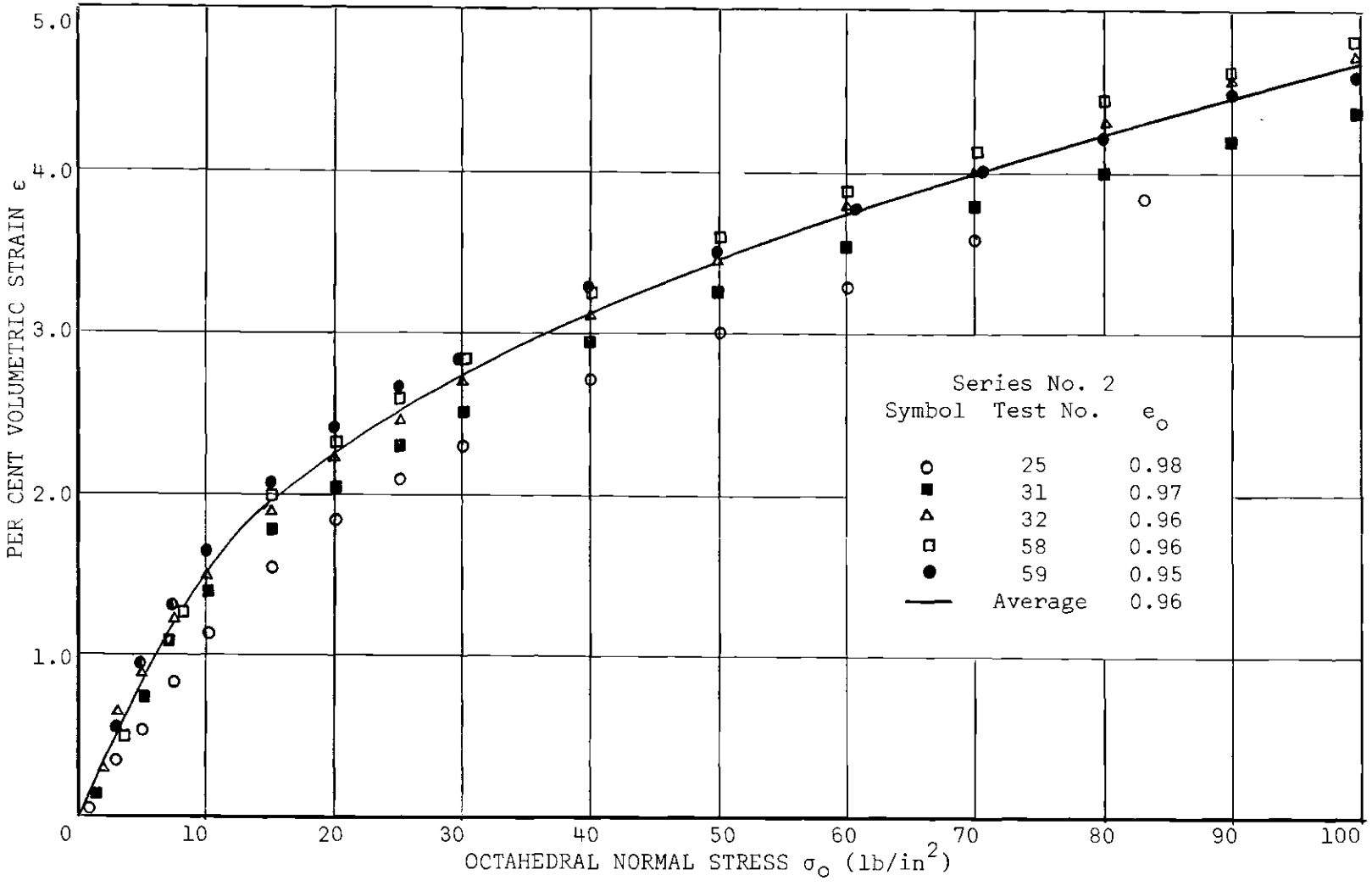

Figure 3. Volumetric Strain versus Octahedral Normal Stress: $D_r = 0.29$.

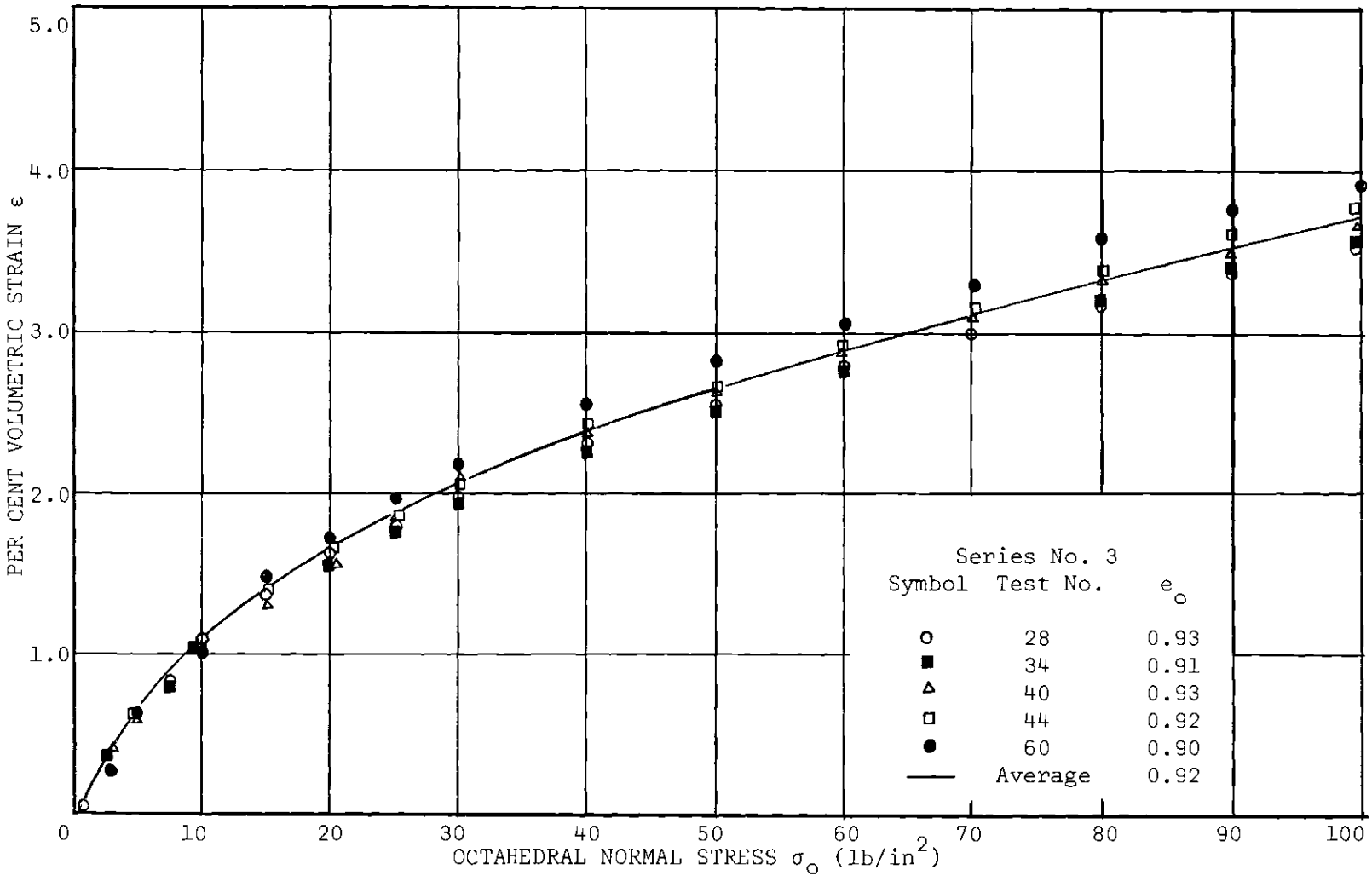

Figure 4. Volumetric Strain versus Octahedral Normal Stress: D_r = 0.37.

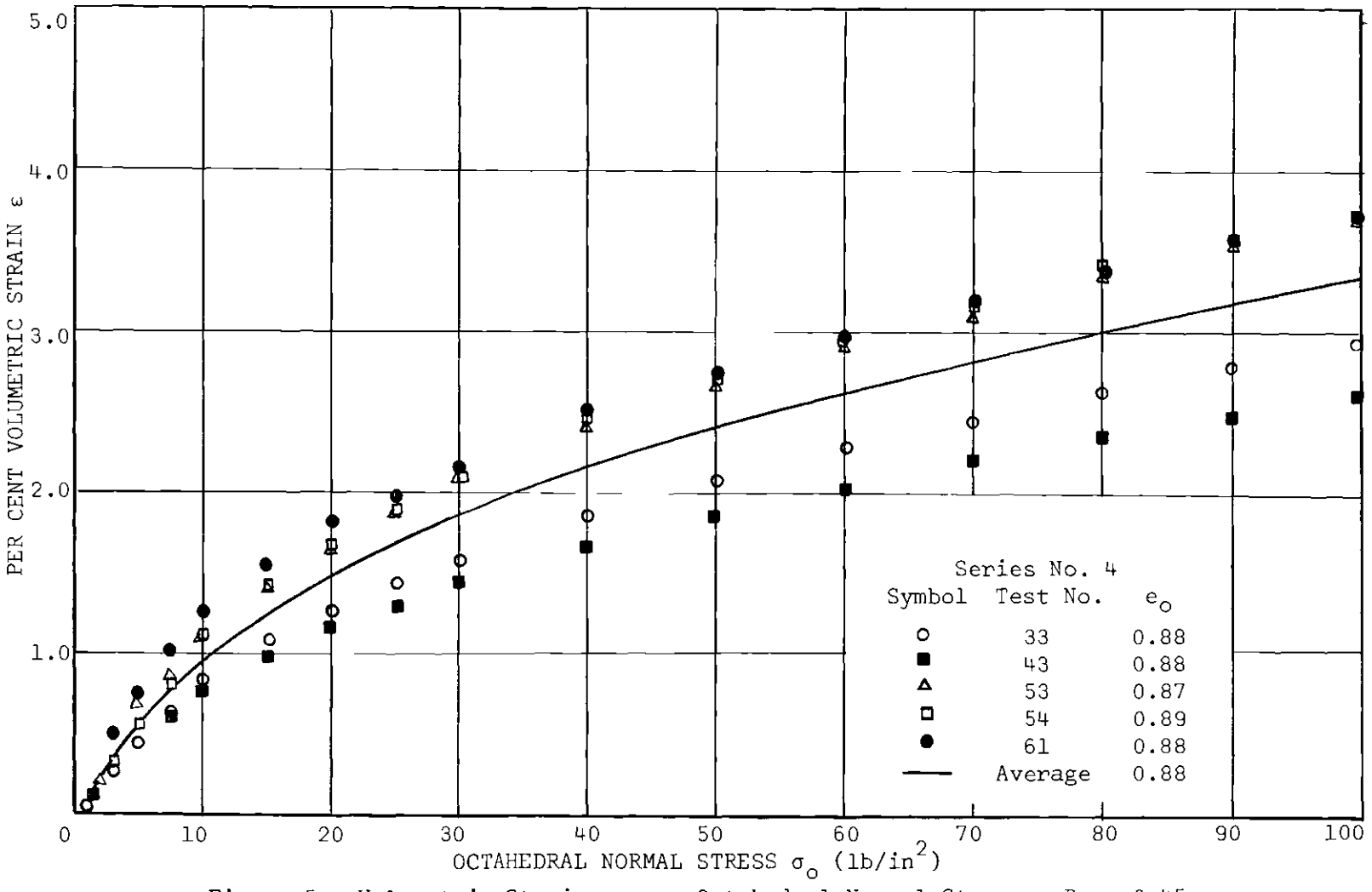

Figure 5. Volumetric Strain versus Octahedral Normal Stress: D_r = 0.45.

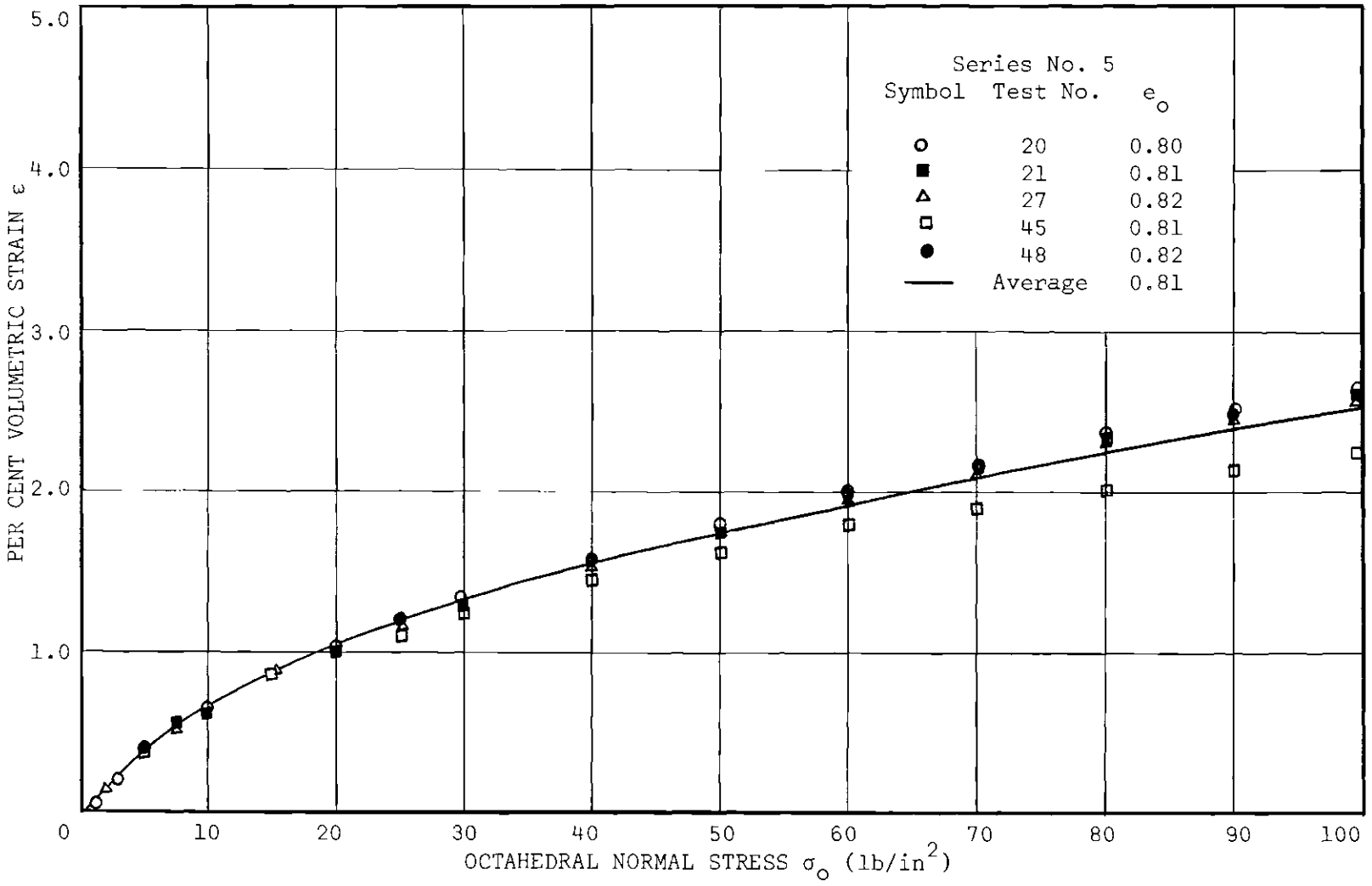

Figure 6. Volumetric Strain versus Octahedral Normal Stress: D_r = 0.60.

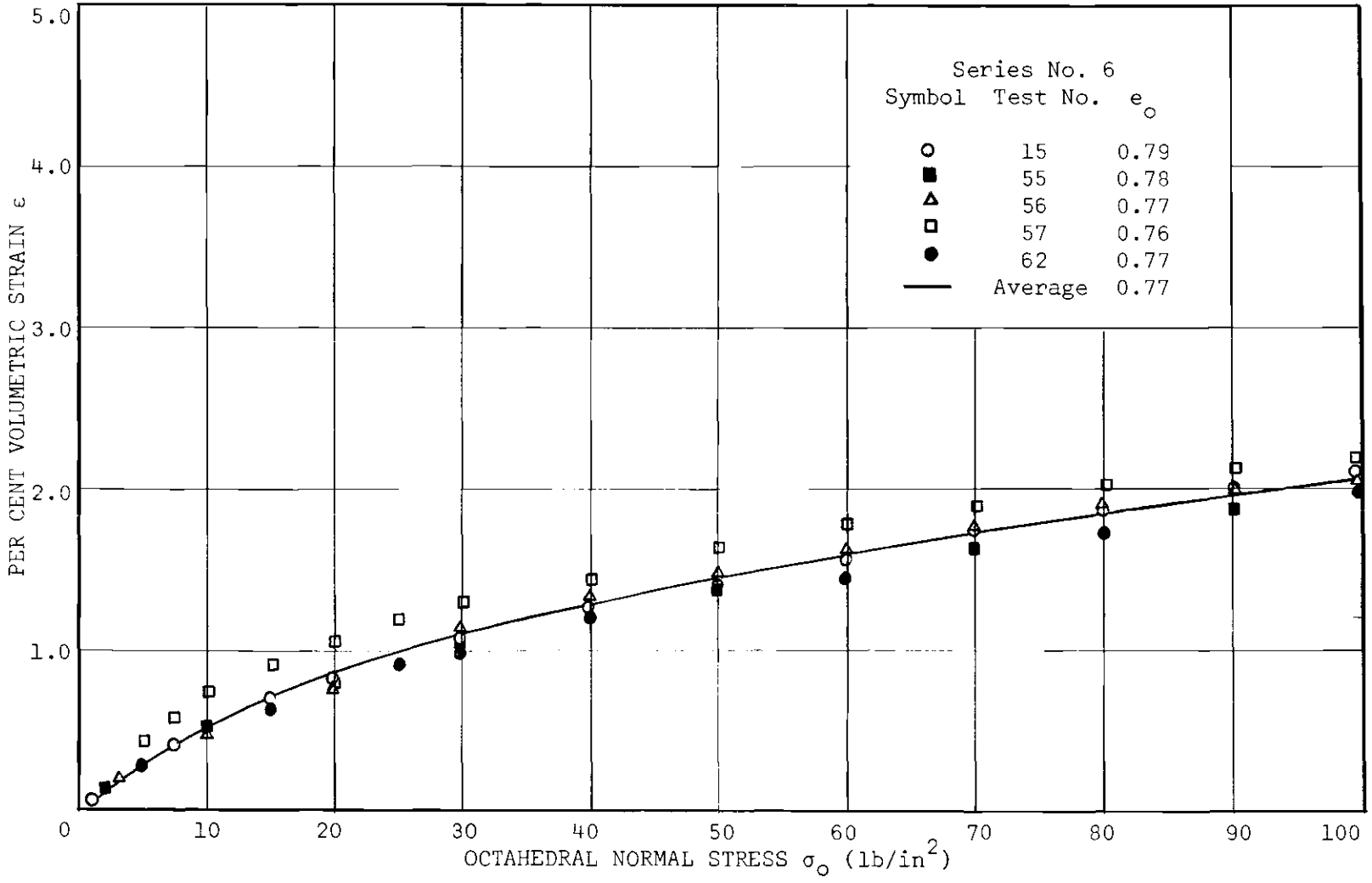

Figure 7. Volumetric Strain versus Octahedral Normal Stress: D_r = 0.68.

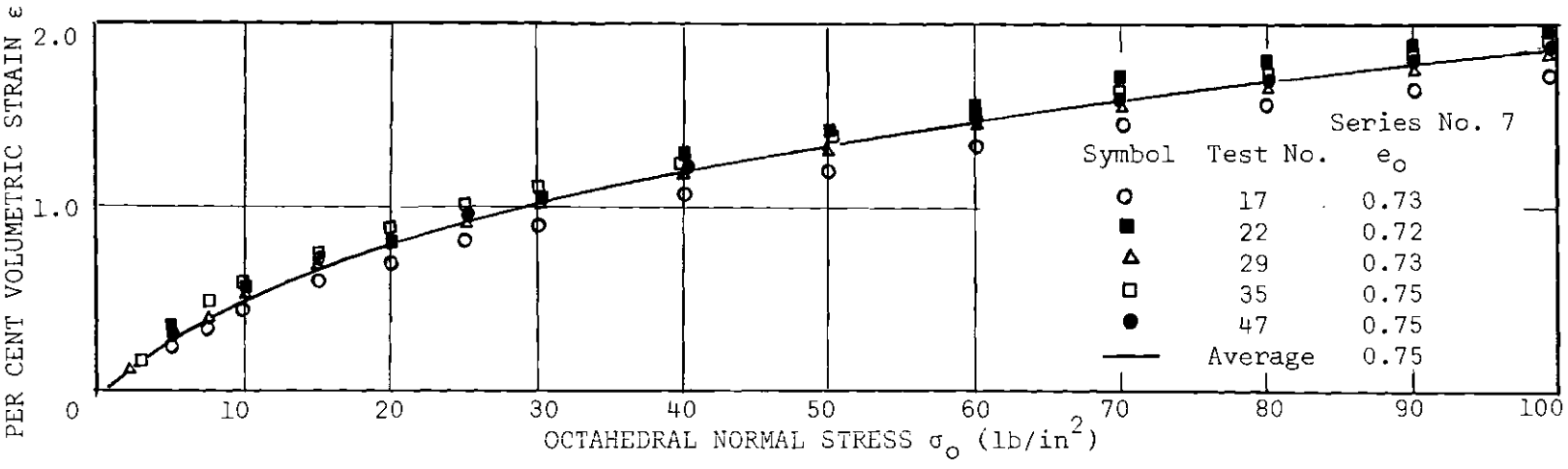

Figure 8. Volumetric Strain versus Octahedral Normal Stress: D_r = 0.74.

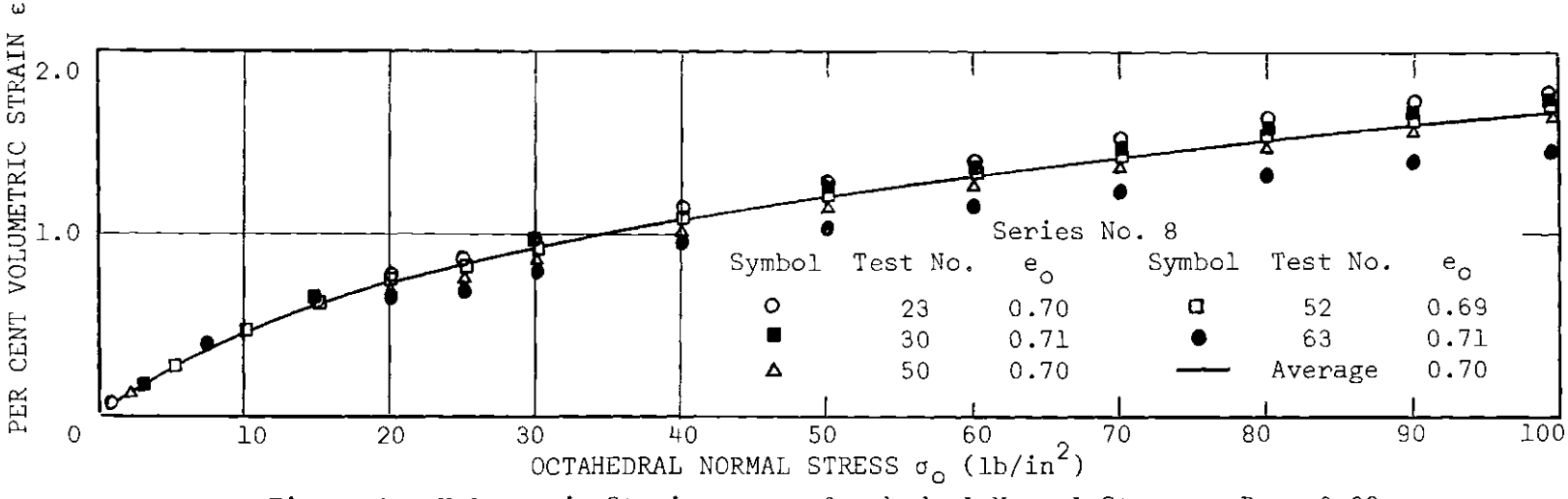

Figure 9. Volumetric Strain versus Octahedral Normal Stress: D_r = 0.82.

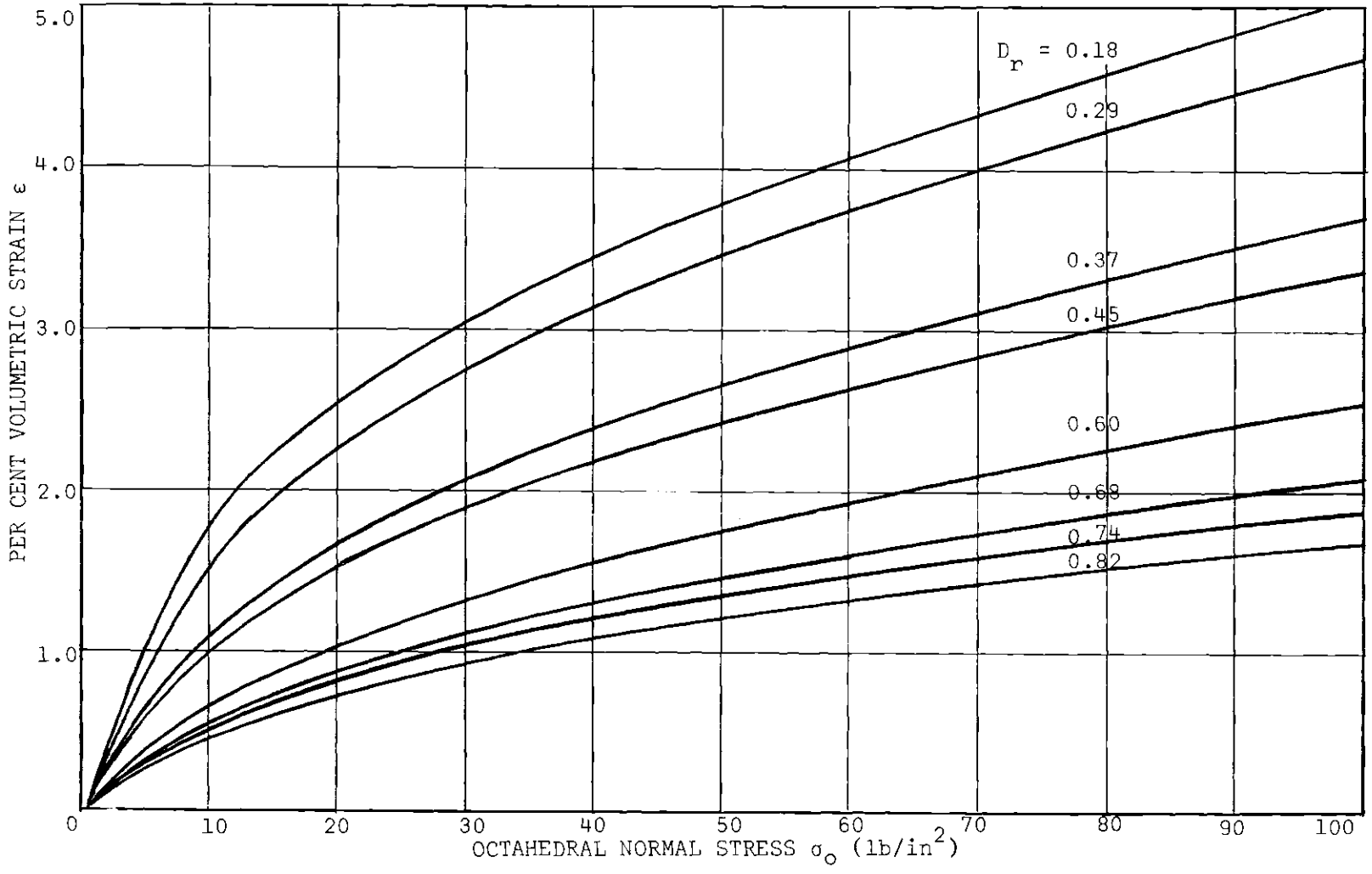

Figure 10. Relationship between Volumetric Strain, Octahedral Normal Stress, and Relative Density.

The scatter of test results in each test series is relatively small with the exception of series No. 4. The scatter may be considered to be the result of:

1. Randomness that all materials can be expected to exhibit when tested under identical conditions.

2. Inaccurate determination of the initial void ratio.

3. Experimental inaccuracies in performing the test.

The effects of each of these will be discussed in subsequent paragraphs.

Randomness

All materials exhibit a randomness when some property of the material is measured under identical testing conditions. In light of this, the probability of an exact duplication of soil test results can not be very high when one considers the material and the process used in forming the samples. A quantitative analysis of the scatter of test data that could be attributed to this in the tests conducted would require a specially designed statistical experiment involving numerous tests. Nonetheless it should be borne in mind that a scatter of test results under identical testing conditions is the rule rather than the exception.

Initial Void Ratio

Much of the scatter is attributable to the variations in initial density. The effect of initial density on the stress-strain relationship is apparent from Figure 10. In Figures 2 through 9 there are some instances in which there is an inconsistency in the relative positions of individual sets of data according to their void ratios. A probable explanation is the possible discrepancy between the observed and the true

initial density.

It can be shown that if the accuracy with which the average dimensions of the sample can be defined is ±0.02 inches (which is a reasonable assumption), then the computed void ratio can only be defined to an accuracy of ±0.015. Consequently, two reportedly identical initial void ratios may in fact vary by as much as 0.03 giving rise to a discrepancy in the stress-strain data. Other discrepancies such as the relative positions of the individual stress-strain curves may be partly explained on this basis.

Experimental Errors

The other experimental errors that can be expected to introduce some scatter of results are:

1. Experimental error in reading the cell pressure. A bourdon gage graduated to the nearest 1 lb. per sq. in. division was used to measure the cell pressure. Since the cell pressure was set at designated values, it is unlikely that the true cell pressure deviated from the observed by more than 0.2 lbs. per sq. in. This deviation would result in a scatter of points obtained during one test and would not be expected to contribute to the scatter between the tests of a series.

2. Temperature effects. One main disadvantage of the method used to measure volume change is the sensitivity of the device to temperature changes. Every effort was made to minimize temperature effects by making certain that the temperature of the cell fluid was the same as the air temperature; by minimizing the volume of air between the sample and the volume change measuring device; and by avoiding as much as possible, large variations in room temperature. To ensure no temperature effects, the

tests would have to have been performed in a temperature controlled room. However due to the relatively short duration of the test, (1.5 to 2 hours) the difference in air temperatures never exceeded more than 1 degree centigrade during any one test. This one degree variation would not be expected to bring about a corresponding change in the temperature of the air in the sample and the volume change device because it is a closed system with considerable insulation from the air surrounding it.

If a one degree (centigrade) change in temperature of the air in the closed system did occur, this could account for a change in volume of approximately 1 cubic centimeter which would constitute a variation in volumetric strain of less than 0.2 per cent. This is not considered to be of significant magnitude.

3. Membrane effects. Roscoe et al. (31) maintain that a significant portion of the observed volume change in triaxial specimens of sand is directly attributed to membrane penetration. Their analysis indicate that for sands having a mean diameter greater than 60 microns the volume change of the soil skeleton is entirely elastic and constitutes a small portion of the observed volume change. Their results and conclusions are subject to conjecture particularly the assumption of purely elastic behavior upon which the entire concept rests. Moreover, the results of tests conducted using relatively stiff membranes (plasticized polyvinyl chloride having a wall thickness of 0.055 inches) on the Chattahoochee sand by Clough (22) (precluding any significant membrane penetration), were of the same nature as those obtained by the author using thin rubber membranes. In conclusion, it is felt that one should be cognizant of the possibility of significant membrane effects particularly in specimens having a large

specific surface and being made up of medium or coarse, poorly graded sand. Further research would be required to establish quantitative corrections that could be applied to observed volume changes to take into account the membrane effect.

With the exception of the membrane effect, the experimental errors in the bulk modulus study have been of a random nature, if not on an individual test basis, then certainly on a test series basis. In view of this it would be expected that their effects were not cumulative. It would be desirable to express some limit of accuracy or degree of confidence regarding the observed test data. However, because of the interaction of the various factors affecting the results, this is not considered to be practical. It is felt that the plot of the test results for each series is a good indication of the reproducibility of results, at least in a qualitative sense.

Permanent and Recoverable Volume Change Components

As a matter of interest, the volume change during isotropic compression and during unloading is shown in Figure 11 for a loose and a dense specimen. The difference between the ordinates of the loading and the rebound curves represents the permanent volume change while the difference between the maximum volume change and the ordinates of the rebound curve represents the recoverable or elastic components of volume change. By inspection it can be seen that the dense sample exhibits less permanent volume change than does the loose specimen as was to be expected.

The magnitude of permanent versus recoverable volume change components, as well as the variation in their relative magnitudes with void

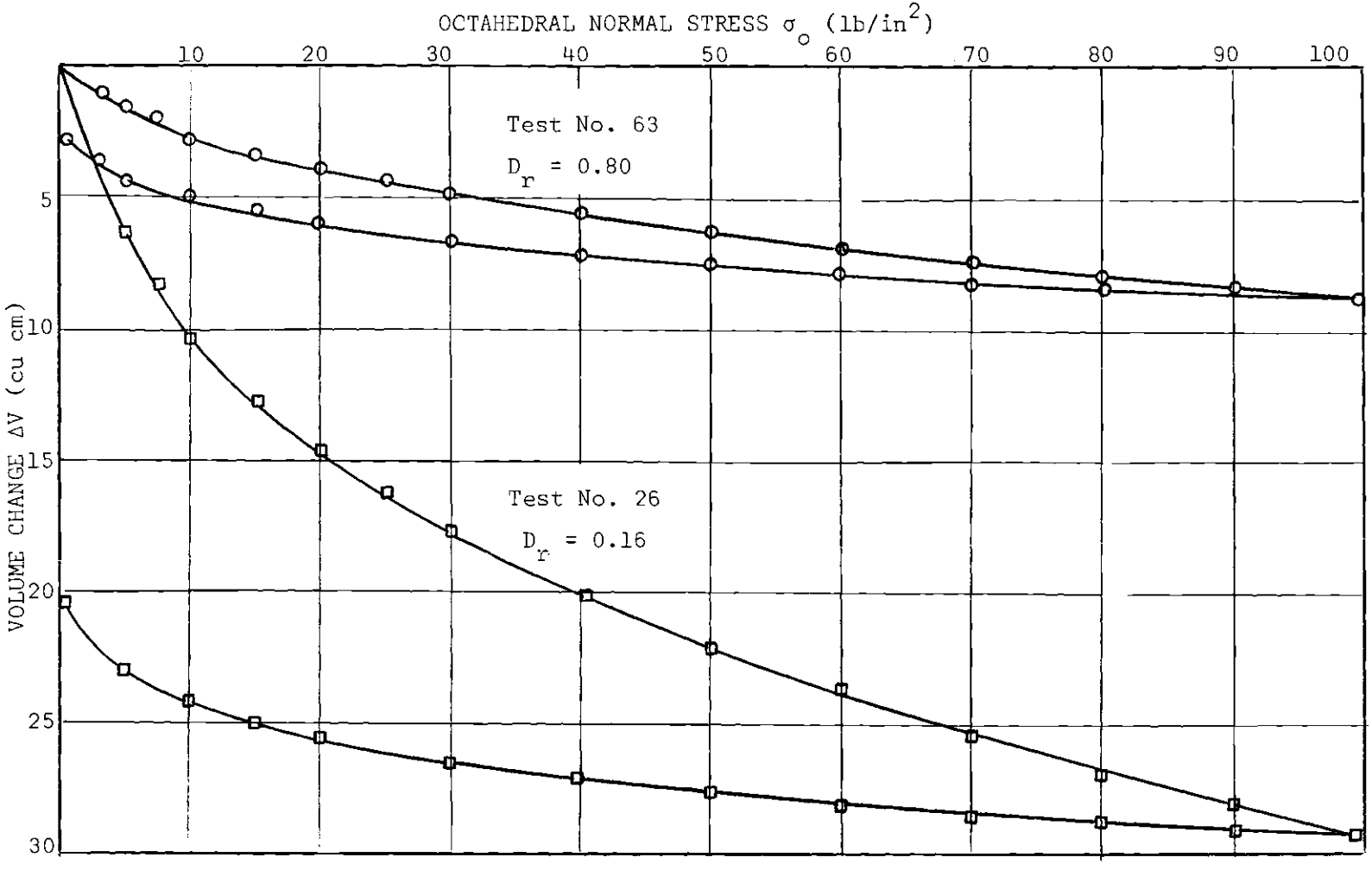

Figure 11. Variation in Volume Change with Octahedral Normal Stress for Loose and Dense Sand.

ratio as based on the entire test series, is shown in Figure 12. The permanent and recoverable portions are expressed as a per cent of the total volume change shown at the left and right hand margins respectively. From the figure it can be seen that there is an approximate linear relationship between the permanent (or recoverable) component of volume change and the relative density of the soil.

An extrapolation of the results would imply the following:

1. At zero relative density under isotropic compression, approximately 80 per cent of the volume change is of a permanent nature and approximately 20 per cent is elastic.

2. At 100 per cent relative density, under isotropic compression, approximately 25 per cent of the total volume change is of a permanent nature and 75 per cent is elastic.

3. Between the aforementioned limits, the magnitudes of the permanent and elastic portion vary linearly with the relative density.

The above statements refer only to the first loading and unloading of a soil. Under repeated loading the relative magnitude of the elastic component would progressively increase.

Bulk Modulus as a Function of the Octahedral Normal Stress

Of primary concern to the investigation was the variation of the bulk modulus with the octahedral normal stress and the initial density of the soil.

Considering first the variation of the bulk modulus with the octahedral normal stress, it is apparent from Figure 10 that the bulk modulus is an increasing function of the octahedral normal stress, since the volumetric strain is a decreasing function of the octahedral normal

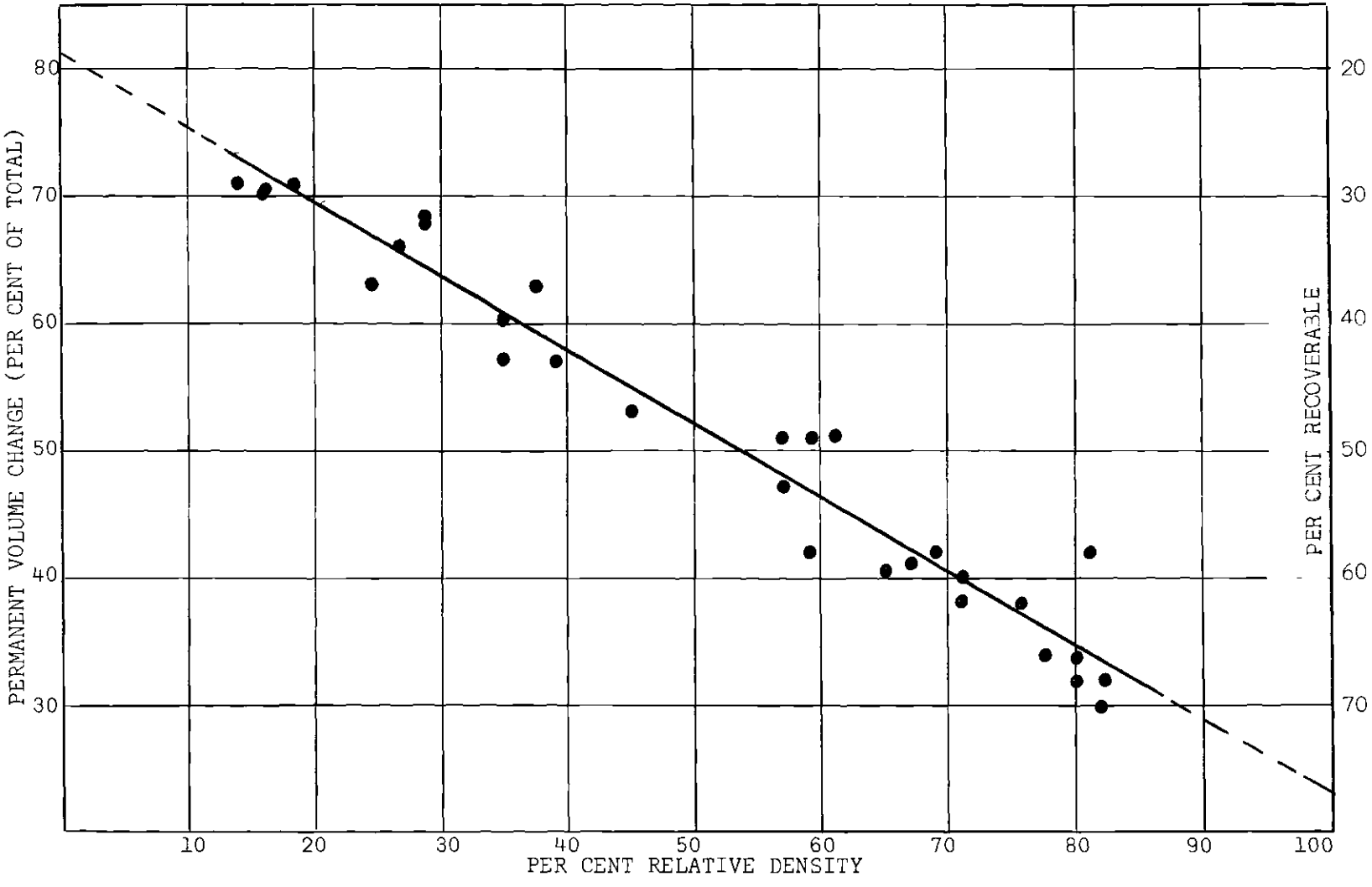

Figure 12. Separation of Total Volume Change into Permanent and Recoverable Components.

stress. An attempt was made to express the volumetric strain as a function of the octahedral normal stress using exponentials, hyperbolic functions, and polynomials of varying degrees. This proved to be unsuccessful primarily because of the difficulty of establishing a set of boundary conditions necessary to the solution of a differential equation. The form of expression suggested by Wilson and Sutton (23) and Jacobson (20) was found to be inapplicable over the range of hydrostatic stresses employed in the test series.

The slope of the stress-strain curve or bulk modulus and its variation with stress was of greater concern to the investigation that the stress-strain curve itself. To obtain an indication of the variation of the slope with stress, the bulk modulus was computed for small increments of stress over the entire stress range. The bulk modulus was then plotted as a function of the octahedral normal stress. One such typical plot is given in Figure 13. An examination of this plot indicated that, as a first approximation, the bulk modulus could be expressed as a linear function of the octahedral normal stress over a specific stress range. Two such functions would serve to relate the bulk modulus to the octahedral normal stress over the stress range investigated.

It should be pointed out that the scatter in this particular plot did not necessarily result from the scatter in the experimental data but was instead the result of not being able to precisely define the change in strain corresponding to a change in stress. The information was taken from a curve representing the average points of a test series.

To obtain the "best fit" straight lines for the eight test series, a linear regression analysis was performed on the test data using the

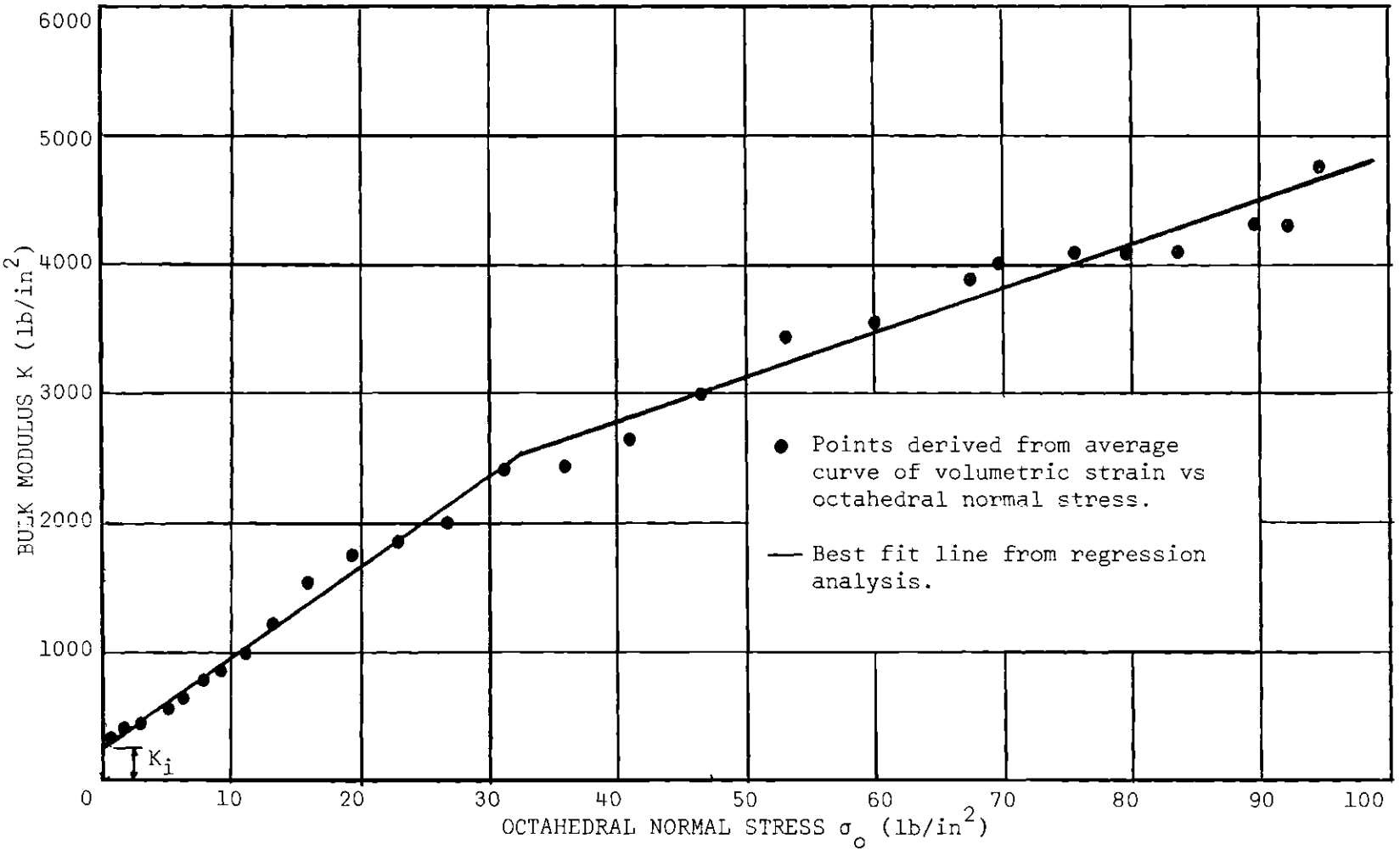

Figure 13. Relationship Between Bulk Modulus and Octahedral Normal Stress: D_r = 0.18.

B220 computer. Using this information an equation was written relating the bulk modulus and the octahedral normal stress. These equations are given in Table 2. Included in the table is statistical information from the regression analysis. The high correlation coefficient, and the level at which the relationship remained significant, is evidence of the validity of an assumed straight line relationship.

To assess the validity of these equations, they were integrated to yield an equation relating volumetric strain and octahedral normal stress. The constant of integration was evaluated by defining the conditions at the point of intersection of the two straight lines. The following illustrates the method used and the form of equation obtained for the data shown in Figure 13.

From the regression analysis the intercept and the slope of the two straight lines were respectively,

$$(259.84, \quad 68.82) \quad \text{and} \quad (1368.89, \quad 34.91)$$

Thus the equation relating bulk modulus $\frac{(d\sigma)}{(d\varepsilon)}$ and octahedral normal stress, written in parts is

$$K = \frac{d\sigma}{d\varepsilon} = 259.84 + 68.82\ \sigma_o \qquad \text{(III-1a)}$$

$$K = \frac{d\sigma}{d\varepsilon} = 1368.89 + 34.91\ \sigma_o \qquad \text{(III-1b)}$$

Equating these two equations yielded the common point of intersection $\sigma_o = 32.70$.

The observed strain at $\sigma_o = 32.70$ is .0316 as taken from the plot of average stress versus average strain for that particular series.

Table 2. Results from Regression Analysis of Bulk Modulus and Octahedral Normal Stress Data

D_r	Derived Equations	Limits of σ_o (psi)	Significance Level (%)	Correlation Coefficient
0.18	$K = 259.84 + 68.82\ \sigma_o$	0 - 32.7	.01	0.99
0.18	$K = 1368.89 + 34.91\ \sigma_o$	32.7 - 100	.01	0.97
0.29	$K = 330.05 + 69.10\ \sigma_o$	0 - 33.6	.01	1.00
0.29	$K = 1452.41 + 35.77\ \sigma_o$	33.6 - 100	.01	0.97
0.37	$K = 501.17 + 82.60\ \sigma_o$	0 - 32.7	.01	1.00
0.37	$K = 1928.47 + 38.94\ \sigma_o$	32.7 - 100	.01	0.99
0.45	$K = 553.36 + 90.99\ \sigma_o$	0 - 26.9	.01	0.99
0.45	$K = 1616.27 + 51.52\ \sigma_o$	26.9 - 100	.01	0.96
0.60	$K = 895.16 + 120.29\ \sigma_o$	0 - 20.1	.01	0.97
0.60	$K = 2135.78 + 58.54\ \sigma_o$	20.1 - 100	.01	0.99
0.68	$K = 955.52 + 154.59\ \sigma_o$	0 - 19.7	.01	0.98
0.68	$K = 2487.19 + 76.69\ \sigma_o$	19.7 - 100	.01	0.98
0.74	$K = 977.62 + 172.90\ \sigma_o$	0 - 18.2	.01	0.97
0.74	$K = 2342.47 + 98.10\ \sigma_o$	18.2 - 100	.01	0.97
0.82	$K = 1055.36 + 210.46\ \sigma_o$	0 - 18.6	.01	0.98
0.82	$K = 2899.39 + 101.68\ \sigma_o$	18.6 - 100	.01	0.99

Integrating the equations we obtain

$$\varepsilon = \frac{1}{68.82} \ln (259.84 + 68.82\, \sigma_o) + C_1 \quad (0 < \sigma_o < 32.7) \qquad \text{(III-2a)}$$

$$\varepsilon = \frac{1}{34.91} \ln (1368.89 + 34.91\, \sigma_o) + C_2 \quad (32.7 < \sigma_o < 100) \qquad \text{(III-2b)}$$

Evaluating the integration constant using the point in common yields

$$C_1 = -0.0821$$

$$C_2 = -0.1926$$

Thus the equation becomes

$$\varepsilon = \frac{1}{68.82} \ln (259.84 + 68.82\, \sigma_o) - 0.0821 \quad (0 < \sigma_o < 32.7) \qquad \text{(III-2c)}$$

$$\varepsilon = \frac{1}{34.91} \ln (1368.89 + 34.91\, \sigma_o) - 0.1926 \quad (32.7 < \sigma_o < 100) \qquad \text{(III-2d)}$$

These equations were then used to obtain an independent curve of volumetric strain versus octahedral normal stress and this curve was compared with the corresponding observed points. The results are shown by the upper curve of Figure 14, which indicates near perfect agreement between the observed points and the expression relating them.

The process was repeated for the other series. The resulting equations are given in Table 3. A comparison of the "best fit" curve having a mathematical basis, and the observed points is given for the entire series, in Figure 14. The validity of the mathematical expression is apparent.

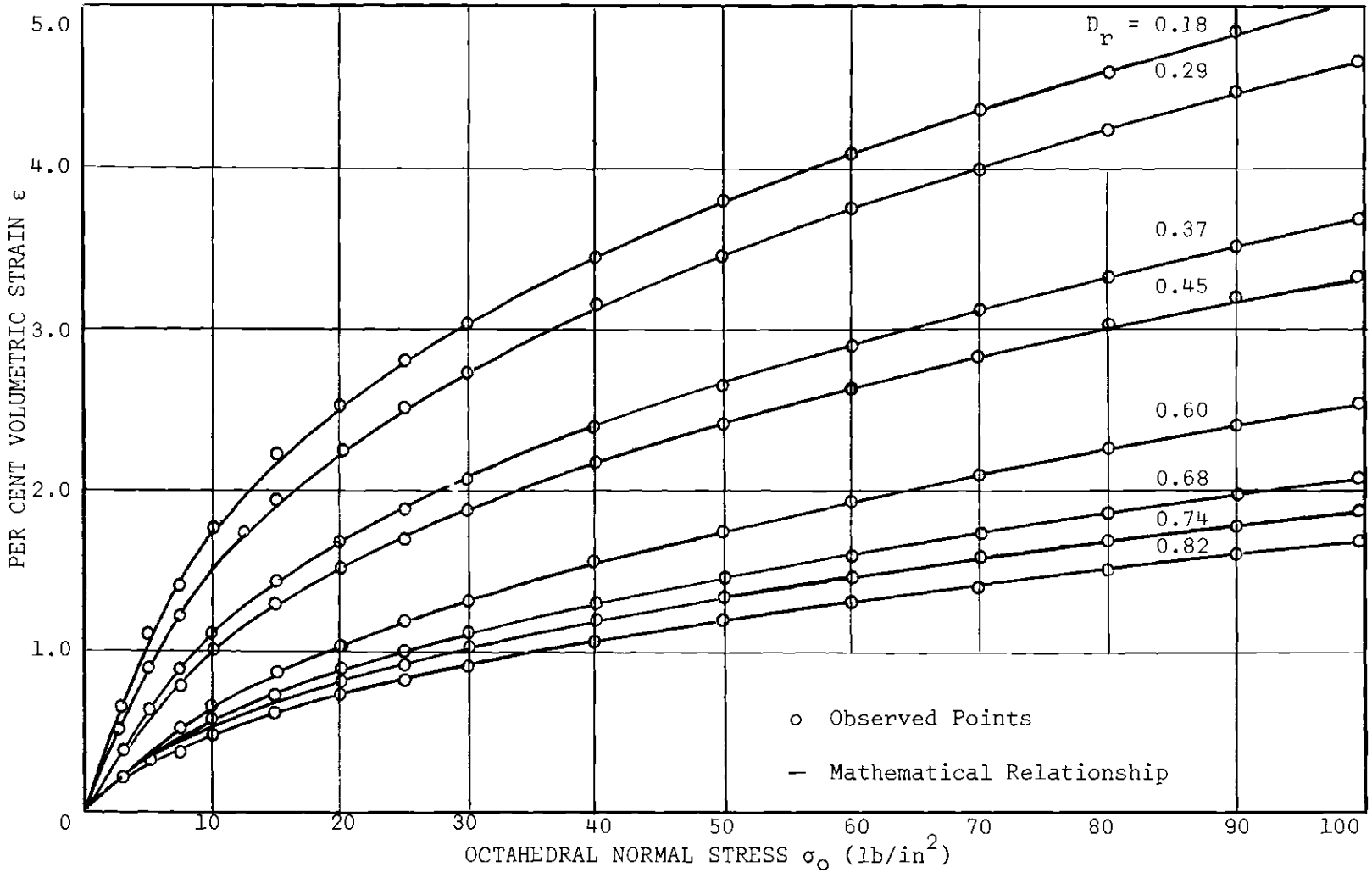

Figure 14. A Comparison of Observed Stress-Strain Data and the Mathematical Stress-Strain Relationship.

Table 3. Equations Relating Volumetric Strain and Octahedral Normal Stress

D_r	Derived Equation	Limits of σ_o (psi)
0.18	$\varepsilon = \frac{1}{68.82} \ln (259.84 + 68.82\,\sigma_o) - 0.0821$	0 - 32.7
0.18	$\varepsilon = \frac{1}{34.91} \ln (1368.89 + 34.91\,\sigma_o) - 0.1926$	32.7 - 100
0.29	$\varepsilon = \frac{1}{69.10} \ln (333.05 + 69.10\,\sigma_o) - 0.0854$	0 - 33.6
0.29	$\varepsilon = \frac{1}{35.77} \ln (1452.41 + 35.77\,\sigma_o) - 0.1915$	33.6 - 100
0.37	$\varepsilon = \frac{1}{82.60} \ln (501.17 + 82.60\,\sigma_o) - 0.0761$	0 - 32.7
0.37	$\varepsilon = \frac{1}{38.94} \ln (1428.47 + 38.94\,\sigma_o) - 0.1856$	32.7 - 100
0.45	$\varepsilon = \frac{1}{90.99} \ln (553.36 + 90.99\,\sigma_o) - 0.0702$	0 - 26.93
0.45	$\varepsilon = \frac{1}{51.52} \ln (1616.27 + 51.52\,\sigma_o) - 0.1378$	26.93 - 100
0.60	$\varepsilon = \frac{1}{120.29} \ln (895.16 + 120.29\,\sigma_o) - 0.0570$	0 - 20.1
0.60	$\varepsilon = \frac{1}{58.54} \ln (2135.78 + 58.54\,\sigma_o) - 0.1282$	20.1 - 100
0.68	$\varepsilon = \frac{1}{154.59} \ln (955.52 + 154.59\,\sigma_o) - 0.0448$	0 - 19.7
0.68	$\varepsilon = \frac{1}{76.69} \ln (2487.19 + 76.69\,\sigma_o) - 0.0995$	19.7 - 100
0.74	$\varepsilon = \frac{1}{172.90} \ln (977.62 + 172.90\,\sigma_o) - 0.0404$	0 - 18.2
0.74	$\varepsilon = \frac{1}{98.10} \ln (2342.47 + 98.10\,\sigma_o) - 0.0772$	18.2 - 100
0.82	$\varepsilon = \frac{1}{210.46} \ln (1055.36 + 210.46\,\sigma_o) - 0.0335$	0 - 18.6
0.82	$\varepsilon = \frac{1}{101.16} \ln (2899.39 + 101.16\,\sigma_o) - 0.0768$	18.6 - 100

Thus it has been demonstrated that for a specific initial density, the bulk modulus of the Chattahoochee River sand can be mathematically related to the octahedral normal stress. It would be desirable to develop a general expression which would include the influence of initial density as well. The feasibility of doing this will be examined in the next section.

Bulk Modulus as a Function of the Octahedral Normal Stress and the Initial Density of the Soil

To study the effects of initial density on the bulk modulus, a plot was made up of the bulk modulus versus octahedral normal stress relationships for the entire series (Figure 15). An examination of this plot indicates the existence of a definite interrelationship between the bulk modulus, the initial density and the octahedral normal stress. The parameters which would define such a relationship are:

1. The bulk modulus intercept (K_i)
2. The rate of change in bulk modulus $(\frac{dK}{d\sigma_o})$
3. The points of intersection of the two straight lines common to one relative density.

Thus a single equation expressing bulk modulus as a function of initial density and octahedral normal stress would have to be developed as a partial differential equation involving two independent variables and a set of parameters that are functions of the independent variables. The complexity of the problem would suggest a graphical method of solution in place of an analytical solution at this stage.

Since the parameters (intercept, rates of change in bulk modulus, and points of intersection) may be considered to be parameters of the soil

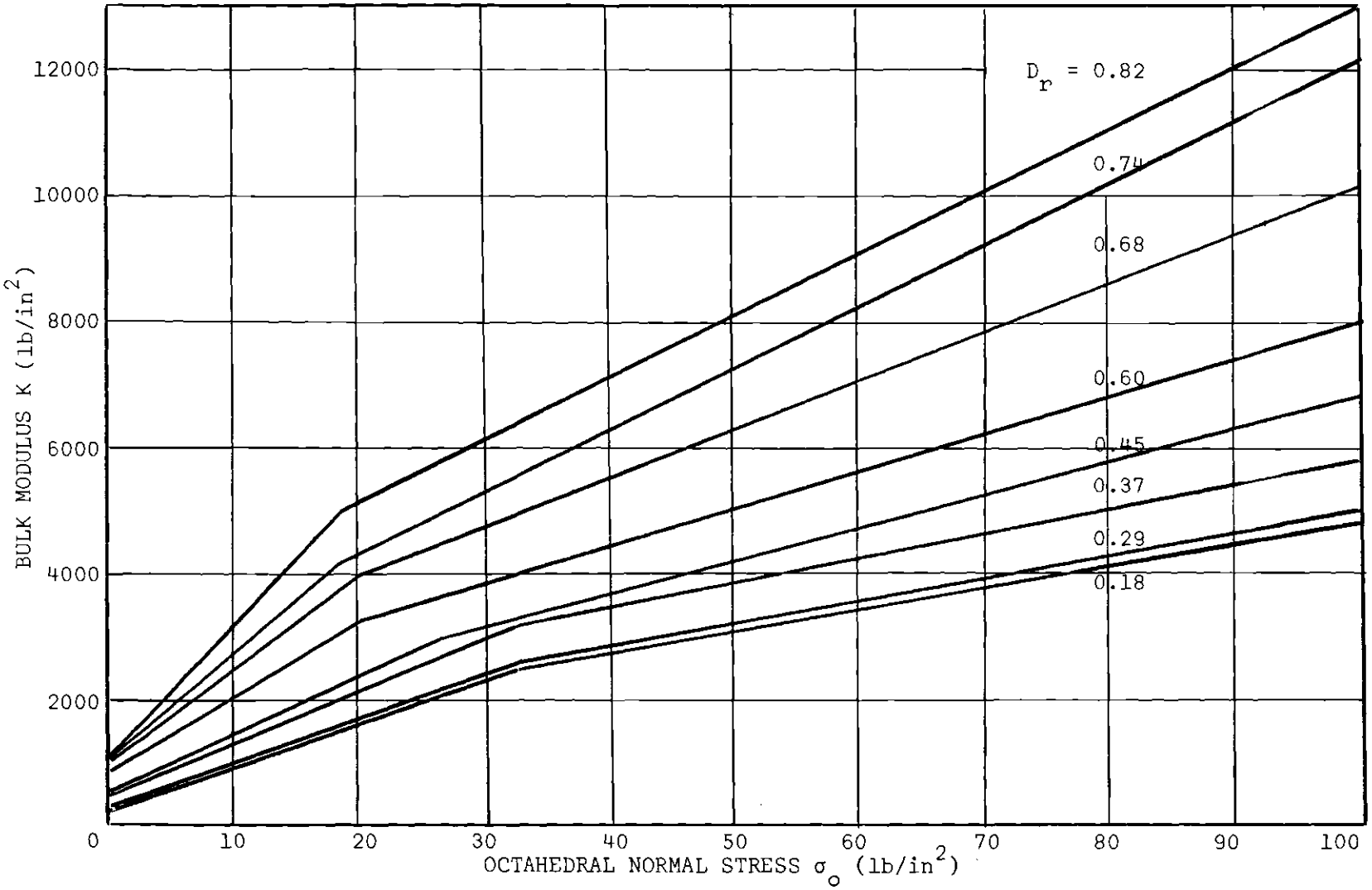

Figure 15. Variation in Bulk Modulus with Relative Density and Octahedral Normal Stress.

(as they reflect or depend upon certain physical properties of the soil) they may be expected to exhibit a definite relationship with one or both of the dependent variables. To ascertain the degree of randomness and existence of a relationship, a plot was made of each of the parameters as a function of initial relative density. The results are depicted in Figure 16 and will be discussed separately.

Bulk Modulus Intercept

The bulk modulus intercept K_i is a function of the initial density of the soil (octahedral normal stress = 0) and it would appear that it bears a straight-line relationship to the initial relative density. The slope of the best fit line was determined by the method of least squares.

Rate of Change in Bulk Modulus

For a specified stress range and a given density, the rate of change in bulk modulus is a constant. The rate of change however is a function of the initial density. As can be seen by the two curves relating the rate of change in bulk modulus and the initial density, the relationship is not a simple function.

Point of Intersection

The point of intersection is intuitively a function of both dependent variables. The relationship may be approximated by a straight line as indicated in Figure 16.

The difficulty of obtaining a general expression relating the bulk modulus, initial relative density, and octahedral normal stress is apparent when one considers the parameters, and their relation to the independent variables. The nature of the relationship may be indicated by the following expressions:

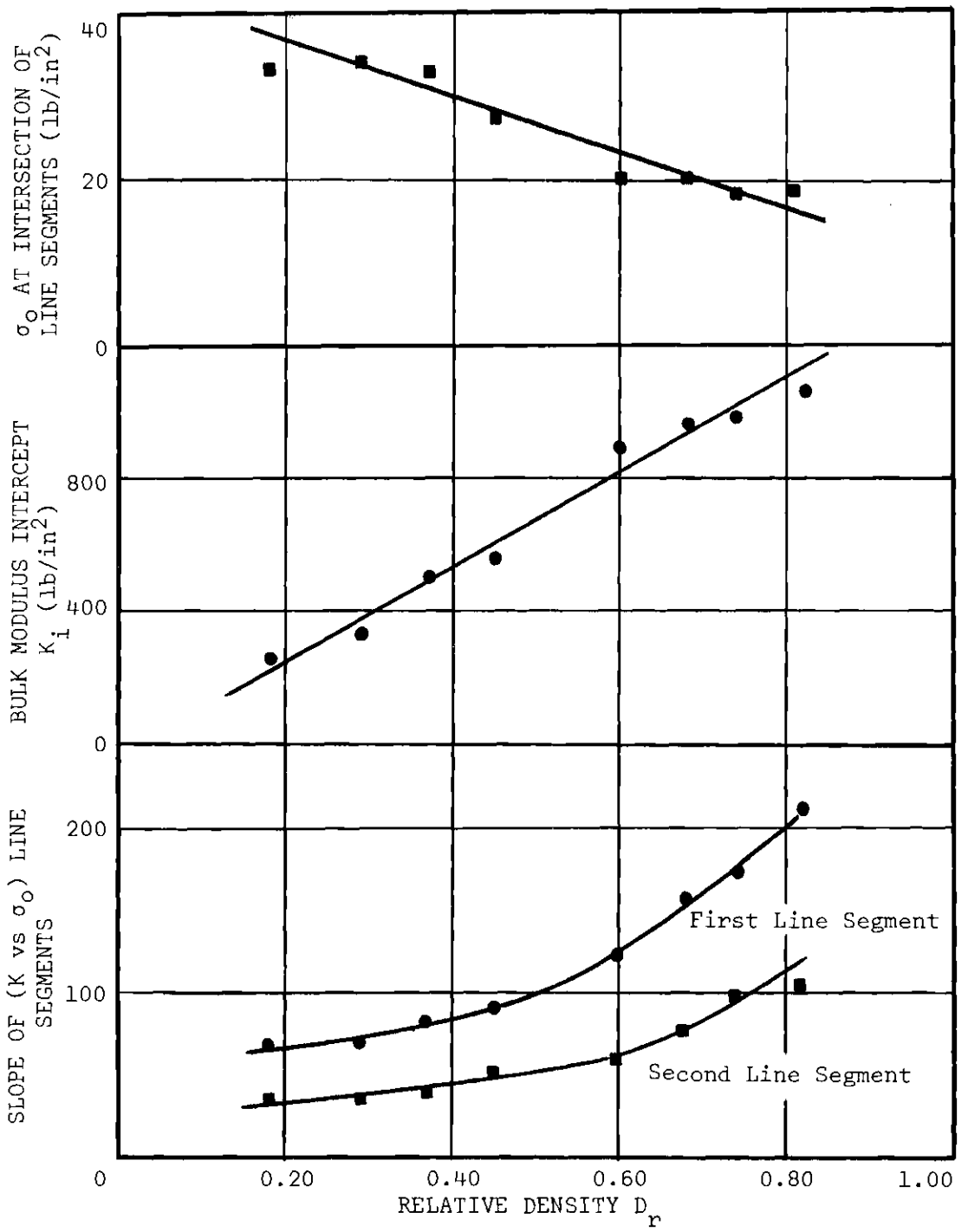

Figure 16. Parameters for Solution of Bulk Modulus.

$$K = A + B\,\sigma_o \qquad 0 < \sigma_o < C \qquad \text{(III-7a)}$$

$$K = D + E\,\sigma_o \qquad C < \sigma_o < 100 \qquad \text{(III-7b)}$$

$$A,\ D,\ = f(e_o)$$

$$B,\ E,\ = g(C,\ e_o)$$

$$C\ = h(\sigma_o,\ e_o)$$

Thus using equations III-7a and III-7b along with the relationships indicated in Figure 14, the bulk modulus may be obtained for any specified initial density and octahedral normal stress.

A graphical solution was obtained using the relationships obtained for these parameters (Figure 16) and using relative densities ranging from 0.10 to 0.90 in increments of 0.10. The solution is shown in Figure 17. This figure differs from Figure 15 in that there has been a "smoothing out" of the parameters. In this respect, it may be considered to be somewhat idealized. In any event the difference between the idealized values and the experimentally observed values is less than one per cent.

Figure 17 permits the direct determination of the bulk modulus of sand for relative densities ranging from 10 to 90 per cent and for octahedral normal stress ranging from 0 to 100 lbs. per sq. in.

Conclusions

On the basis of the preceding outline of results the following pertinent conclusions may be cited regarding the bulk modulus of the Chattahoochee river sand, as based on triaxial, isotropic compression tests.

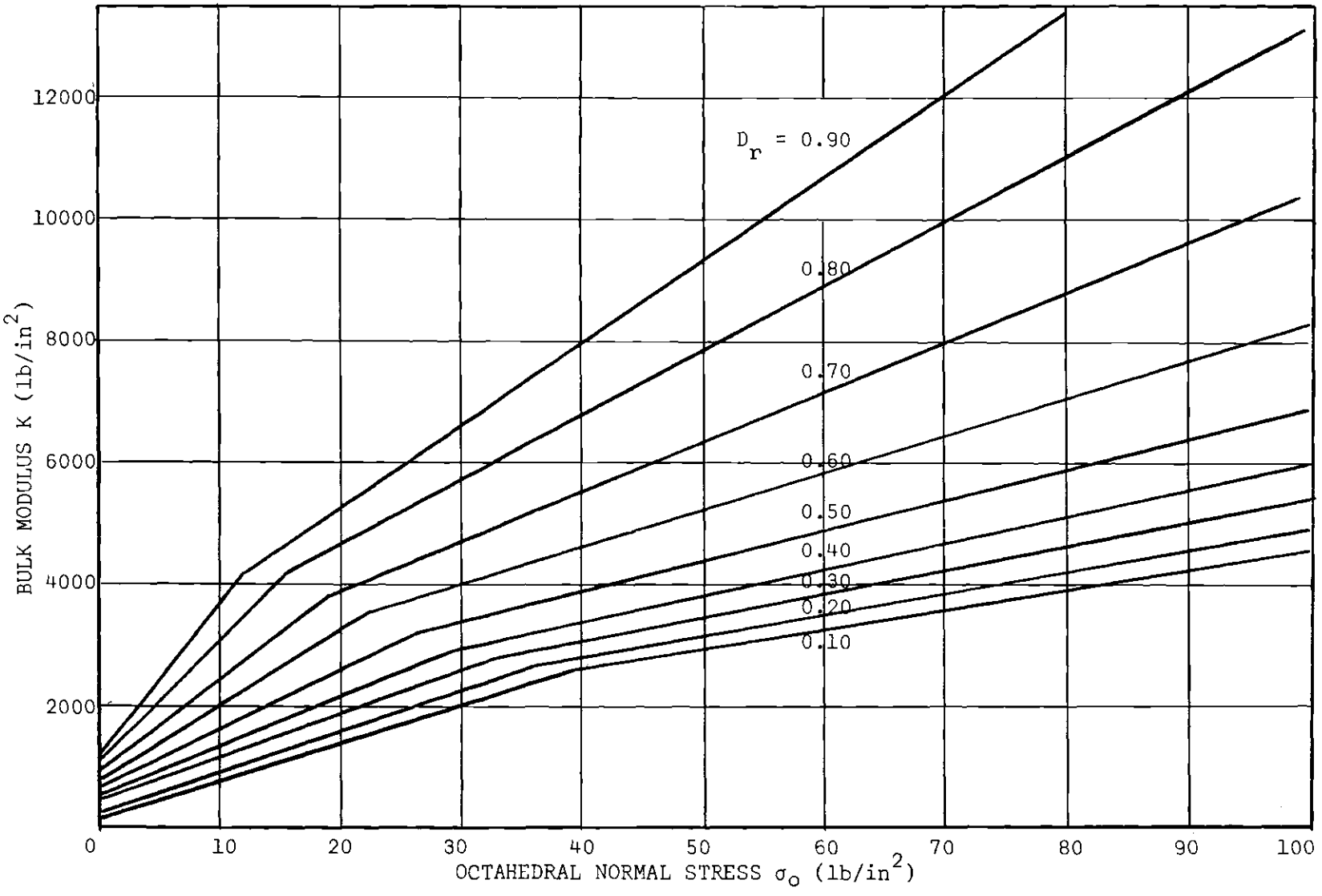

Figure 17. Idealized Bulk Modulus-Relative Density-Octahedral Normal Stress Relationship.

1. The bulk modulus is a function of the initial density of the soil, and the magnitude of effective normal stress to which it is subjected.

2. For a given initial density the relationship between the bulk modulus and the octahedral normal stress can be approximated by a straight line over a limited stress range.

3. The stress-strain relationship for the isotropic compression of the sand can be expressed by a mathematical equation of the form

$$\varepsilon = \frac{1}{m} \ln (A + m \sigma_o) + D$$

in which:

m, A, B = constants which are functions of the soil and the stress level.

4. A mathematical expression for the bulk modulus in terms of the initial density and the octahedral normal stress would have to incorporate 4 parameters, three of which are functions of the initial density only and the fourth a function of both the initial density and the octahedral normal stress.

5. The solution for the bulk modulus as a function of initial density and octahedral normal stress can be readily expressed in graphical form.

CHAPTER IV

EXPERIMENTAL INVESTIGATION OF THE SHEAR MODULUS

Laboratory Method of Determining the Shear Modulus

As mentioned previously the shear modulus of soil may be determined by any one of the following methods:

1. Torsion tests
2. Pure shear tests
3. Wave propagation
4. Constant octahedral triaxial compression tests

The author chose the fourth method for determining the shear modulus for the following reasons:

1. The triaxial cell is widely used in the determination of soil properties and may be considered to be standard laboratory equipment. The alternative methods required more elaborate equipment not readily available in most soil mechanics laboratories.

2. The triaxial cell method better simulates the mechanics of the behavior of a soil under a loaded area than do the other methods. That is, the triaxial test constitutes a special case of a three dimensional axially symmetrical problem.

3. It is readily divisible into the octahedral and deviatoric components of stress which is the basis for this particular investigation.

The equations necessary for the determination of the shear modulus from a constant octahedral triaxial compression test are as follows:

$$G = \frac{\tau_o}{\gamma_o} \qquad \text{(IV-1)}$$

In terms of principal stresses σ_1, σ_2, σ_3,

$$\tau_o = \frac{1}{3}\sqrt{(\sigma_1 - \sigma_2)^2 + (\sigma_2 - \sigma_3)^2 + (\sigma_1 - \sigma_3)^2} \qquad \text{(IV-2a)}$$

For the triaxial compression test in which $\sigma_2 = \sigma_3$, the equation reduces to

$$\tau_o = \frac{\sqrt{2}}{3}(\sigma_1 - \sigma_3) \qquad \text{(IV-2b)}$$

Similarly, in terms of principal unit strains ε_1, ε_2, ε_3,

$$\gamma_o = \frac{2}{3}\sqrt{(\varepsilon_1 - \varepsilon_2)^2 + (\varepsilon_2 - \varepsilon_3)^2 + (\varepsilon_1 - \varepsilon_3)^2} \qquad \text{(IV-3a)}$$

which for the triaxial compression test reduces to

$$\gamma_o = \frac{2\sqrt{2}}{3}(\varepsilon_1 - \varepsilon_3) \qquad \text{(IV-3b)}$$

Assuming the soil to be isotropic, the stress and strain tensors are coaxial and the equation for the shear modulus may be written

$$G = \frac{1}{2}\,\frac{(\sigma_1 - \sigma_3)}{(\varepsilon_1 - \varepsilon_3)} \qquad \text{(IV-4)}$$

For the test in question

$$\varepsilon_1 = \frac{\Delta L}{L_c} \qquad \text{(IV-5)}$$

in which: ΔL = change in length of the test specimens

L_c = length of the test specimen just prior to shear

$$\epsilon_3 = \frac{\Delta d}{d_c} \qquad \text{(IV-6a)}$$

in which Δd = change in the diameter of the test specimen

d_c = diameter of the sample just prior to shear

The change in diameter may be determined by physical measurements or may be computed from the following equation, the derivation of which is included in the Appendix:

$$\epsilon_3 = -\sqrt{\frac{1 - \frac{\Delta V}{V_c}}{1 - \frac{\Delta h}{h_c}}} - 1 \qquad \text{(IV-6b)}$$

Equation (IV-6b) will be used in the analysis and the test results will be presented in terms of octahedral shear stresses and strains.

Scope of the Investigation

Intuitively, the variables affecting the shear modulus are, density of the soil, octahedral normal stress, and the octahedral shear stress. To ascertain the influence of each, it was decided to perform a series of constant octahedral triaxial compression tests varying the initial density and the octahedral shearing stress. A test series consisted of three tests performed at each of four different densities at a constant octahedral normal stress. Six such series were conducted at constant octahedral normal stresses of 100, 80, 60, 40, 20 and 10 lbs per sq. in. Thus 72 tests were performed to determine the shear modulus under varying

conditions of octahedral normal stress, octahedral shear, and initial density.

Materials and Test Apparatus

Chattahoochee river sand was used in these tests and was taken from the same batch as that used for the isotropic compression tests. The sand was in an air-dry state and was tested under drained conditions.

A 2.8 inch standard triaxial cell was used for the tests. The loading apparatus consisted of a hydraulic ram activated by compressed air. The advantage of this loading system was that it was stress controlled with no manual adjustment required while the sample was undergoing deformation. Also it lent itself to incremental loading which was necessary for reasons explained in the test procedure. Two hydraulic rams having different capacities were used. A small bore ram was used for the tests conducted at low octahedral normal stresses while the larger capacity ram was used for the tests conducted at the higher octahedral normal stresses. This provided consistency in the accuracy with which the major principal stress could be controlled. The calibration chart for the hydraulic rams is included in the Appendix.

The volume change apparatus previously described was used for measuring volume changes and a dial extensometer was used for measuring axial deformation.

The end platens were polished and sprayed with Teflon to minimize end restraint. A schematic of the test apparatus is shown in Figure 18.

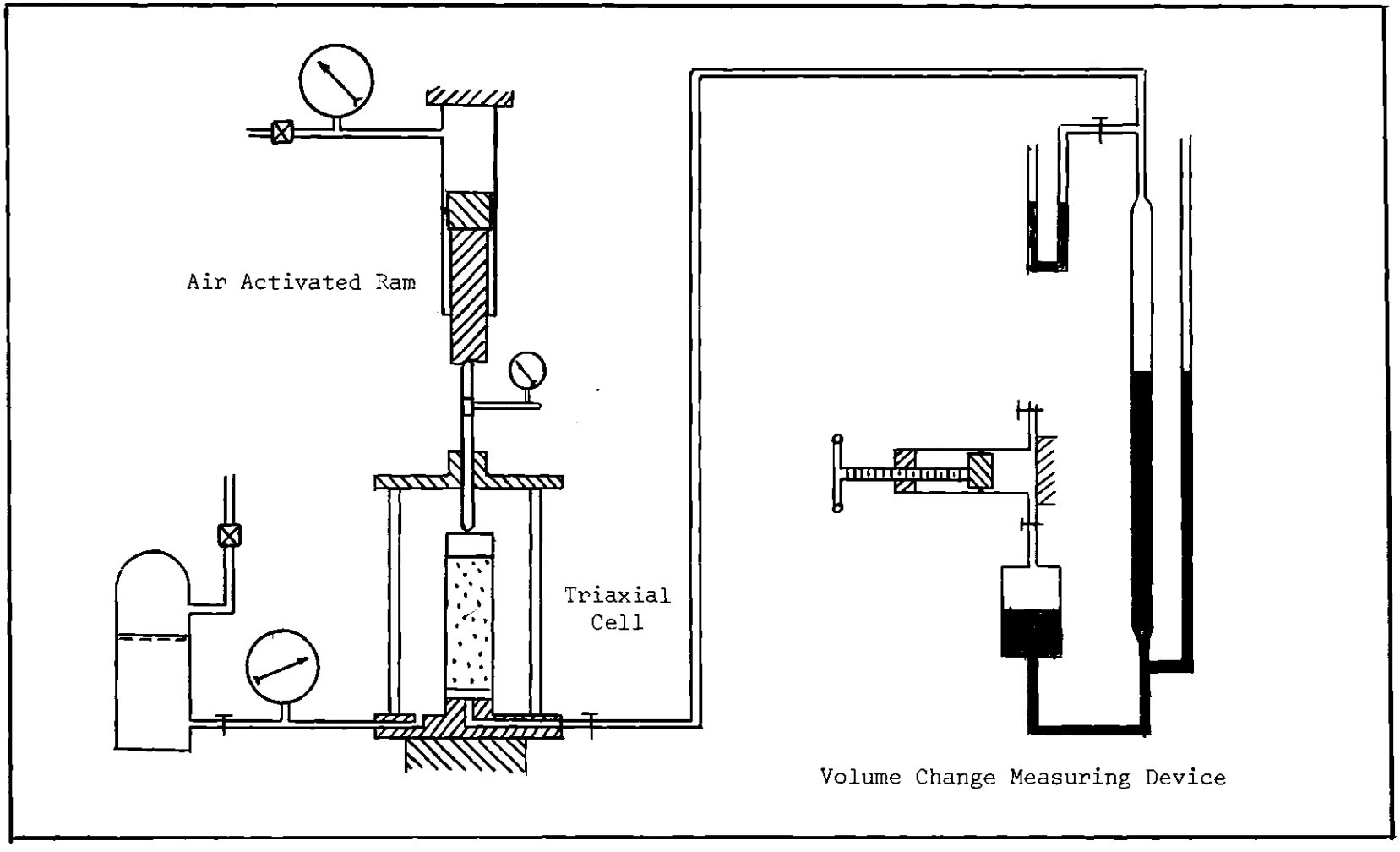

Figure 18. Schematic of Apparatus Used in Shear Modulus Study.

Test Procedure

Sample Preparation

The samples were formed in a manner identical to that described in the bulk modulus study. An attempt was made to obtain the loosest possible state of density, a very dense state, and two intermediate states of density. Triplicate specimens were formed in an effort to obtain at least a duplication of density within plus or minus 0.02 lbs per cu. ft.

Test Technique

After the specimen was formed, its dimensions obtained, and the cell assembled, the cell pressure was brought up to the desired value of the octahedral normal stress. During this phase, the volume change and axial deformation were measured to enable the redefinition of the initial conditions of the sample for the shear tests.

After equilibrium of the isotropic compression had been attained, the sample was tested to failure in small load increments. The cell pressure was lowered and the axial load was increased almost simultaneously so as to maintain a constant octahedral normal stress. Because of symmetry a reduction in cell pressure of a given magnitude, required an increase in σ_1 by twice the given decrement. All pressure decrements varied from 0.5 lbs. per sq. in. in the case of the low octahedral normal stresses to 2.0 lbs. per sq. in. for the high octahedral normal stresses.

To determine the axial load increment required to maintain a constant mean normal stress, the cross sectional area of the sample corresponding to that stress had to be estimated. This was done by calculating and recording the change in cross sectional area as the test progressed and using this as a guide to predicting the area for the next load increment.

The predicted and the actual cross-sectional areas were almost in perfect agreement until failure was imminent. It is noteworthy that failure developed rapidly, and was characterized by bulging followed by a shear failure surface. The bulging and development of the failure surface generally took place in the last 2 or 3 load increments. Up to that point there was no visual evidence of bulging. Thus end restraint was only appreciable when failure was occurring, and the assumption that the specimen remained a cylindrical during deformation was valid.

Discussion of Test Results

The results of the constant octahedral triaxial compression tests are tabulated in the Appendix (Table 5), and are represented in Figures 19 through 28 in the form of a plot of octahedral shear stress versus octahedral shear strain. This particular form of presentation was used since it will later be used for determining the shear modulus, and all parameters will be related to octahedral stress and strain components. Each figure depicts the results of a series of tests conducted at a constant octahedral normal stress, and at varying initial densities* of the soil. Some series encompassed four different densities while others encompassed only three. This is because the isotropic compression governed to a great extent, the possible initial density range. Under high isotropic compressive stresses, the possible range of initial densities was relatively small and hence only 3 significantly different densities were obtained. The results of the three tests conducted at approximately the same density were plotted

---

*Initial density refers to the density of the soil after isotropic compression and just prior to the beginning of the shear test, and will be denoted by the subscript c.

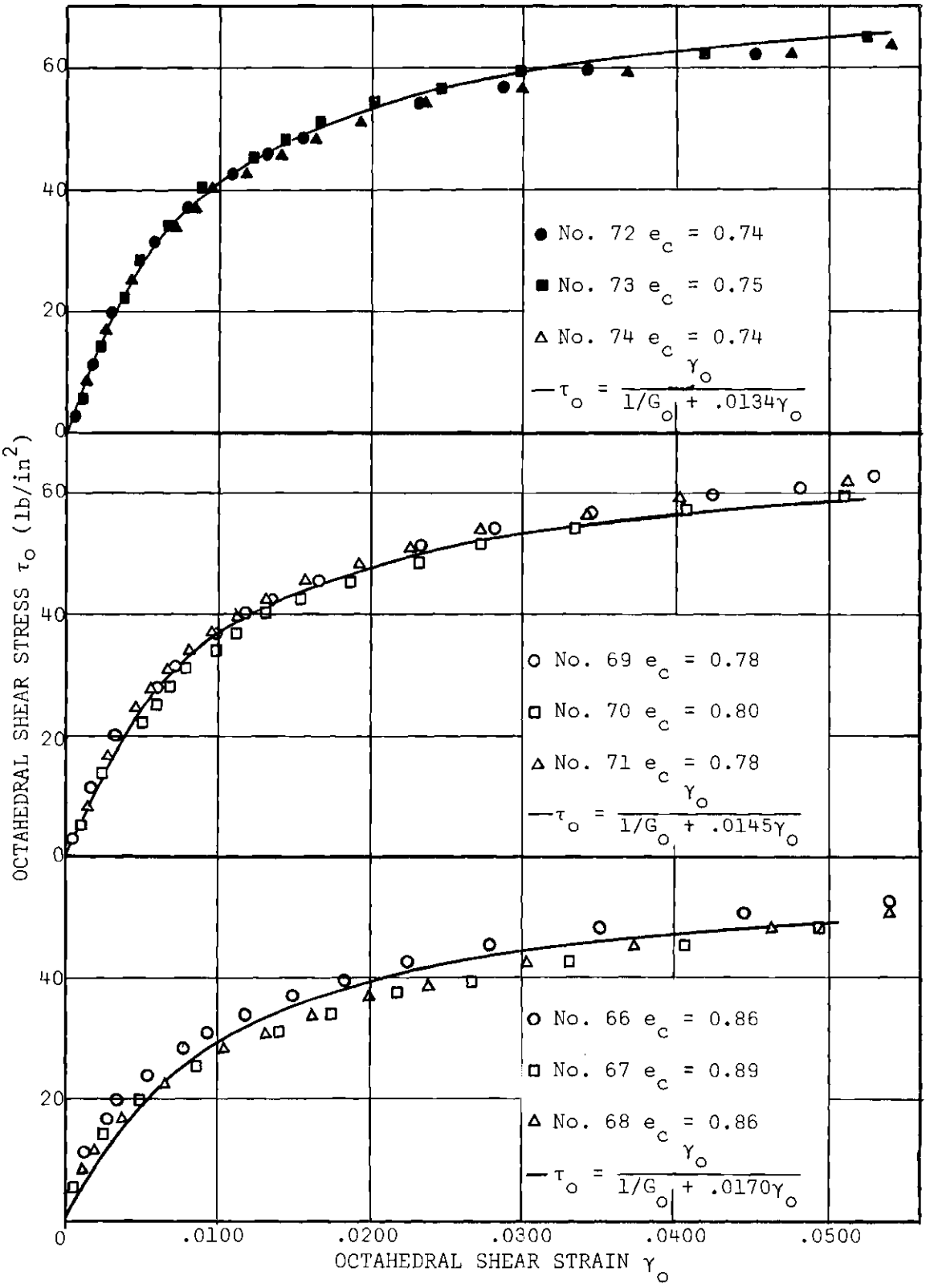

Figure 19. Stress-Strain Relationship for Constant σ_o = 100 lb/in^2.

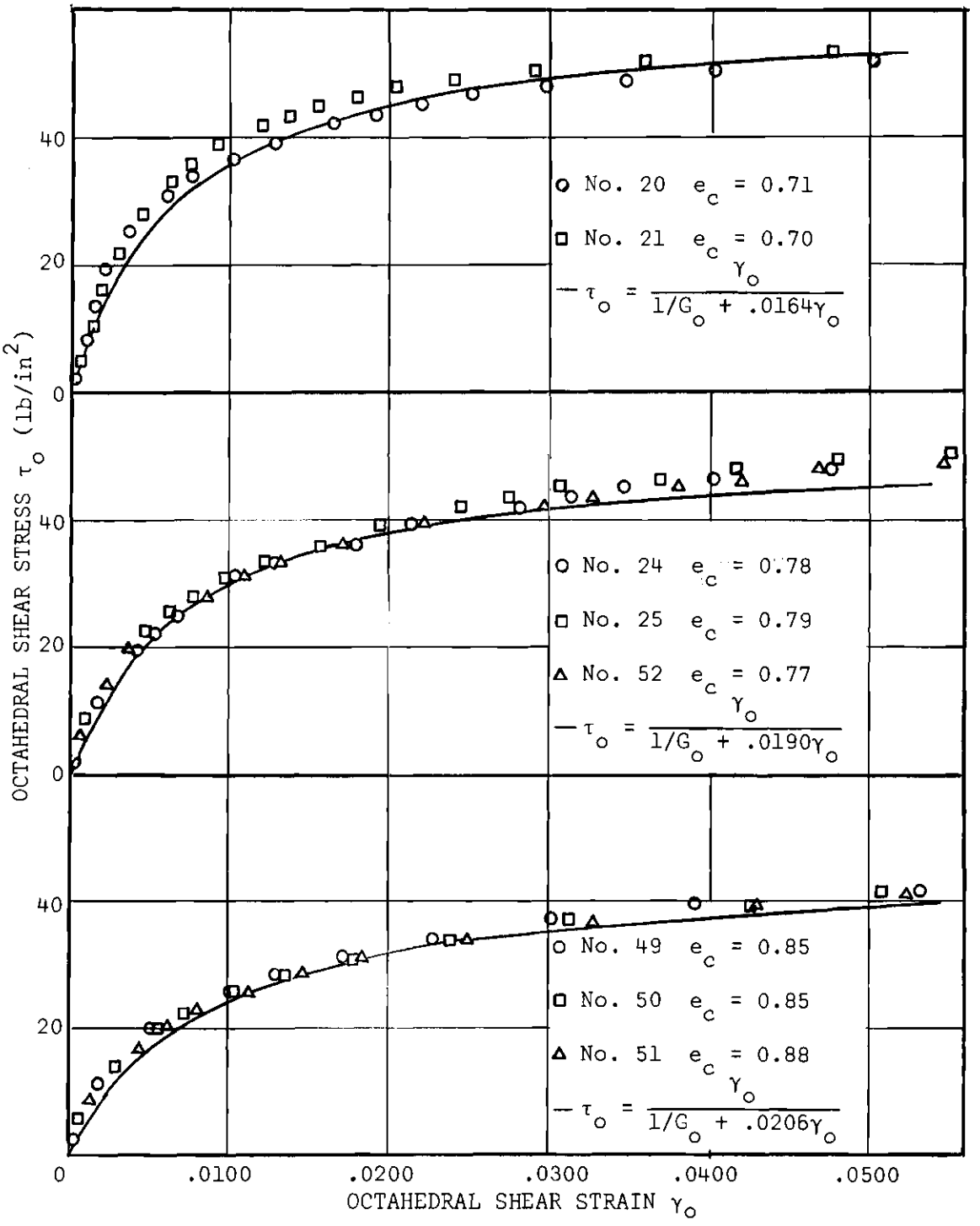

Figure 20. Stress-Strain Relationship for Constant σ_o = 80 lb/in^2.

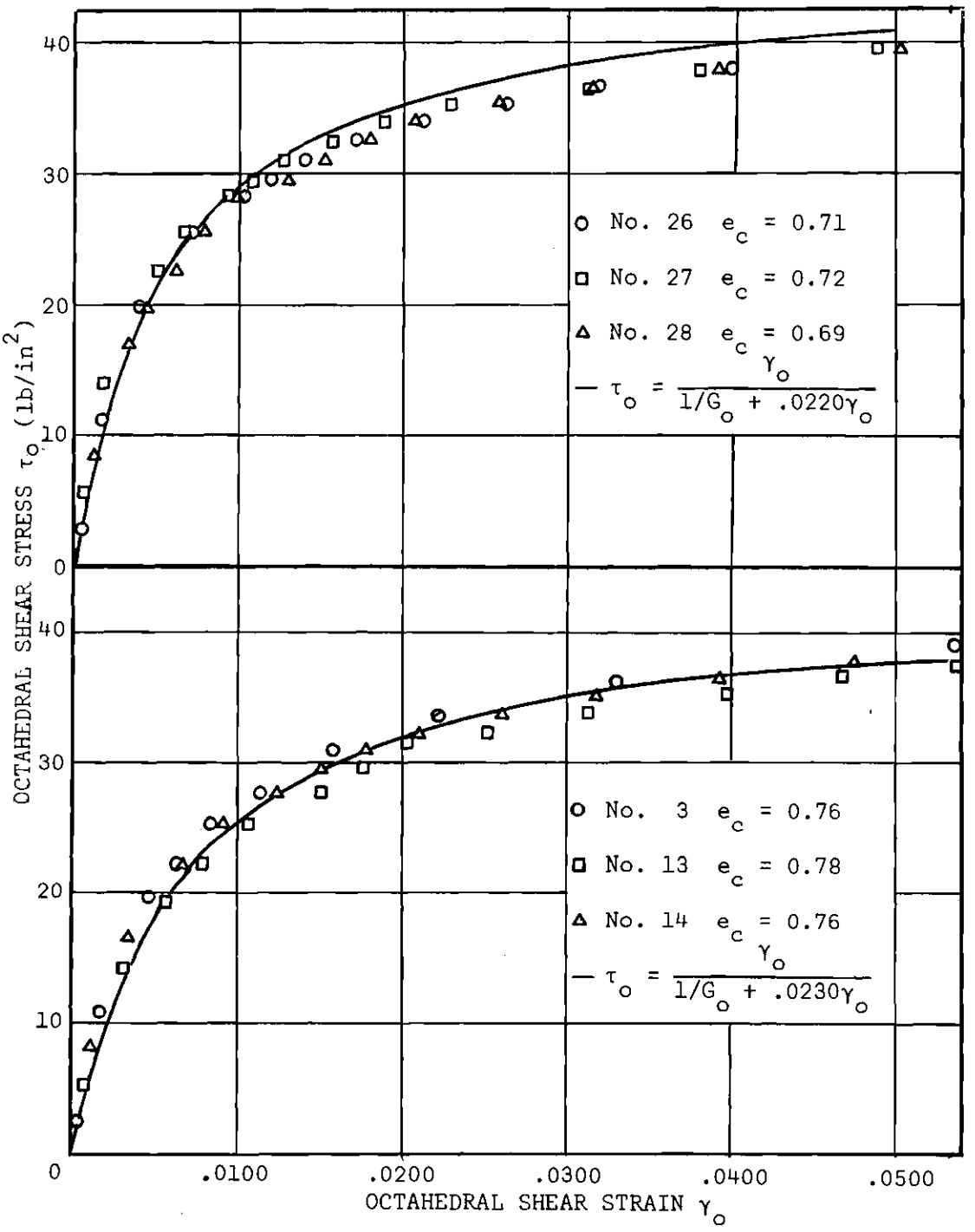

Figure 21. Stress-Strain Relationship for Constant σ_o = 60 lb/in^2.

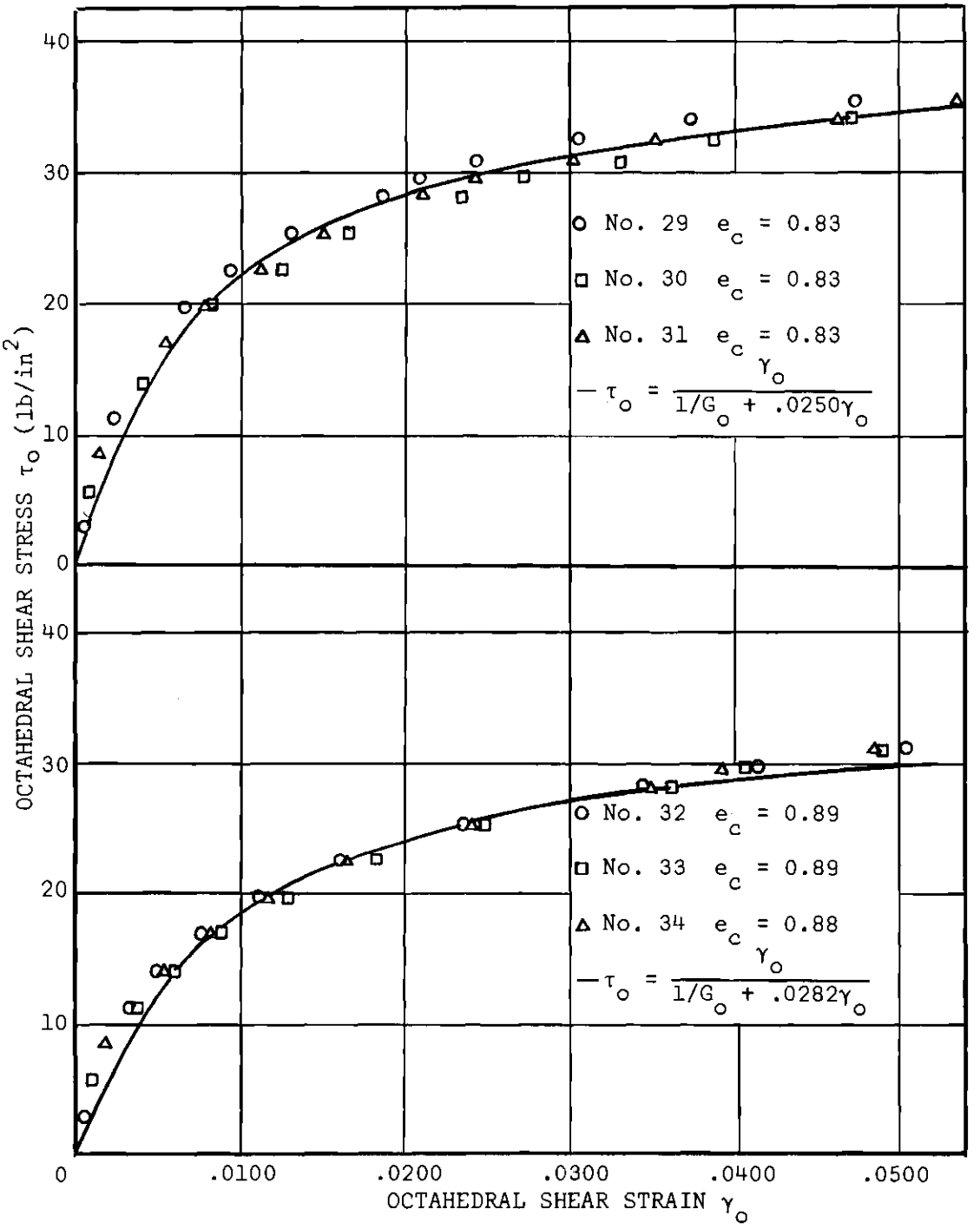

Figure 22. Stress-Strain Relationship for Constant σ_o = 60 lb/in^2.

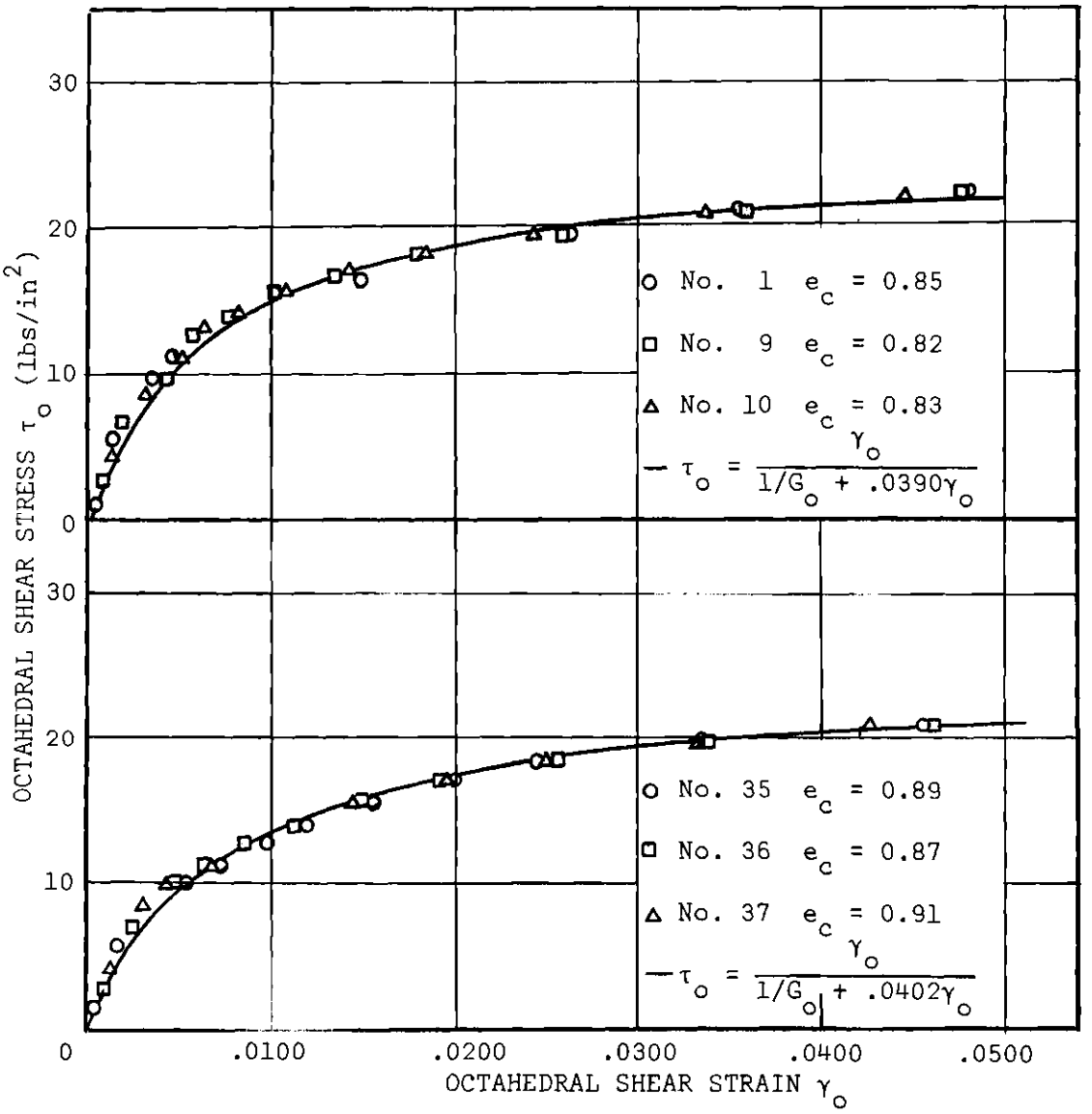

Figure 23. Stress-Strain Relationship for Constant σ_o = 40 lb/in^2.

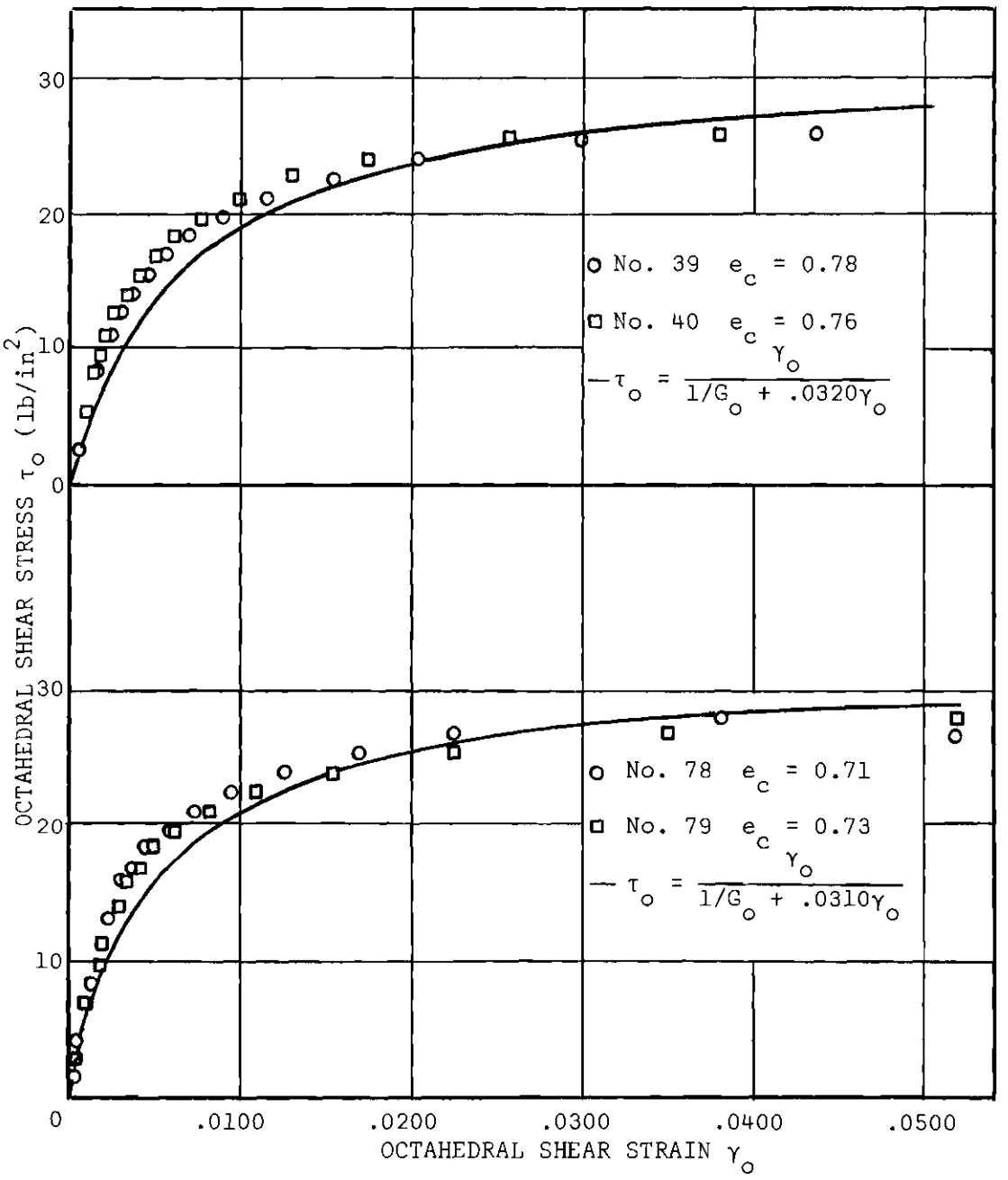

Figure 24. Stress-Strain Relationship for Constant σ_o = 40 lb/in^2.

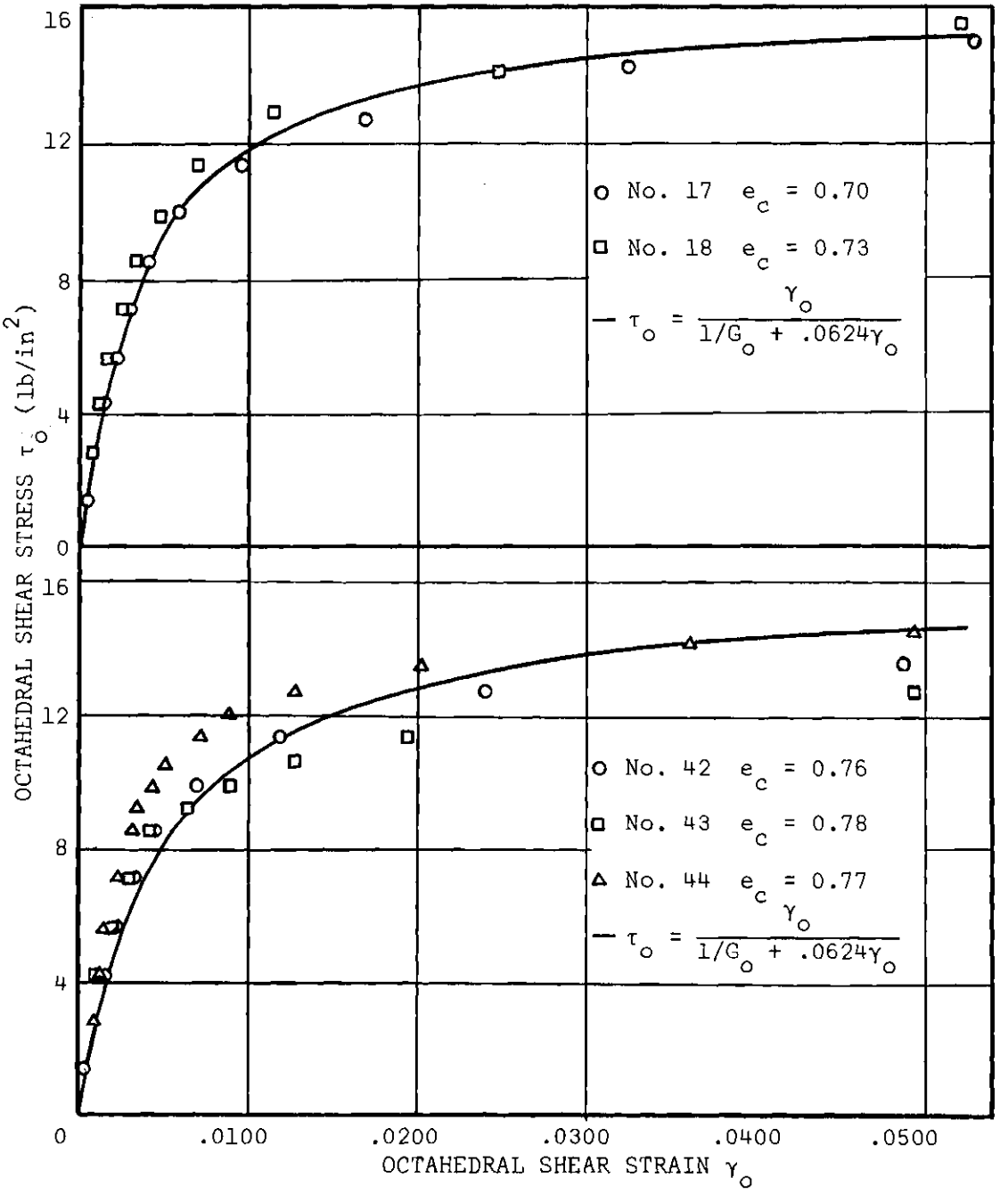

Figure 25. Stress-Strain Relationship for Constant σ_o = 20 lb/in^2.

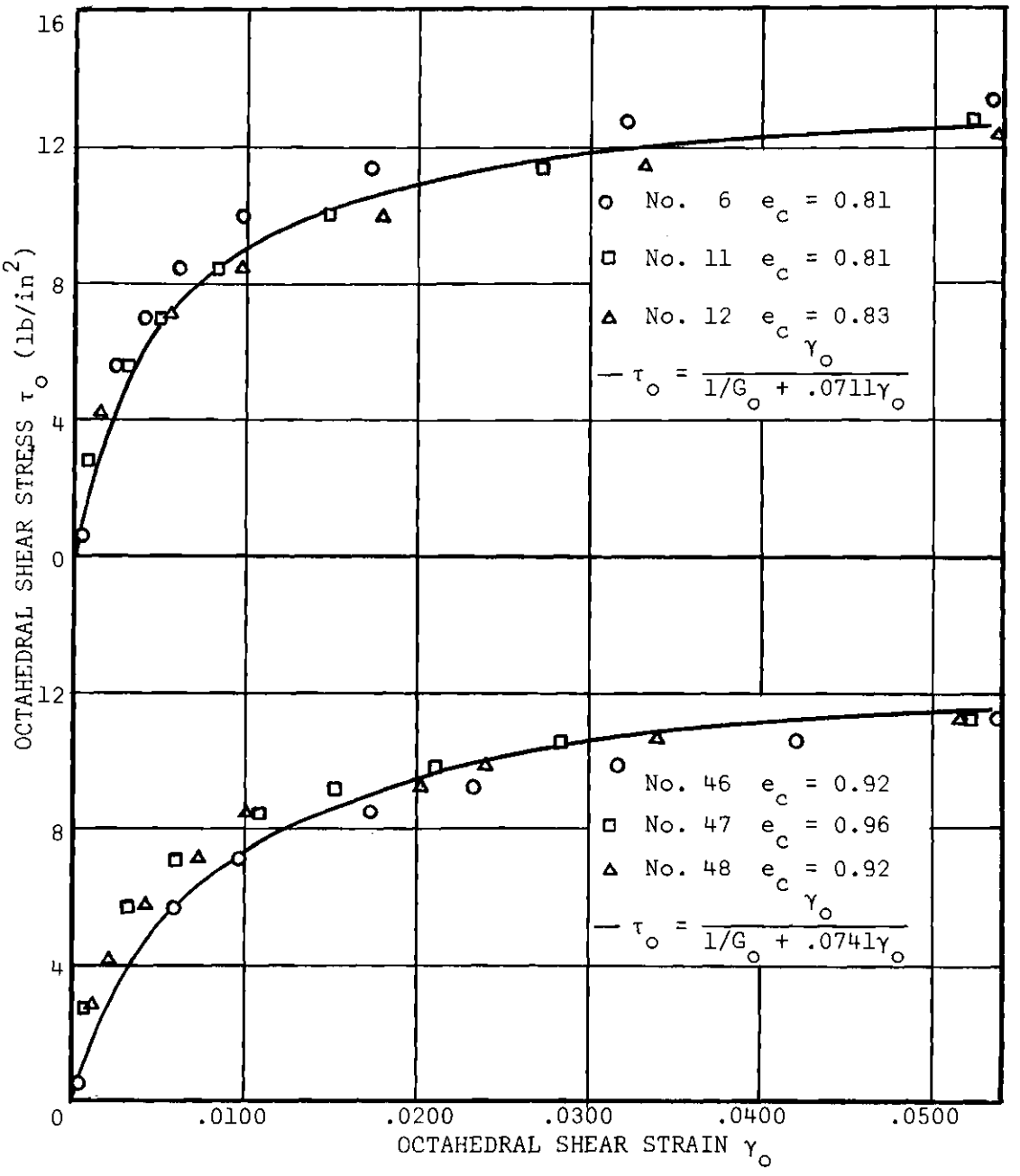

Figure 26. Stress-Strain Relationship for Constant σ_o = 20 lb/in^2.

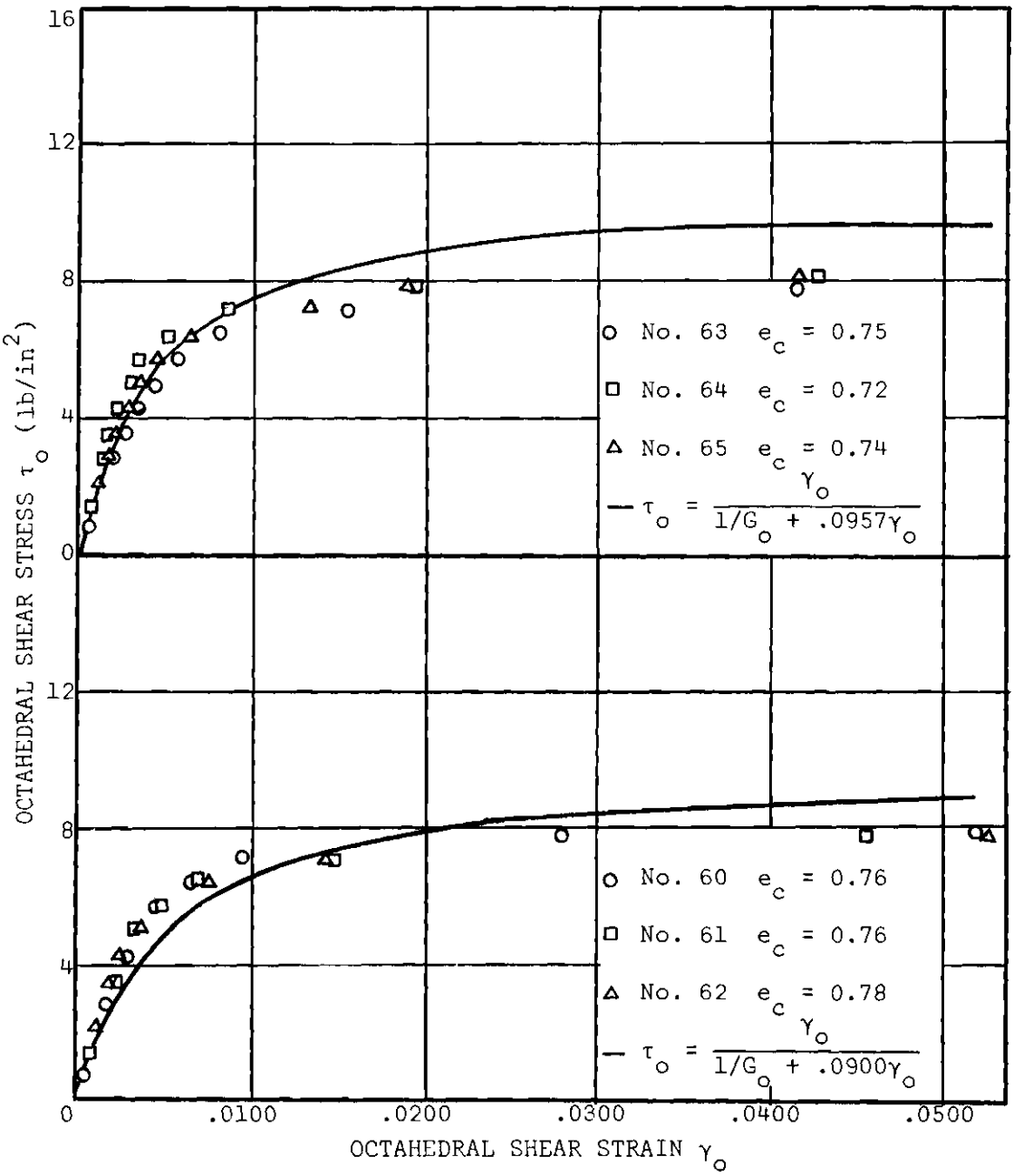

Figure 27. Stress-Strain Relationship for Constant σ_o = 10 lb/in^2.

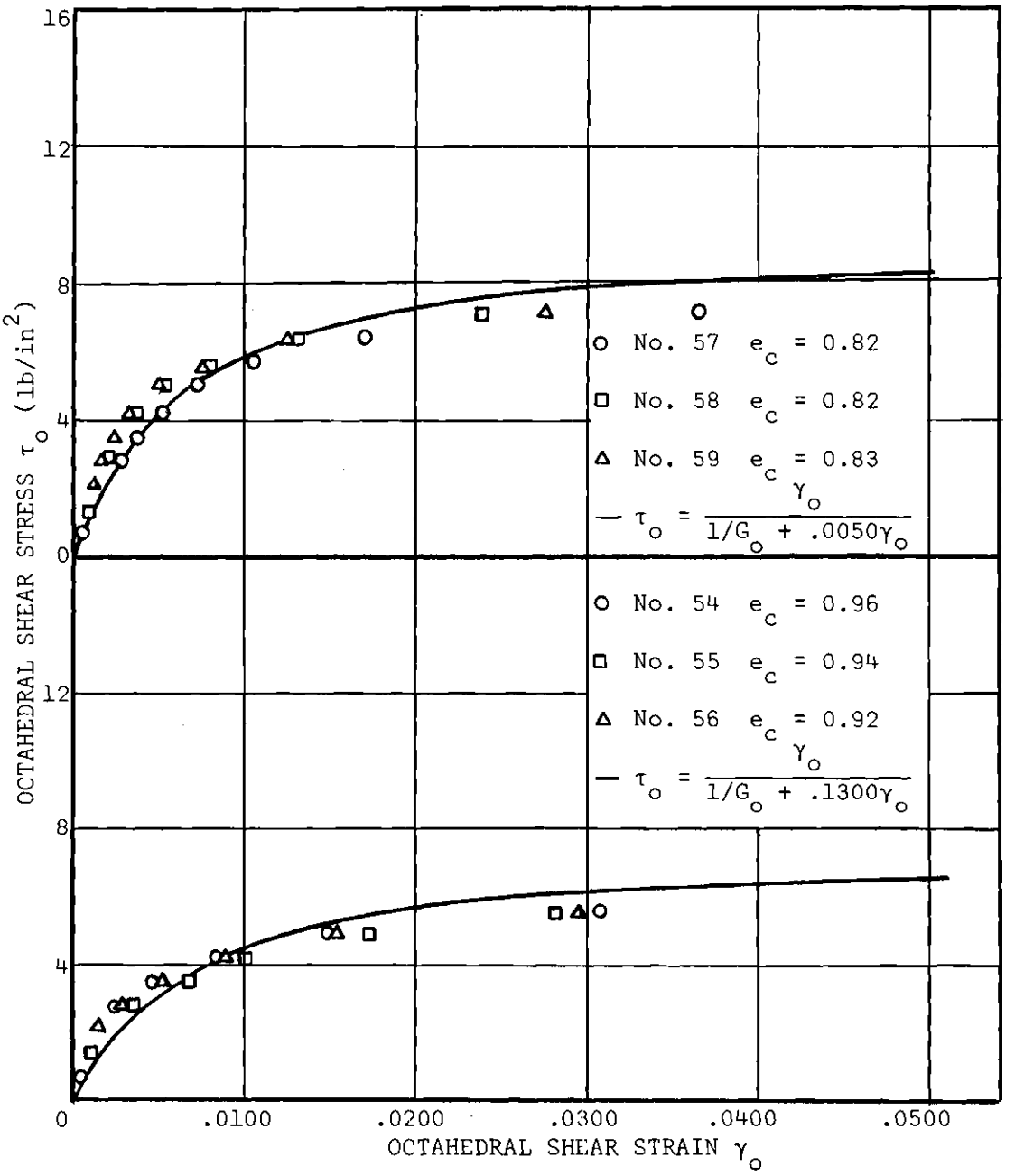

Figure 28. Stress-Strain Relationship for Constant σ_o = 10 lb/in^2.

to indicate the scatter in test results. The solid lines are the stress-strain relationships according to the mathematical expressions indicated on the figures. Details regarding how they were arrived at will be given in a later section.

The density corresponding to each set of test results is indicated on the figure.

To ascertain the effect of density on the stress-strain relationship, best-fit curves were obtained for each of the three tests representing different densities, and these best-fit curves were presented on a common plot. The results are shown in Figures 29 through 34.

To show the influence of the octahedral normal stress on the stress-strain relationship, best-fit curves corresponding to approximately the same density but different octahedral normal stresses were presented on a common plot (Figure 35). The octahedral normal stress and the relative density to which the best-fit curve corresponds is indicated in parenthesis.

Considering first the separate plots obtained for each constant octahedral normal stress, it can be seen that there is some scatter of data but the scatter is quite small. Some of the possible causes of scatter are as follows:

1. Variation in initial densities. The argument presented in Chapter III regarding this point applies in this series of tests as well, and will not be repeated.

2. Discrepancy between the computed or observed principal stresses and the actual principal stresses. The cell pressure and hence σ_3 could be read reasonably accurately to within ±0.25 lbs. per sq. in. Consequently

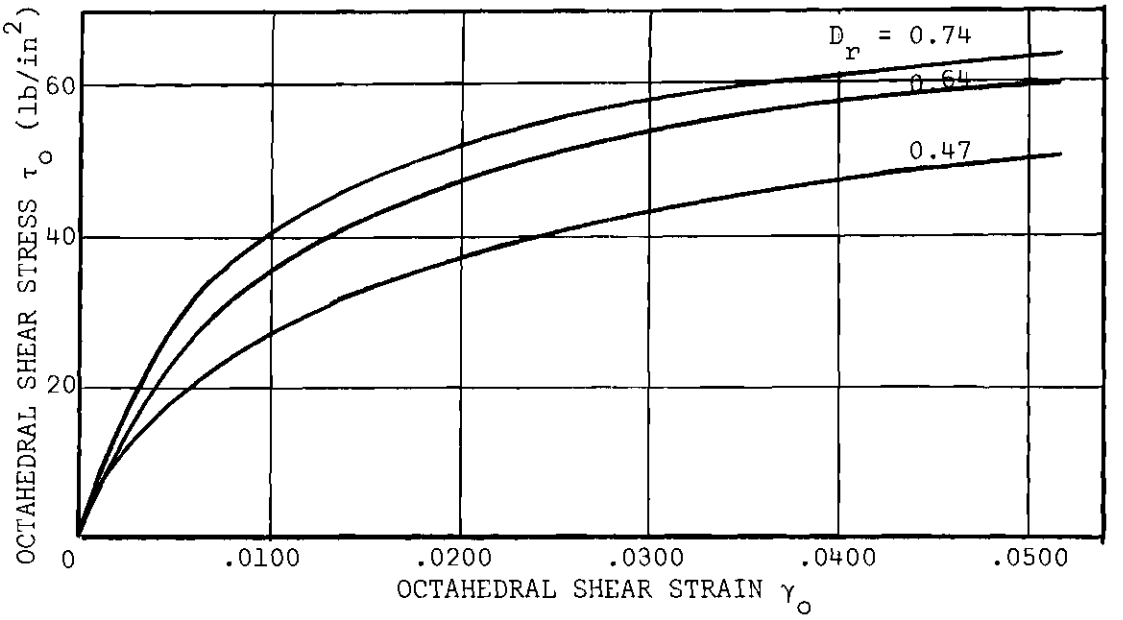

Figure 29. Stress-Strain Relationship for Various Densities and Constant σ_o = 100 lb/in^2.

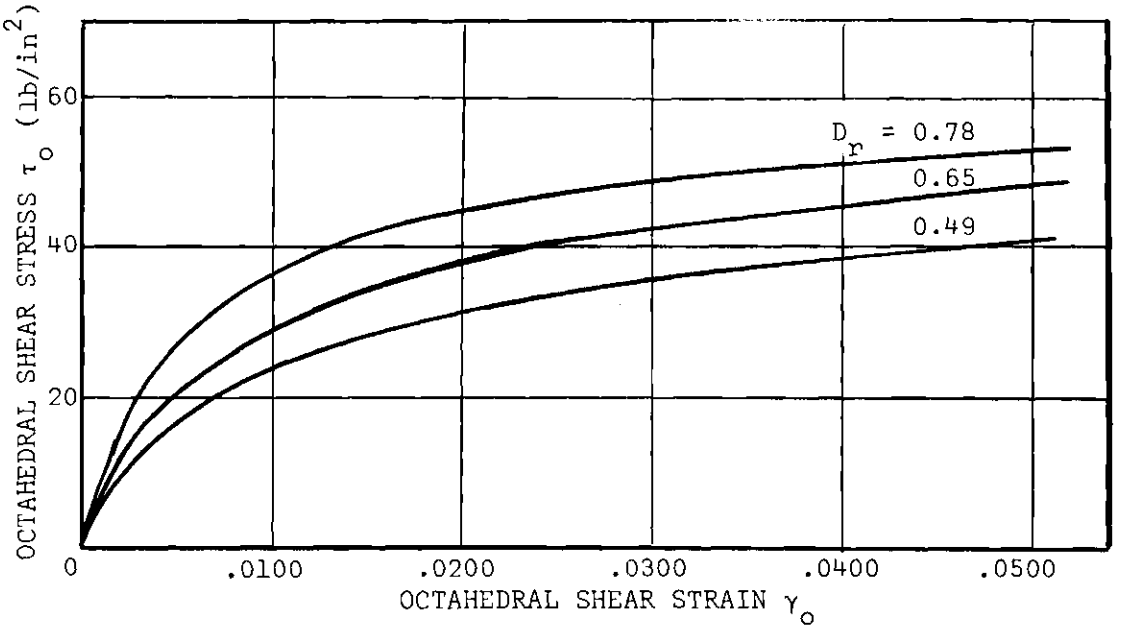

Figure 30. Stress-Strain Relationship for Various Densities and Constant σ_o = 80 lb/in^2.

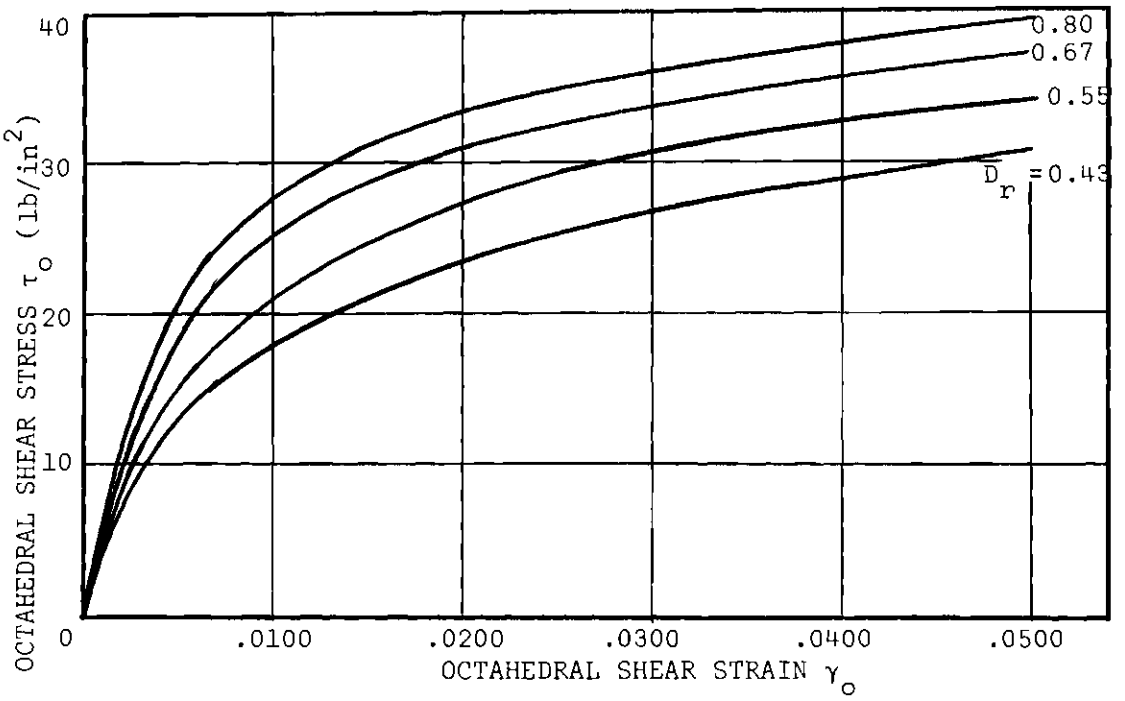

Figure 31. Stress-Strain Relationship for Various Densities and Constant σ_o = 60 lb/in^2.

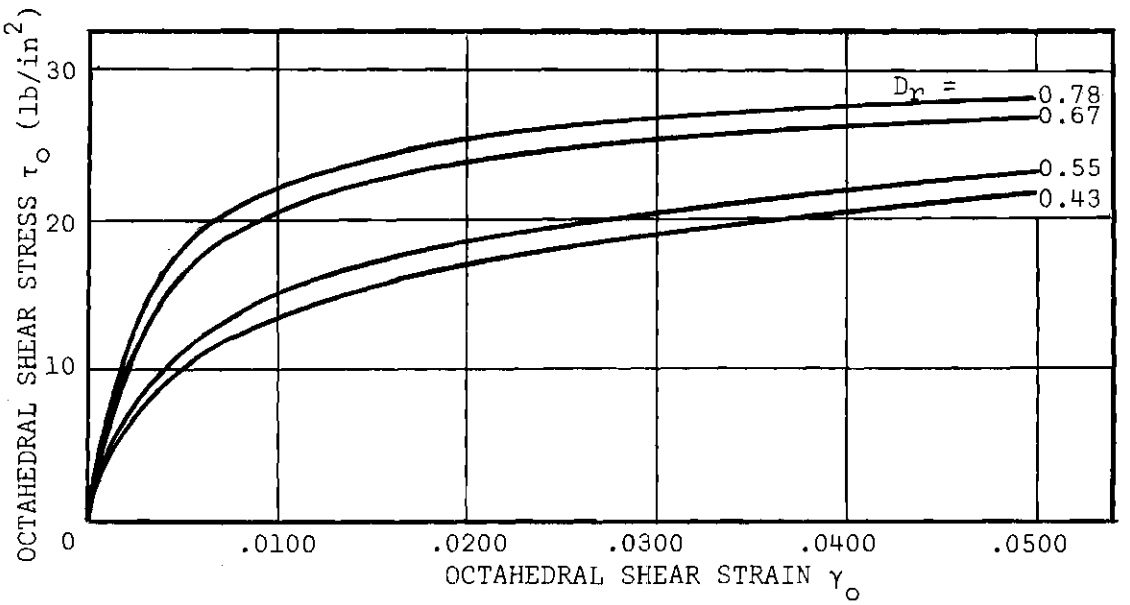

Figure 32. Stress-Strain Relationship for Various Densities and Constant σ_o = 40 lb/in^2.

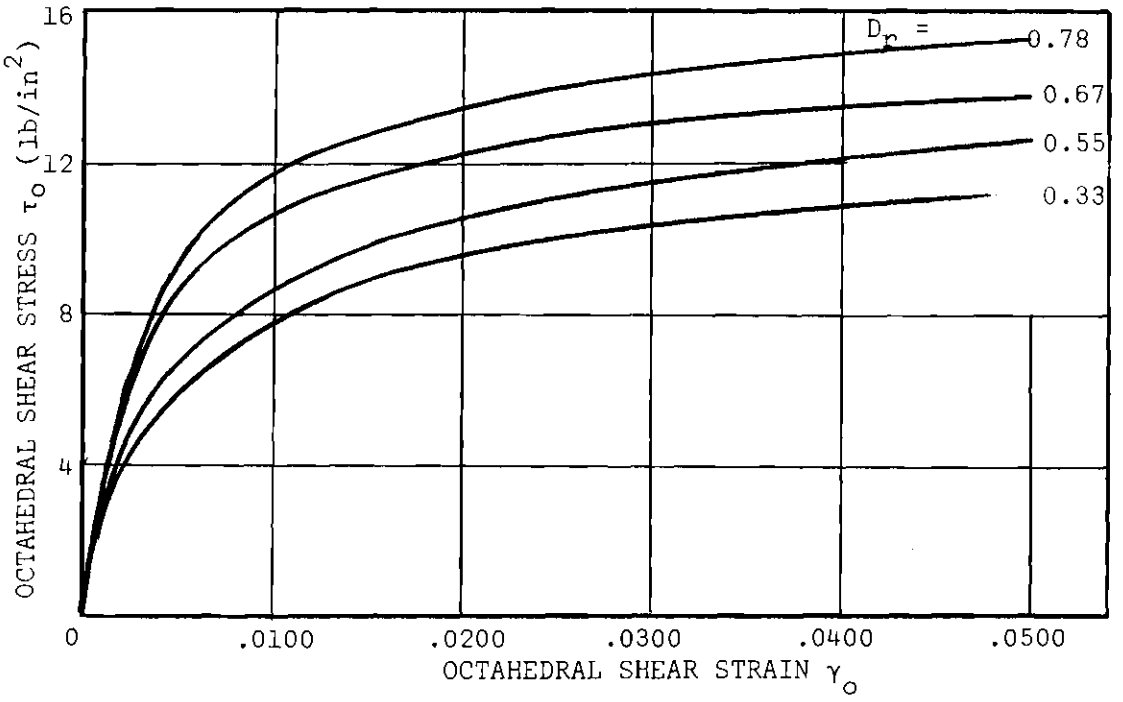

Figure 33. Stress-Strain Relationship for Various Densities and Constant σ_o = 20 lb/in^2.

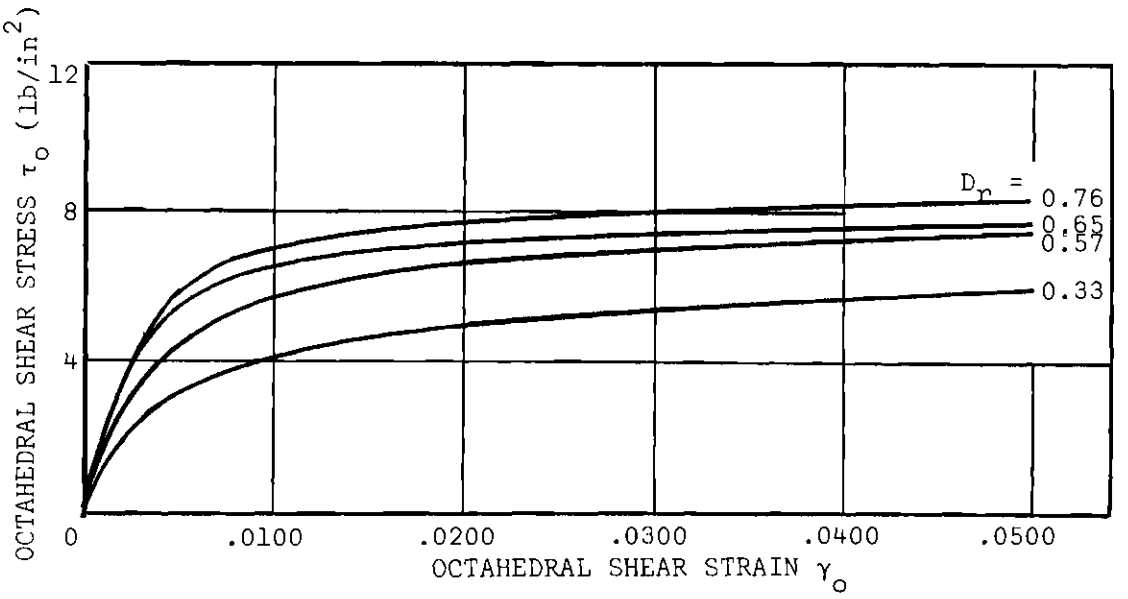

Figure 34. Stress-Strain Relationship for Various Densities and Constant σ_o = 10 lb/in^2.

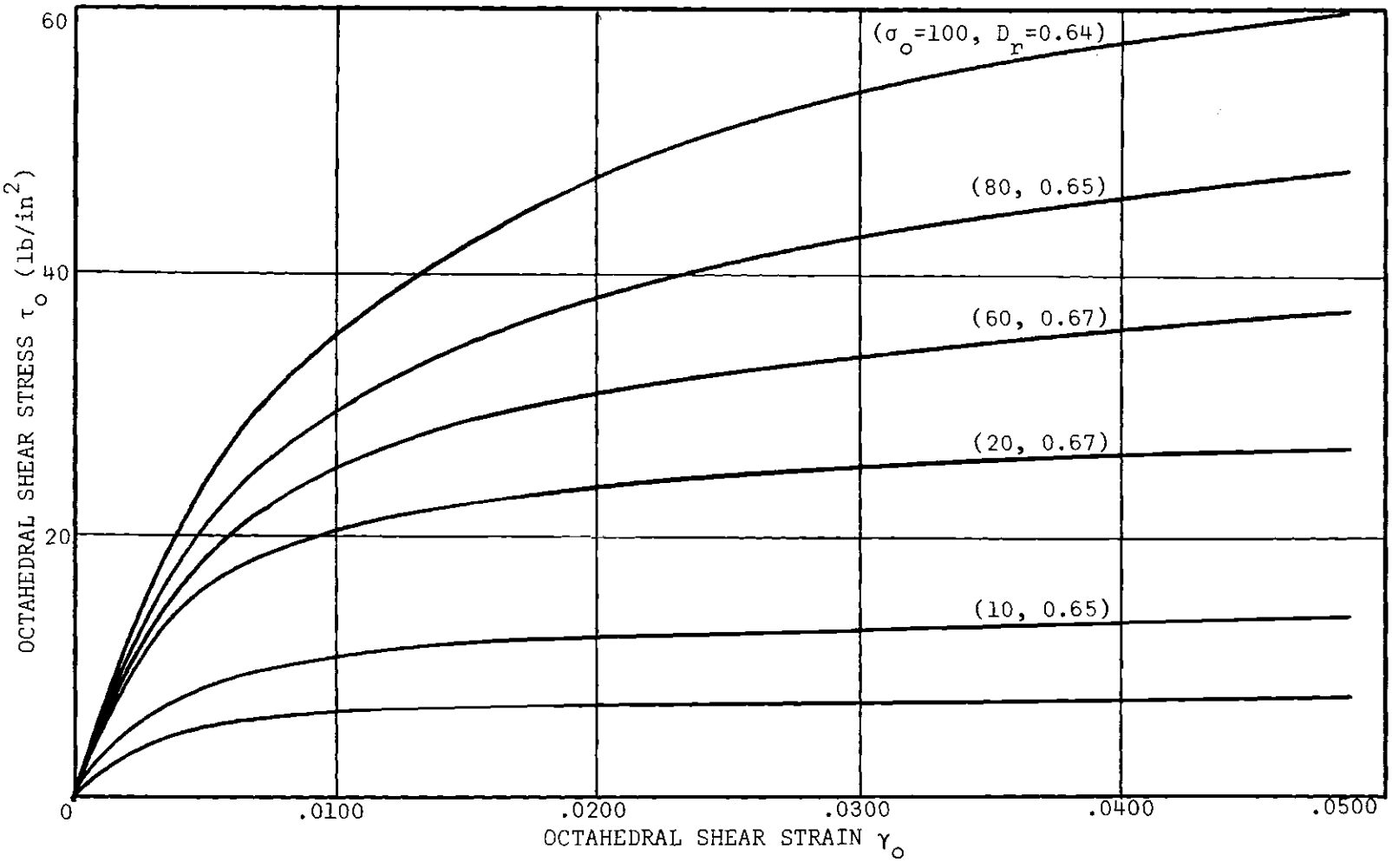

Figure 35. Stress-Strain Relationship for Constant Density and Various Octahedral Normal Stresses.

the relative or per cent error increased as the cell pressure was decreased. This was particularly significant in the "low" constant octahedral normal stress tests.

The pressure activating the hydraulic ram could also be read to within ±0.25 lbs. per sq. in. Since the area of the large ram was approximately the same as the area of the sample it can be assumed that the error in σ_1 due to variations in the applied load was approximately the same as the error in the ram pressure. The influence of this was the greatest at low ram pressures because of the larger per cent error. There is also the possibility of a discrepancy between the observed and true values of σ_1 due to piston friction resulting from a horizontal component of force acting on the piston at the platen. This effect is most pronounced near failure conditions when tilting of the sample is most likely to occur. The design of the piston should theoretically minimize side friction.

3. Discrepancy between predicted and actual cross sectional area. As pointed out previously, in order to attain a given change in σ_1, the corresponding change in area had to be predicted. The predicted and the actual areas proved to be in near perfect agreement until failure conditions were approached. Beyond this point the discrepancy in some instances was appreciable.

4. Deviation from constant octahedral normal stress conditions. The possibility of such a deviation arises from discrepancies between observed and actual stresses. A study of Figure 35 reveals that the stress-strain relationship is fairly sensitive to the octahedral normal stress and therefore deviations from a constant σ_o condition could be expected to cause some scatter in the test results.

5. Strain and Volume Change Measurements. To determine the axial strain which occurred during the build up of the cell pressure, it was necessary to apply a counterbalancing force to the piston, to keep it in contact with the top platen. The accuracy with which this could be done was limited to the accuracy with which the piston load could be controlled. Any error introduced by an inaccurate seating of the piston on the top platen was evident in the stress-strain plot, and the necessary zero correction was applied.

There is very little likelihood of any appreciable error being attributable to volume change observations.

In summary it may be said that scatter in the test results was to be expected for reasons cited above and that in a qualitative sense at least the degree of scatter was within tolerable limits. The consequences of the scatter is most pronounced at the initial portion of the curves since defining initial conditions is of utmost importance to this study.

Considering Figures 29 through 35, it is apparent that the stress-strain relationship is a function of the initial density of the soil and the octahedral normal stress. Specifically, for a given constant octahedral normal stress there is a reduction in the maximum shearing strength with a decrease in the initial density. This is of course consistent with the results of standard triaxial compression tests. Since the tests were performed as stress-controlled tests it was not possible to distinguish between peak and ultimate strengths.

From Figure 35 it can be seen that the octahedral normal stress has a substantial influence on the shearing strength of a sand tested at a given initial density. This phenomena has been cited by other

investigators and is the basis of the extended Huber-Von Mieses and the Tresca failure hypothesis.

To illustrate the effect of the octahedral normal stress on the shearing strength of the soil, a plot of the octahedral normal stress versus the octahedral shear stress at failure was prepared for the sand in a dense and in a loose state (Figure 36). From the figure it can be seen that there is a linear relationship between the octahedral shear stress at failure and the octahedral normal stress. The slope of the line represents the ratio of the octahedral normal stress to the octahedral shear stress at failure. The ratio was found to be 1.4 and 1.6 for the soil in a dense and loose state respectively indicating that the initial density has a minor influence on the stress conditions at failure. This is attributed to the fact that as failure is approached, dense soils dilate while loose soils consolidate. Consequently the difference in densities at failure is much less than at the beginning of the test.

The existence of this definite relationship does lend support to the Huber-Von Mieses and the Tresca failure concepts.

Of greater significance to this particular investigation is the apparent decrease in initial tangent modulus with a decrease in density for a given constant octahedral normal stress. This will be considered in greater detail in a subsequent analysis.

Evaluation of the Shear Modulus

The modulus of shear as defined by equation (IV-1) is the slope of octahedral shear stress-strain curve obtained for a constant octahedral triaxial compression test. From Figures 29 through 35 it is evident that the shear modulus is:

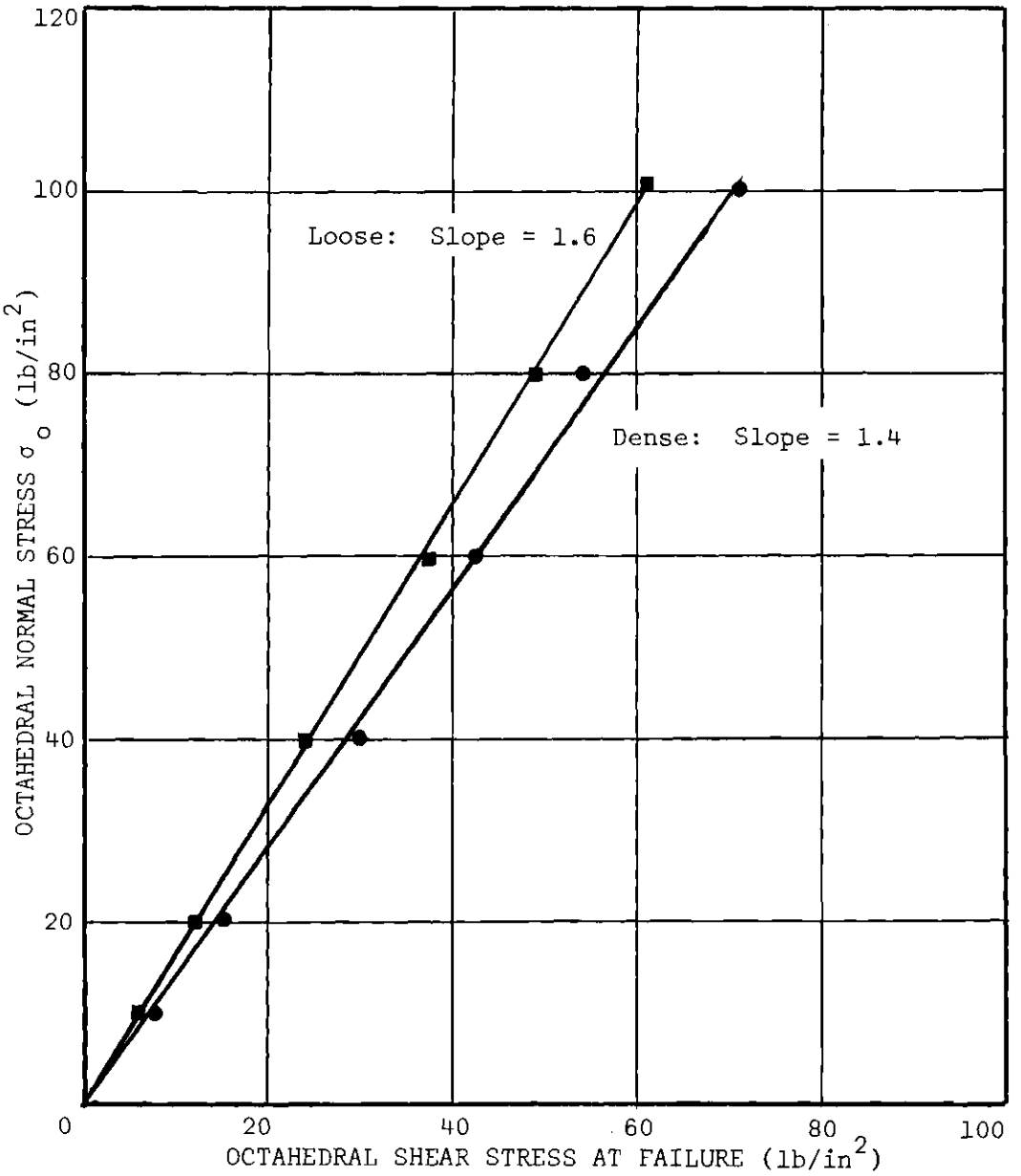

Figure 36. Relationship Between Octahedral Normal Stress and Octahedral Shear Stress at Failure.

1. A decreasing function of the octahedral shear stress for a given initial density and a constant octahedral normal stress.

2. An increasing function of the initial density for a given constant octahedral normal stress.

3. An increasing function of the octahedral normal stress for a given initial density.

Thus the shear modulus may be expressed in a very general form by

$$G = f(\sigma_o, \tau_o, e_c)$$

In developing the above relationship either analytically or graphically it is necessary to define the limits of each independent variable. The limits of the octahedral normal stress and the initial density must necessarily be limited to the range investigated. The selection of a limit for the octahedral shear stress is however somewhat more arbitrary.

Since the shear modulus is by definition, an elastic constant, then its application in soil mechanics problems should correspondingly be limited to that range of stresses for which the accompanying strains are of a relatively small magnitude. This would eliminate the stress range just prior to and during failure, where strains are relatively large.

On the basis of the above reasoning and the fact that in practical soil mechanics problems the working stress is generally based on a safety factor of 3 or more, it was decided to develop a solution for the modulus of shear over an octahedral shear stress range of 0 to 40 per cent of the ultimate stress.

Equations of the following form were used to relate stress and

strain.

$$\gamma_o = C - \frac{1}{B} \ln (G_o - B \tau_o) \qquad \text{(IV-7)}$$

in which B = the variation in shear modulus with octahedral shear

G_o = the initial tangent shear modulus for a specified density

C = integration constant evaluated on the basis of initial conditions.

It was subsequently discovered that the equations were inadequate for the solution of the settlement of a rigid plate on the surface of a cohesionless soil. The inadequacy is a consequence of the fact that, although the average stress under a loaded area may be well below the ultimate, there are points at which the combination of stresses are such that failure conditions exist. Since the analysis was based on the actual rather than the average stresses, it became necessary to define the stress-strain relationship up to and including failure.

As a result, new stress-strain relationships had to be established. The form previously used was not suitable when extended to include failure. Kondner and Zelasko (12) have shown that the stress-strain curve for a triaxial compression test performed on a sand can be expressed by means of a two parameter rectangular hyperbolic function. In their solution, the principal stress difference is related to the axial strain. In view of the similarity of such a curve to the octahedral stress-strain curve* it was decided to express octahedral shear stress-strain relationship by a hyperbolic function.

---

*Although the principal stress difference may be converted directly to the octahedral shear stress by the use of an appropriate constant, the axial strain cannot be similarly converted to octahedral shear strain.

The details of Kondner's method of obtaining the parameters and the function are given in reference (12) and will not be repeated here since only the form of the equation, and not the method was used. The following is a brief outline of the principle of Kondner's method.

Considering Figure 37 as representing the nature of a typical stress-strain curve for a triaxial compression test in which the specimen is tested to failure, it is seen that at very large strains, or as failure is manifested, the stress-strain curve approaches a horizontal line. Thus it can be assumed to be asymptotic to a horizontal line. As well, it may be considered to be asymptotic to a vertical line passing through a point to the left of the origin. The asymptotes may be expressed as:

$$\varepsilon + \alpha = 0 \qquad \text{(IV-8a)}$$

$$\sigma - \beta = 0 \qquad \text{(IV-8b)}$$

in which σ denotes the principal stress difference and ε denotes the axial strain.

The equation of the associated hyperbola may be written as:

$$\varepsilon\sigma - \beta\varepsilon + \alpha\sigma = 0 \qquad \text{(IV-9)}$$

Letting $a = \frac{\alpha}{\beta}$, and $b = \frac{1}{\beta}$ then equation (IV-9) may be rewritten as:

$$\sigma = \frac{\varepsilon}{a + b\varepsilon} \qquad \text{(IV-10)}$$

By evaluating the derivative of equation (IV-10) at $\varepsilon = 0$ and by

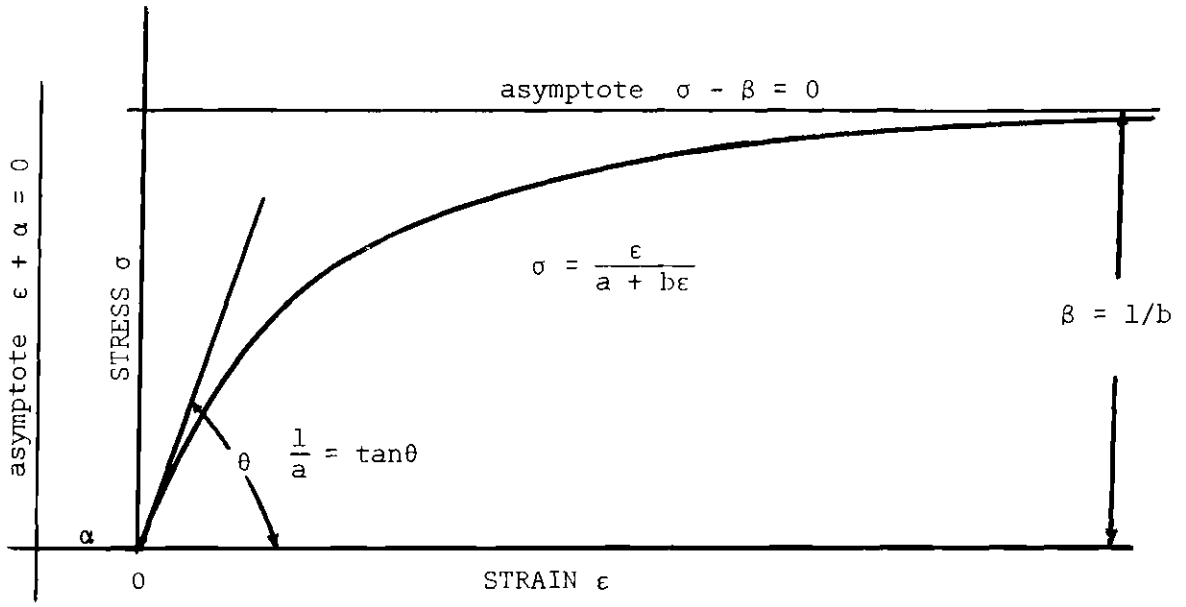

Figure 37. Illustration of the Use of a Two Parameter Hyperbolic Function to Relate Stress and Strain.

taking its mathematical limit, it can be shown that $1/a$ represents the initial tangent modulus while $1/b$ represents the ultimate stress of the soil.

Kondner defines $1/a$ and $1/b$ by the following expressions:

$$\frac{1}{a} = C + D\,\sigma_o$$

$$\frac{1}{b} = A + B\,\sigma_o$$

in which A, B, C, and D are constants that are obtained from the analysis of triaxial test results. It is noteworthy that he expresses both the initial tangent modulus $1/a$, and the ultimate stress $1/b$, as a function of the octahedral normal stress. The expressions however are not of a general form and for any specific density a series of triaxial compression tests at the specified density are required for their solution.

The author made use of the hyperbolic function in the form given by equation (IV-10). By the selection of proper coordinates for the stress-strain plot, the initial tangent modulus was made to represent the initial shear modulus while the ultimate stress was expressed in terms of octahedral shear. As applied to this set of coordinates equation (IV-10) may be rewritten as

$$\tau_o = \frac{\gamma_o}{a + b\,\gamma_o} \qquad \text{(IV-11)}$$

General expressions and particular solutions were obtained for the parameters $1/a$ and $1/b$. These parameters were expressed as functions of the octahedral normal stress, the octahedral shear stress, and the initial

density of the soil. The following sections deal with the development of the stress-strain hyperbolic function. The terms "initial tangent parameter" and the "ultimate stress parameter" will be analogous to the $1/a$ and $1/b$ parameters respectively. They are not identical in that Kondner relates them to principal stress difference and axial strain whereas the author relates them to octahedral shear stresses and strains as well as initial density.

Initial Tangent Parameter, a

To obtain the initial tangent shear modulus parameter for the test series, the aforementioned "average" stress-strain curves were plotted to an enlarged scale, zero corrections were applied where necessary and the initial tangent moduli were computed. The moduli for a given octahedral normal stress were plotted as a function of relative density and a smooth curve was then drawn through the points. A family of curves was thus obtained as depicted by Figure 38. A second family of curves was then drawn showing the relationship between the initial tangent shear modulus and octahedral normal stress for varying magnitudes of relative density (Figure 39). It will be noted that the curves were extended to pass through the origin. This implies that under a zero octahedral normal stress, the soil has no measurable shearing resistance. This assumption is not strictly correct but it is felt that it is a valid approximation of a condition that cannot be experimentally verified.

Insofar as the relationship between the initial shear modulus, the initial density, and the octahedral normal stress is concerned, it can be stated that no simple function relates these three variables. Figure 39 implies that, contrary to Kondner's assertion, the initial tangent modulus

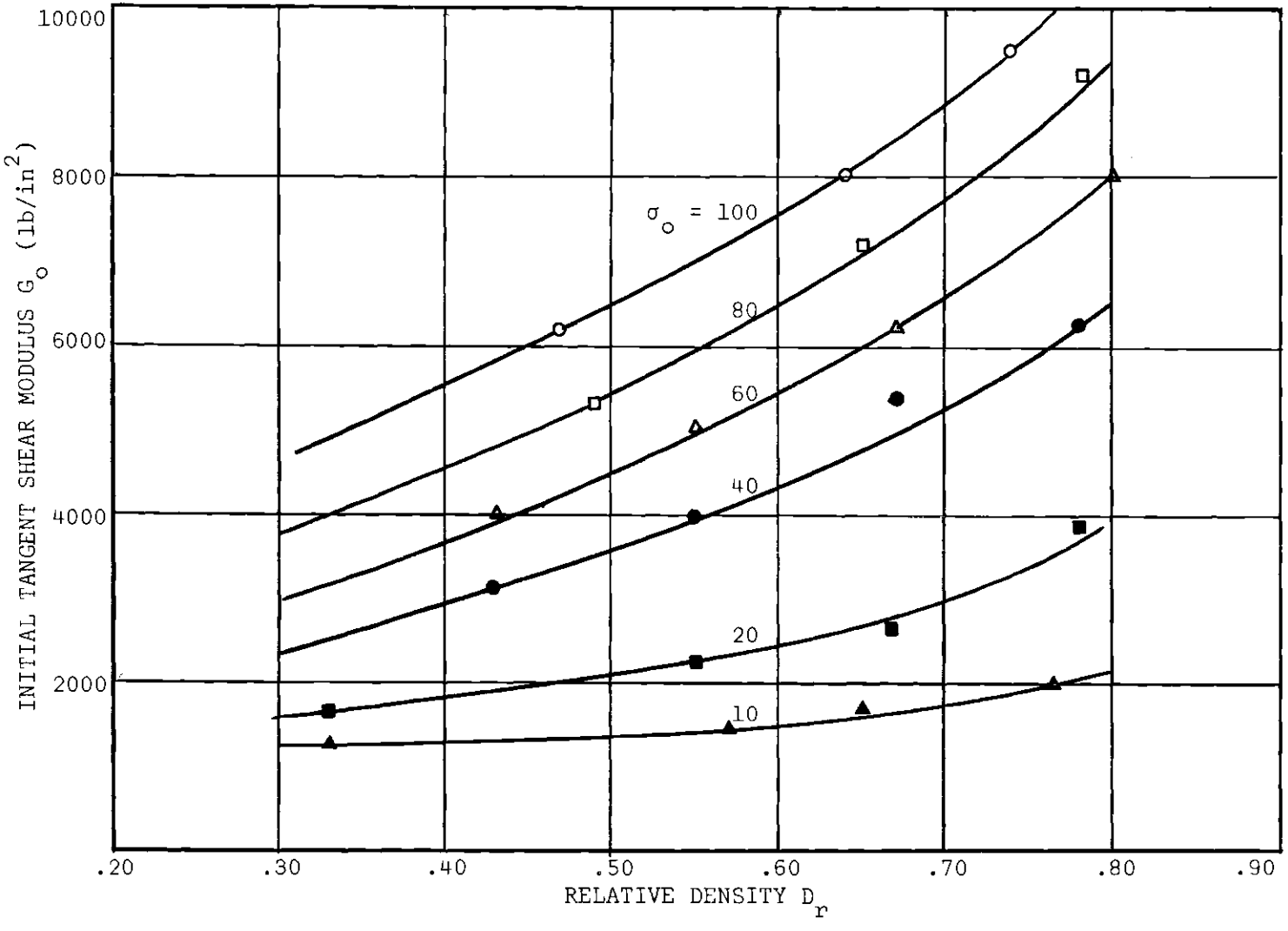

Figure 38. Relationship Between Initial Tangent Shear Modulus and Relative Density for Different Octahedral Normal Stresses.

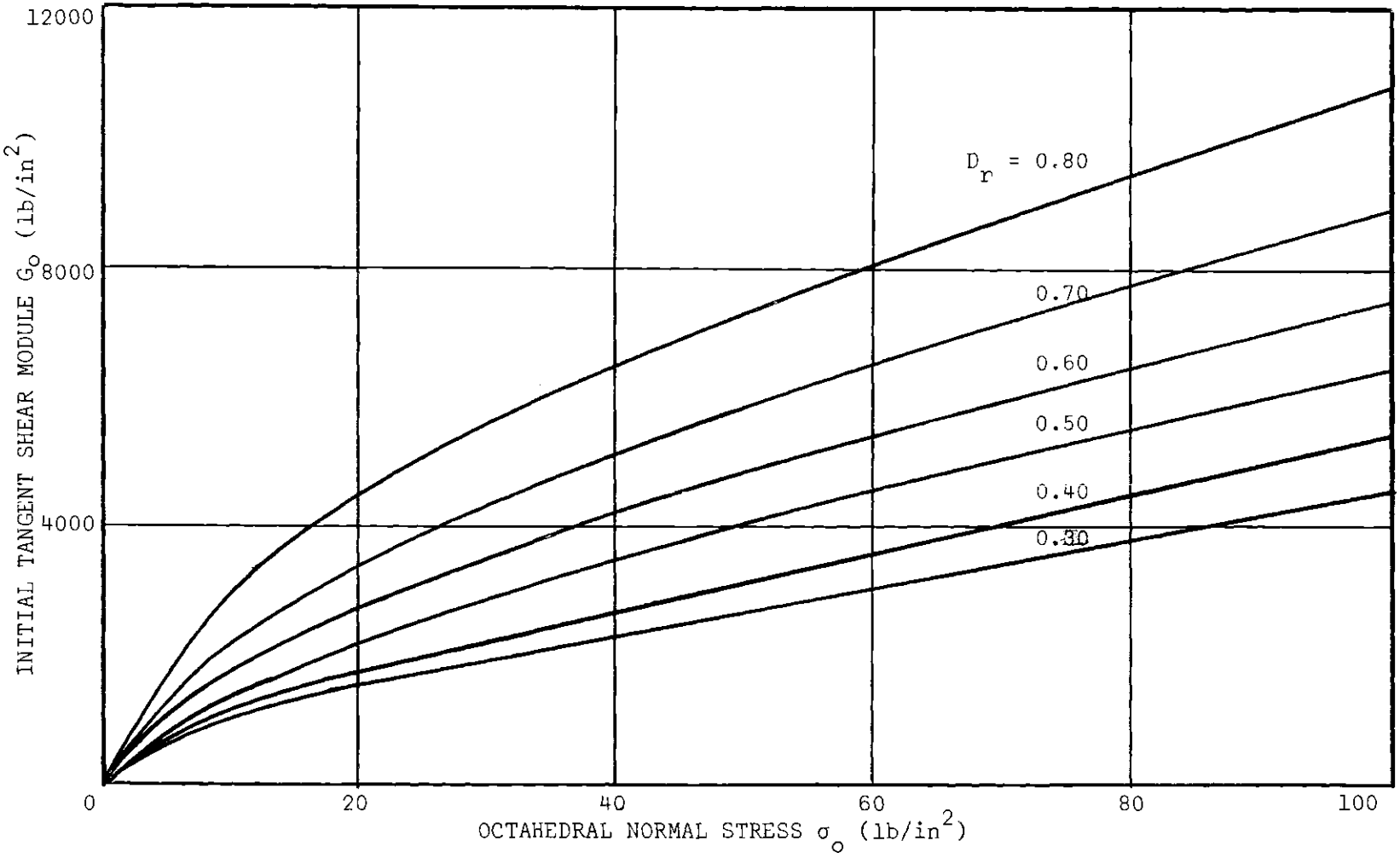

Figure 39. Relationship Between Initial Tangent Shear Modulus and Octahedral Normal Stress for Different Relative Densities.

is not a linear function of the octahedral normal stress for a given density. The deviation from linearity is particularly significant at low octahedral normal stresses. However in view of the difficulty of defining the intergranular stresses under small externally applied normal stresses, any conclusive statement regarding the response of a soil under low "observed" normal stresses is presumptuous. As mentioned previously, the existence of prestress in granular soils has been verified experimentally. This prestress would intuitively become highly significant at small externally applied normal stresses.

No serious attempt was made to obtain an expression relating the three variables since it was felt that an extended investigation should precede any such analysis. The graphical solution as depicted by Figure 39 was used throughout the investigation.

Ultimate Stress Parameter, b

The b parameter contained in equation (IV-10) was solved for directly in the following manner. Several corresponding sets of stress-strain data were taken from the average stress-strain curve of a test series. By means of equation (IV-11) and the solution for the initial tangent modulus (Figure 38), the corresponding values of b were computed. The average of the several b values representing one test series was used in the mathematical expression relating the octahedral shear stress and strain. This was repeated for each test series and the mathematical expressions and their associated plots are included in the figures presenting the experimental stress-strain data (Figures 19 through 28).

From a comparison of the experimental data and the relationship based on the mathematical expression, it can be concluded that the two-

parameter hyperbolic function is a good representation of the response of a cohesionless soil undergoing a constant octahedral triaxial compression test.

The effect of initial density and octahedral normal stress on the b parameter, is illustrated by Figures 40 and 41. Figure 40 is a plot of the computed values of b versus relative density for constant values of octahedral normal stress. It is seen that a straight line can be used to approximate the relationship between relative density and the b parameter for a constant octahedral normal stress.

Figure 41 illustrates the variation in the b parameter with octahedral normal stress for a constant relative density as based on the assumed straight line relationship between b and relative density. The curves imply a rapid increase in the b parameter with decreasing octahedral normal stress. At zero octahedral normal stress, the magnitude of b must approach infinity. Considering equation (IV-10) the mathematical limit as the axial strain approaches infinity is given by:

$$\tau_o = \frac{1}{b} \qquad \text{(IV-12)}$$

Moreover for the condition of $\tau_o = 0$, we have that $\sigma_o = 0$ in which case b must equal infinity, in order that equation (IV-12) be satisfied. Consequently the solution for the b parameter could only be properly defined between the limits of σ_o = 10 to 100 lbs. per sq. in. for the investigation concerned. This solution is given in graphical form in Figure 41. An analytical solution was not attempted but the nature of the relationship would suggest the feasibility of a mathematical representation.

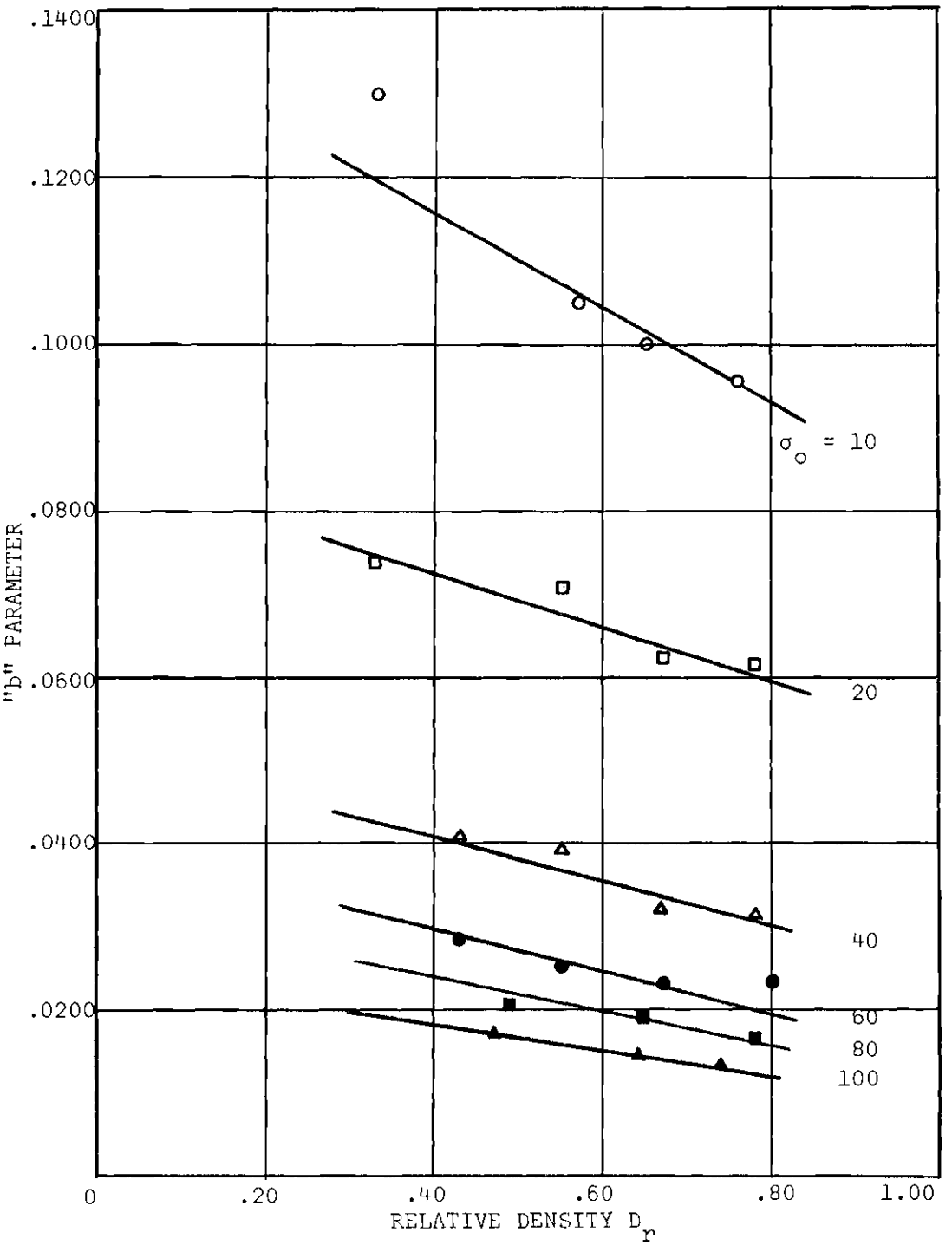

Figure 40. Relationship Between "b" Parameter and Relative Density for Different Octahedral Normal Stresses.

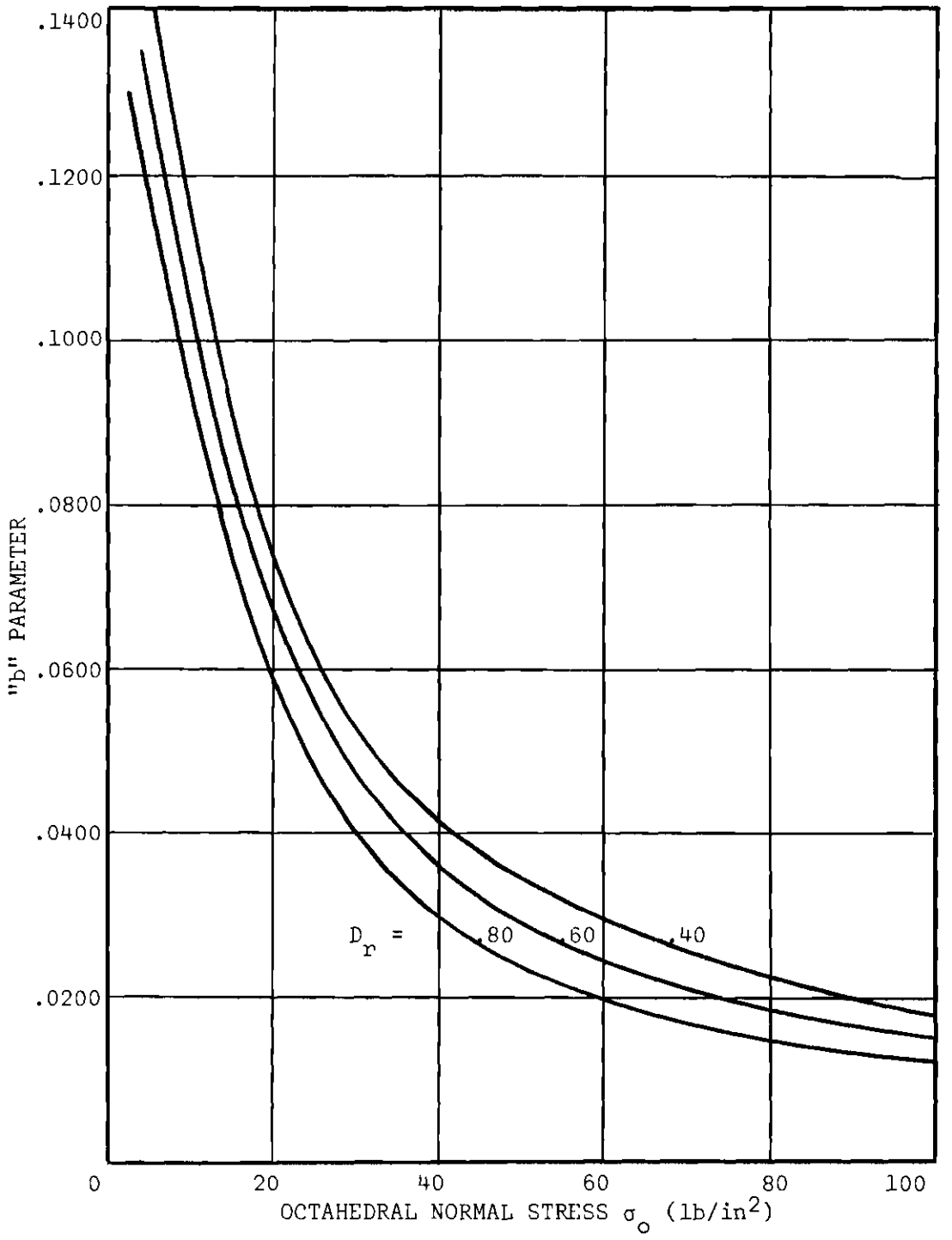

Figure 41. Relationship Between "b" Parameter and Octahedral Normal Stress for Different Densities.

Shear Modulus as a Function of Octahedral Normal Stress, Octahedral Shear and Initial Density

In general, the shear modulus (G) is a function of the initial density of the soil, the octahedral normal stress, and the octahedral shear stress and can be expressed by:

$$G = f(\sigma_o, \tau_o, e_c)$$

Based on the investigation, the following expression, which is the derivative of equation (IV-11), may be used to relate the variables:

$$G = G_o(1 - b\,\tau_o)^2 \qquad \text{(IV-12)}$$

in which:

$G_o = \frac{1}{a}$ = shear modulus for a specific density and octahedral normal stress, and zero octahedral shear stress.

$= f(\sigma_o, e_c)$ as given by Figures 39 and 40.

b = parameter defining ultimate stress for a specific octahedral normal stress and initial density.

$= g(\sigma_o, e_c)$ as given by Figure 41.

Conclusions

Based on the previously outlined investigation and analysis, the following conclusions pertaining to the shearing characteristics of the Chattahoochee River sand may be made:

1. Constant octahedral triaxial compression tests offer an expedient means of evaluating the response of a cohesionless soil to shearing action.

2. At failure, there is a unique relationship between the octahedral normal stress and the octahedral shear stress: for the soil in a dense state, the ratio between the octahedral normal stress and the octahedral shear stress is approximately 1.4 while for the soil in a loose state it is approximately 1.6.

3. The experimental octahedral shear stress-strain data may be represented by a two parameter hyperbolic function of the form

$$\tau_o = \frac{\gamma_o}{a + b\,\gamma_o}$$

4. The shear modulus defined as the instantaneous slope of the octahedral shear stress-strain curve is a function of the initial density of the soil, the octahedral normal stress and the octahedral shear stress, and may be expressed by the equation

$$G = G_o(1 - b\,\tau_o)^2$$

in which: G_o = shear modulus corresponding to zero octahedral shear, and which is a function of the initial density of the soil and the octahedral normal stress.

b = a parameter that is a function of the octahedral normal stress and the initial density of the soil, and which is the inverse of the ultimate stress of the soil at the designated density and octahedral normal stress.

PART B

THE ANALYSIS OF DEFLECTION UNDER A UNIFORMLY DISTRIBUTED LOAD ACTING OVER A CIRCULAR AREA

CHAPTER V

THEORETICAL CONSIDERATIONS

Present Methods of Analysis

The subject of stresses and displacements in a semi-infinite body due to a force acting on the boundary has received considerable treatment since its inception by Boussinesq (32) in 1885. The Boussinesq solutions yielded the stresses and displacements for any point in a semi-infinite mass due to a vertical concentrated force acting on the boundary. The solutions have been extended to distributed loads acting over a finite portion of the boundary. This was first done by Love (33) in 1928, who developed general solutions in partial derivative form. Since then, numerous particular solutions have been developed by many investigators to include: distributed loads of variety of nature; a variety of boundary conditions; and non-homogeneity and non-isotropy of the soil. It is not the author's intent to review these particular solutions here because of the vast number of them and because they have been well reviewed in the writings of such authors as Scott (34), Florin (35), Jurgenson (36) and Sowers and Vesic (37).

The solution for the deflection of a point on the surface of a semi-infinite, homogeneous isotropic, elastic solid due to a distributed load acting on the boundary as based on the Boussinesq stress distribution is generally in the form of equation (V-1).

$$w = \frac{2pa\ (1 - \nu^2)}{E}\ I_w \qquad (V\text{-}1)$$

in which: w = deflection of the point

p = average unit load on the boundary

ν = Poisson's ratio

E = Young's modulus or modulus of deformation

$2a$ = a measurement of the geometry of the loaded area; (diameter for circular area, side for square, etc.)

I_w = settlement factor the magnitude of which depends upon; the shape of the loaded area; the position of the point with respect to the loaded area; and the nature of the distribution of the boundary force.

The equation was obtained by the integration of the Boussinesq stress distribution. The solution is based on the assumption of a semi-infinite, homogeneous, isotropic medium, having a constant Poisson's ratio and a constant modulus of deformation. According to equation (V-1), the deflection is sensitive to variations in the modulus of deformation but is much less sensitive to variations in Poisson's ratio. For this reason it is not uncommon to find the solution written in terms of the modulus of deformation and an assumed Poisson's ratio of 0.5.

It is generally contended that the above equation when applied to cohesionless soils is inadequate primarily because of the assumption of a constant modulus of deformation. It is recognized that the modulus of deformation is a function of the confining pressure and must not only vary from point to point within the mass, but must also change with each change in magnitude of the unit load on the boundary.

Several investigators have attempted, with varying degrees of success, to take into account the variation of the deformation modulus.

Mazanti (38) established an empirical relationship between the modulus of deformation and the lateral confining pressure based on triaxial compression tests performed at constant cell pressures. The modulus of deformation was taken as the instantaneous slope of the principal stress difference versus axial strain curve. In his settlement analysis he considered the soil to consist of several horizontal layers having different moduli. The moduli were obtained on the basis of his predetermined relationship, using a computed lateral pressure in the soil. The lateral pressure was taken as a percentage of the vertical pressure which was computed on the basis of a pyramidal stress distribution. The deflection of the plate was taken to be the sum of the vertical strains of a column of soil under the plate. A criticism of his analysis is the method of correlation of laboratories and field stress conditions. Principal stresses were used to define the modulus of deformation in the laboratory, while vertical and horizontal stresses were used in the field. These are only identical along the axis of symmetry.

A solution for the stresses and deflection in a layered solid system has been developed by Burmister (39), and Acum and Fox (40), for the purpose of flexible pavement design.

In predicting the settlement of circular foundations resting on a cohesionless soil, it may be stated that equation (V-1) receives widest use because of its simplicity and the lack of a better approximation. Moreover, it is obvious that equation (V-1) will yield a solution that provides excellent agreement between the predicted and the observed deflection for a specific footing diameter, and footing load. It merely requires a judicious selection of elastic constants E and ν. However,

the same constants will not yield good agreement if either, or both, footing size and footing load are changed. It is generally an accepted fact that to obtain good agreement, the elastic constants must be changed.

With regard to changing the elastic constants according to footing size and/or footing load, or some other measure of the change in stress conditions, it is the author's contention that E as conventionally defined by the instantaneous slope of a stress-strain curve is not a parameter that can be properly correlated to stress conditions in a soil mass. It pertains to and is defined only in terms of, stresses and strains manifested in a triaxial compression test. Alternatively, the use of a bulk and shear modulus permits a direct correlation between stress conditions in the field and the stress conditions that define the two moduli. The following sections deal with the development of a settlement equation in terms of bulk and shear moduli.

Method of Analysis

It was proposed to define the stress-strain response of a cohesionless soil mass under the action of a circular, uniformly loaded area, in terms of volumetric and shearing components. The bulk and shear moduli were used to characterize the respective components. The soil was treated as a multilayered system, with each layer having a shear and bulk moduli in accordance with the prevailing stress conditions in that layer. Existing equations for settlement based on the theory of elasticity and expressed in terms of Young's modulus were modified so as to include the bulk and shear moduli in place of Young's modulus and Poisson's ratio.

Stress Distribution

The stress distribution throughout the soil mass was required since the elastic parameters K and G are functions of the stress system. The moduli have been defined in terms of prevailing effective stresses and therefore stresses due to body forces as well as stresses due to the distributed load acting on the boundary must be considered.

Stresses Due to Body Forces. The stresses due to body forces in terms of cylindrical coordinates are as follows:

$$\sigma_z = \gamma z \qquad \text{(V-2)}$$

$$\sigma_\theta = \sigma_r = K_o \sigma_z \qquad \text{(V-3)}$$

$$\tau_{rz} = 0 \qquad \text{(V-4)}$$

in which: γ = effective unit weight of the soil

z = depth at which stresses are being evaluated

K_o = coefficient of earth pressure at rest.

The coefficient of earth pressure at rest of the Chattahoochee sand was investigated by Moore (41). His investigation showed that K_o was relatively independent of the density of the sand and was approximately equal to 0.48. This value was used in equation (V-3).

Stresses Due to Distributed Load Acting on the Boundary. The stresses due to the distributed load were obtained from the solutions developed by the U. S. Waterways Experiment Station (42, 43) for a uniformly loaded circular area. The solutions are based on the Boussinesq theory of stress distribution for a semi-infinite homogeneous isotropic elastic solid, and on the theory of superposition.

An experimental investigation of the stress distribution in a homogeneous sand was conducted by the U. S. Waterways Experiment Station (43). Their results indicated that in general there was reasonable agreement between the measured stresses and the computed stresses based on the Boussinesq theory. The largest discrepancy in the vertical stresses was directly below the loaded area at shallow depths, where the measured stresses were approximately 20 per cent larger than the computed stresses. The deviations diminished considerably with depth and/or horizontal distance from the loaded area. The measured horizontal stresses were found to be somewhat lower than the theoretical stresses at shallow depths but the trend was reversed at greater depths.

The Boussinesq theory of stress distribution was adopted because of the generally good agreement found between the measured and theoretical stresses and because of the lack of a better method applicable to this investigation. It is recognized that the Boussinesq theory can only serve to approximate the actual stresses and also that there is an incompatibility between the assumptions on which the stress computations are based (homogeneity and isotropy) and the assumptions on which the deflections are based (non-homogeneity and isotropy).

The method for determining the octahedral normal and shear stresses was as follows:

Stresses due to the distributed load were computed in terms of cylindrical coordinates, using the developed solution for a Poisson's ratio of 0.33. The stresses due to the body forces were added.

The stresses in terms of cylindrical coordinates were converted to principal stresses by means of the following equations.

$$\sigma_1, \sigma_2 \text{ or } \sigma_3 = \frac{\sigma_z + \sigma_r \pm \sqrt{(\sigma_z - \sigma_r)^2 + (2\tau_{rz})^2}}{2} \qquad \text{(V-5)}$$

$$\sigma_1, \sigma_2 \text{ or } \sigma_3 = \sigma_\theta \qquad \text{(V-6)}$$

The principal stresses were converted to the octahedral normal and shear stresses by means of equations (IV-2) and (IV-3).

Evaluation of the Bulk and Shear Moduli

Stress Computations. As mentioned previously, because of the availability of particular solutions for stress distribution it is possible to develop a 3 dimensional model of stress contours. A corresponding 3 dimensional model of moduli contours may be obtained which would yield surface deflection contours due to any boundary force system.

This study however was limited to the analysis of the deflection under the circular area over which the load is applied. Specifically, the deflection at the center and the edge of the circular area was determined.

The stresses were computed at the following depths (expressed as multiples of the plate radius): 0, 0.2, 0.4, 0.6, 0.8, 1.0, 1.2, 1.5, 2.0, 2.5, 3.0, to 26.0 in one plate radius increments. The depth of 26 plate radii represents the bottom of the cylindrical concrete pit in which the tests were conducted.

The stresses were computed for every two lbs. per sq. in. boundary stress increment. Thus, for every load increment, the stresses were computed at 34 depths in terms of cylindrical coordinates. These stresses were then converted to principal stresses and then to octahedral stresses. In view of the numerous calculations involved, the stress distribution analysis was carried out by means of a computer program.

Computation of the Bulk Modulus. At each depth at which the octahedral normal and shear stresses were evaluated, the corresponding bulk and shear moduli were determined.

It will be remembered that the bulk modulus was a function of the octahedral normal stress for a given initial relative density. Moreover, it was shown that over a specific stress range the modulus was linearly related to the octahedral normal stress. Two such linear expressions served to define the relationship over a stress range of 0 to 100 lbs. per sq. in. A computer program was used to solve for the bulk modulus utilizing the parameters given in Figure 16.

Computation of the Shear Modulus. The general solution for the shear modulus as given by equation (IV-12) is:

$$G = G_o (1 - b \tau_o)^2$$

This solution applies only to a stress system in which the ratio of the octahedral normal to the octahedral shear stress is greater than 1.4 for dense soils and 1.6 for loose soils. If the ratio is less, then failure conditions prevail. Preliminary calculations indicated that failure conditions did in fact prevail under the loaded area at very shallow depths. It was therefore necessary to assign a shear modulus to the zone of local failure for which there was no experimental data since the laboratory tests were carried out to incipient failure only. The method used was to assign a constant shear modulus (G_{min}) to the zone based on failure conditions measured in the laboratory. This implied that the ratio of the octahedral normal stress to the octahedral shear stress could not be smaller than some predetermined value.

It was also necessary to approximate the shear modulus for low values of the octahedral normal stress. The investigation of the ultimate stress parameter indicated that at very low octahedral normal stresses, the b parameter was very large and approached infinity as the octahedral normal stress approached zero. This made it difficult to establish a value for b at low octahedral normal stresses and so a second approximation of the shear modulus was established for the case where the octahedral normal stress was less than 5 lbs. per sq. in. The approximation was of the following form

$$G = G_o - \frac{\tau_o (G_o - G_{min})}{0.67\, \sigma_o} \qquad (V\text{-}7)$$

which merely indicates that the shear modulus decreases linearly with the octahedral shear from the initial tangent modulus to the minimum value. The rate of decrease is based on the octahedral shear stress at failure expressed as a function of the octahedral normal stress.

The shear modulus for all other situations was calculated on the basis of equation (IV-12), and the graphical solutions for G_o and b as given by Figures 39 and 41 respectively.

Thus the solution for the shear modulus was obtained in accordance with one of the following categories:

1. Failure conditions prevailed.

2. The octahedral normal stress was less than 5 lbs. per sq. in. but failure conditions did not prevail.

3. All other stress conditions.

A computer program was used to obtain the solutions. Since only

graphical solutions were developed for "G_o" and "b," it was necessary to provide the computer with a set of specific values in place of a general expression. This was done by considering a single curve to consist of a series of straight lines for which the slopes could be defined.

It should be pointed out that the procedure as outlined could be simplified in the following two ways:

1. By assigning to the parameter b a finite value when $\sigma_o = 0$. This would enable the determination of G for all values of σ_o and τ_o by means of equation (IV-12) and would eliminate the second category.

2. By establishing mathematical expressions for the relations between the initial tangent shear modulus and the independent variables, and for the relationship between the ultimate stress parameter b and its independent variables. This would avoid the need of approximating the relationships by a series of short straight lines.

Deflection Analysis

The deflection of a point on the surface of a semi-infinite mass due to a uniformly distributed load acting over a circular area can be obtained from equation (V-1) using the appropriate settlement factor I_w. The solution in this form cannot be used to obtain the deflection at any point within the mass.

More general solutions yielding the deflection at any point within a semi-infinite mass have been developed which permit the computation of the contribution of any layer within the mass by the method of differences. Such an equation has been developed by the U. S. Waterways Experiment Station (42, 43) for the case of a uniformly distributed load. It is a very complex equation involving several functions and will not be

repeated here since it is not in a form which is readily comprehensible. To facilitate its use, the functions have been evaluated and tabulated for a coordinated pattern of points within the semi-infinite mass.

For the special case of the settlement of a point along the vertical axis of symmetry the general expression is reduced to the following form (44):

$$w_z = (1 + \nu) \frac{pa}{E} \left[\sin \alpha + (1 - 2\nu) \frac{1 - \cos \alpha}{\sin \alpha} \right] \qquad \text{(V-8)}$$

in which: w_z = settlement of a point at a vertical distance of z from the boundary.

$$\alpha = \tan^{-1} \frac{a}{z}$$

It can be seen that equation (V-8) reduces to equation (V-1) (with a settlement factor of 1.0) for a point at the surface.

Equation (V-8) as well as making possible the computation of the contribution of any specific layer, permits the separation of the deflection into volumetric and shearing components. This is accomplished by multiplying through by $(\frac{1 + \nu}{E})$ and making the substitution

$$K = \frac{E}{3(1 - 2\nu)}, \quad G = \frac{E}{2(1 + \nu)}, \quad \nu = \frac{3K - 2G}{2(3K + G)}$$

Equation (V-8) can be written as:

$$w_z = pa \left[\frac{1}{2G} \sin \alpha + \frac{1 + \frac{3K - 2G}{2(3K + G)}}{3K} \frac{1 - \cos \alpha}{\sin \alpha} \right] \qquad \text{(V-9)}$$

Equation (V-9) permits the computation of the settlement of the center of a uniformly loaded area for the following conditions: a multi-

layered mass of finite depth; each layer a homogeneous isotropic solid having elastic constants G and K which are functions of the soil and the stress system in the layers. It should be pointed out that in reality the equation is the solution for a non-homogeneous, isotropic mass with the non-homogeneity arising from variations in the stresses rather than from a variation in soil properties.

A computer program was used to solve equations (V-9). A program was used that solved first for the stresses, then the associated bulk and shear moduli, then the compression of the layer. The compression of the individual layers were summed up to obtain the deflection at the surface.

Another computer program was set up for determining the stresses, bulk and shear moduli, and deflections for the same number of layers along a vertical line passing through the periphery of the plate. The method for determining the stresses and moduli was similar to that discussed earlier. The general expression for the settlement at any point within the mass could not be simplified for the case of deflection along the edge, and so the following procedure was adopted.

In a previous investigation by Vesic and Domaschuk (45) numerical values of the various functions contained in the general expression for deflection were combined into a single settlement factor which reduced the equation to a form identical with that given the equation (V-1). The equation could not be used in this form for the author's investigation since it is in terms of Young's modulus. Nonetheless, by means of these settlement factors, the settlement at points other than along the axis of symmetry can be expressed as a fraction of the settlement of corresponding

points along the axis of symmetry, due regard being paid to the use of appropriate moduli.

Figure 42 illustrates the relationship between the settlement of a point along a vertical line passing through the periphery of the plate and the corresponding point along the axis of symmetry for constant elastic parameters. This relationship was used in computing the deflection of a point on the edge of the uniformly loaded circular area.

Load-Settlement Analysis of a Rigid Plate Resting on the Surface of a Cohesionless Soil

The contact pressure under an absolutely rigid plate resting on the boundary of a semi-infinite mass was solved for by Boussinesq (32) and is given by:

$$p = \frac{P}{2\pi a \sqrt{a^2 - r^2}} \qquad \text{(V-10a)}$$

in which: p = contact pressure

P = total load on the plate

a = plate radius

r = horizontal distance of the point in question from the center of the plate.

Thus, in accordance with the equation, the contact pressure varies from a minimum

$$p_{min} = \frac{P}{2\pi a^2} \qquad \text{(V-10b)}$$

at the center of the plate, to a maximum of infinity at the edge of the

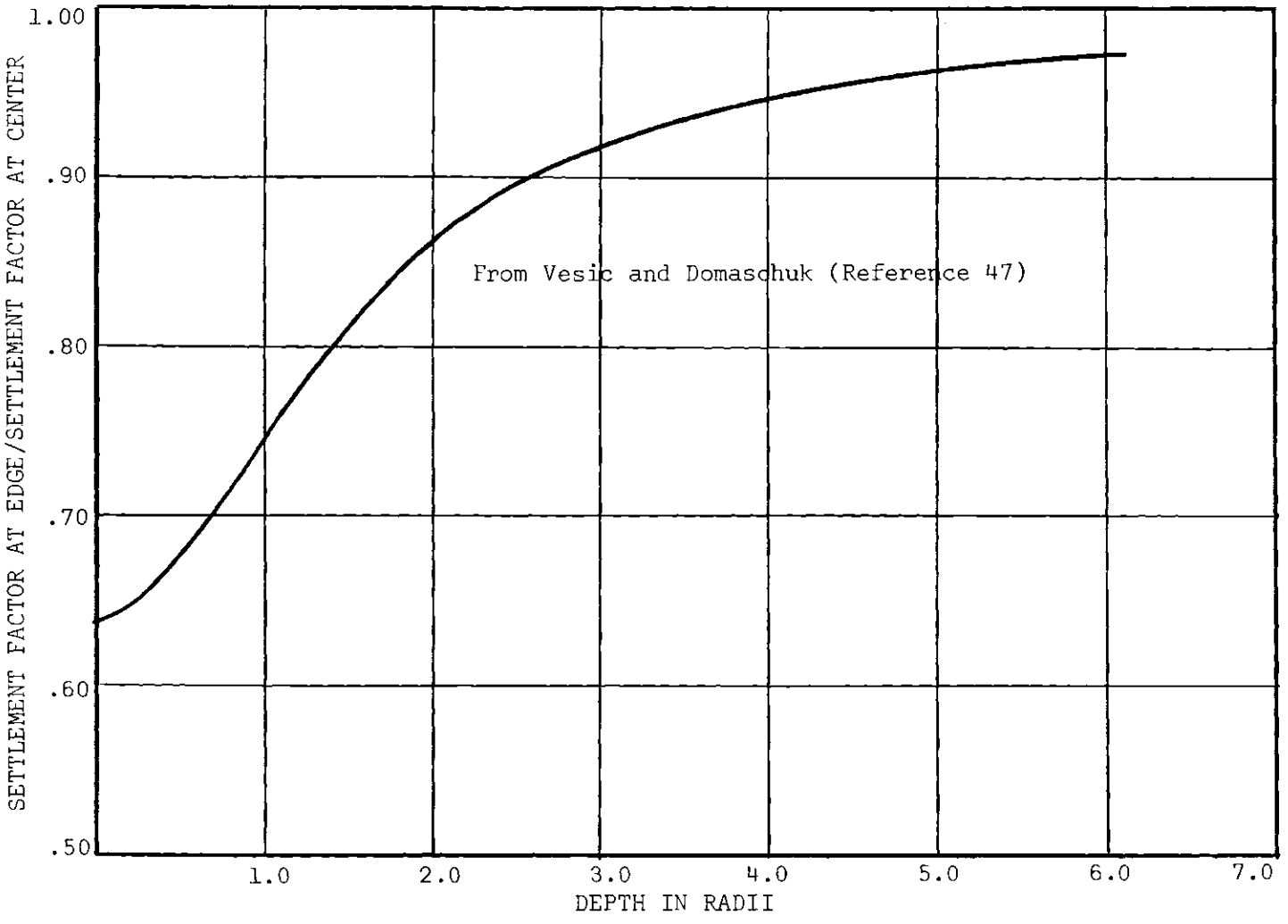

Figure 42. Ratio of Settlement Factors versus Depth for a Uniformly Loaded Circular Area.

plate where $r = a$ (Figure 43a). In reality, the material along the edge yields causing a redistribution of pressure. The redistribution of pressure is governed by the shear strength of the medium in the immediate vicinity of the edge of the plate. The net result is a considerable decrease in pressure from the theoretical at the edges, and an associated increase in pressure towards the center of the plate. Figure 43b illustrates such a pressure distribution for the case of a medium exhibiting a relatively constant shear strength.

For a rigid plate resting on the surface of a cohesionless soil, the pressure that can be developed at the periphery of the plate is necessarily limited because of the soil's dependence on lateral confinement for shearing resistance. In this respect the edge effects are more significant in the pressure redistribution under small plates than under large plates.

Experimental investigations of the nature of the contact pressure distribution under a rigid foundation resting on a cohesionless soil have been conducted. Early experiments using model tests by Kögler and Scheidig (46) indicated a convex parabolic pressure distribution which became more uniform as the size of the footing was increased or as the depth of foundation was increased. More recent tests by Schultze (47) and Bub (48) have indicated that by increasing the footing size and/or footing depth, a concave parabolic pressure distribution may be manifested.

Schultze compiled the results of eleven case histories involving the measurement of rigid footing contact pressures in buried foundations. Out of the eleven case histories, eight showed an accumulation of pressure at the edges. On the basis of his findings he has developed an

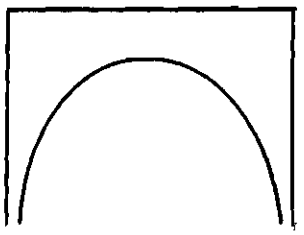

(a) Theoretical After Boussinesq

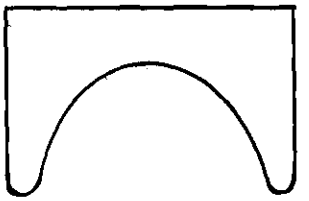

(b) Effect of Local Failure Along the Periphery

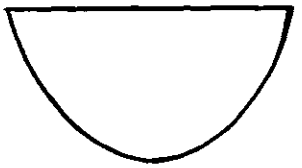

(c) As Determined Experimentally Using Small Plates

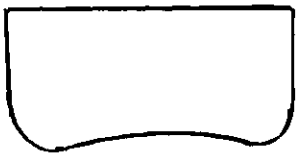

(d) As Determined Experimentally Using Large Plates or Increasing Footing Depth

Figure 43. Illustration of the Pressure Distribution Under a Rigid Footing.

elastic-plastic expression for rigid footing contact pressures, which combines the stress calculated according to the Boussinesq theory and the ultimate stress that can be developed at the edges in accordance with the Prandtl-Buisman theory of plastic equilibrium. The resulting pressure distribution is a function of the factor of safety against shear failure and may vary from full convex parabolic for a safety factor of one, to concave parabolic for a safety factor of two or three.

Figures 43c and 43d illustrate the nature of the pressure distribution as determined by experimental investigations.

Thus the experimental evidence indicates that for footings resting on the surface of cohesionless soil, the boundary pressure distribution can vary from convex parabolic to concave parabolic depending upon footing size. In many instances it approaches a uniform pressure distribution. In view of this, a uniform pressure distribution was assumed for all theoretical calculations. To utilize a pressure distribution other than uniform, would require its determination by experimentation since it has been demonstrated to be influenced by footing size and depth.

The solution for the settlement of a rigid circular plate resting on the surface of a semi-infinite mass was developed by Schliecher (49) and is of the form given by equation (V-1). The corresponding settlement factor is 0.79.

The settlement factors for the centre, the edge, and the average settlement, of a circular uniformly loaded area are 1.0, 0.64, and 0.85 respectively.

Thus it is seen that the average settlement of a flexible circular footing is very nearly identical to that of a rigid circular footing

despite the vastly different natures of assumed boundary pressure distributions. This would infer that the nature of the boundary pressure distribution has only a small influence on the magnitude of overall deflection of the footing. The difference in deflections lies primarily in the shape of the deflection bowl within and immediately adjacent to the loaded area, the importance of which lies in the computation of stresses in the foundation itself.

Since the experimental investigations have indicated that the pressure distribution under a rigid plate tends towards a uniform distribution, and since the overall deflection is not significantly affected by the nature of the pressure distribution it was felt that rigid plate bearing tests could be used to assess the validity of the concept of using stress dependent shear and bulk moduli for deflection computations.

Furthermore, to develop an apparatus that would ensure a uniform pressure distribution, and that would be sufficiently flexible to deflect without any restraint, would have been time consuming and costly.

A more deciding factor was the practical application of the concept. There are very few instances in which the member through which the distributed load is applied is completely flexible. One such instance would be a wheel load on a flexible pavement. However, the solution of this particular problem is better treated by methods incorporating repetitive and dynamic loading. The author's intent was to apply the concept to the settlement of foundations on cohesionless soils. In this respect the load transmitting member is generally semi-rigid to rigid with the exception of thin slabs which are often flexible. As well, by extending the concept to the settlement of foundations, it is possible to test its

validity by analyzing case histories.

CHAPTER VI

EXPERIMENTAL INVESTIGATION OF THE SETTLEMENT OF A RIGID PLATE RESTING ON THE SURFACE OF A SAND

Equipment and Materials

Test Pit and Loading Equipment

The tests were conducted in a cylindrical pit, 8 ft. 4 in. in diameter and 22 feet deep. The pit consists of corrigated pipe incased in concrete and has a concrete floor.

A 200 ton capacity frame over the pit acts as the reaction for loading purposes. The frame may be readily moved off the pit when not in use. Attached to the frame is a 200 ton capacity hydraulic jack that may be used for loading purposes or may be used for the vertical positioning of other loading apparatus.

The loading head of a Karol-Warner Conbell high pressure consolidometer was used up to its capacity of approximately 6 tons. For larger loads a 20 ton hydraulic jack was used.

The advantage of the Conbel loading apparatus was, that it was air activated and hence required no manual adjustments to compensate for the plate deflections that occurred. It provided a more accurate method of load application than could be achieved with the hydraulic jack.

Deflection measurements were made by micrometer dial gages (0.001 inch precision) mounted on the edges of the plate.

The test apparatus is shown in Figures 44 and 45.

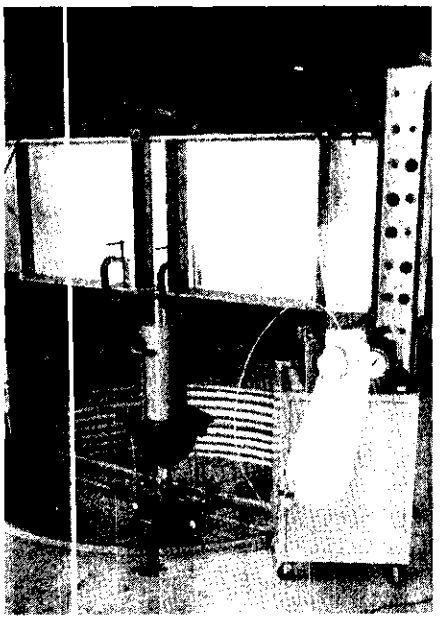

Figure 44. View of Test Pit and Loading Apparatus.

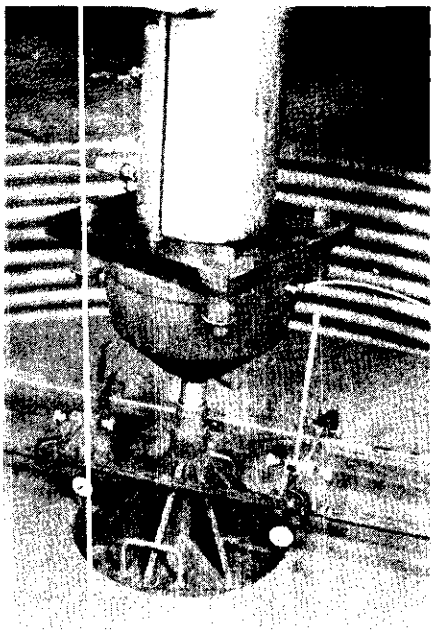

Figure 45. View of Instrumentation.

Model Foundation

A 17.5 inch diameter steel plate, made rigid by use of radial stiffeners, was used as the model foundation. The size was selected so as to maintain minimal side effects due to the rigid walls of the pit.

Soil

A micaceous sand identical to that used in the bulk and shear modulus studies was used for the plate load tests.

Test Procedure

Placing of Sand and Control of Density

A plate load test was conducted on the sand in a loose, medium, and dense state.

The loose state was achieved by pouring the sand through a long flexible six-inch diameter tubing. The sand was not permitted to drop into place but was allowed to accumulate in the bottom of the tubing from which it was poured into place.

A medium state of density was achieved by allowing the sand to fall through a distance of approximately three feet. The previously established relationship between height of fall and density indicated that for heights of fall in excess of 30 inches the density remained practically constant. An eight-foot diameter container with a perforated bottom was used for controlling the height of fall. It was lowered and raised as required by means of an overhead winch.

The dense state was attained by placing the sand in approximately six-inch layers and vibrating it by surface vibrators.

In each instance, a cone penetrometer was used to determine the

density by a method devised in conjunction with previous tests on the same sand (29). The cone penetrometer was forced into the sand by means of a screw jack at a rate of approximately four in. per minute. Total resistance to penetration was recorded at two inch depth intervals. The resistance was converted to an equivalent unit end resistance which was then converted to density according to an empirical relationship.

The density tests were performed at three different locations in the pit. The densities thus obtained varied in a random manner and the mean was used in the theoretical considerations.

Loading Procedure

The load was applied in two lbs. per sq. in. increments for the medium and dense sand and in one lb. per sq. in. increments in the case of the loose sand.

After each load increment, sufficient elapsed time was permitted to ensure almost complete static equilibrium. A new load increment was applied after the rate of deflection was equal to or less than 0.002 inches in a period of five minutes. The time required to reach this rate increased with load from approximately 10 minutes at small loads to 60 minutes as failure was approached.

Discussion of Test Results

The results of the plate load tests along with other pertinent information is given in Figure 46.

The load-settlement curves corresponding to the medium (Test No. 1) and dense (Test No. 3) sands are typical. They exhibit an initial portion in which small increases in load cause small increases in deflection,

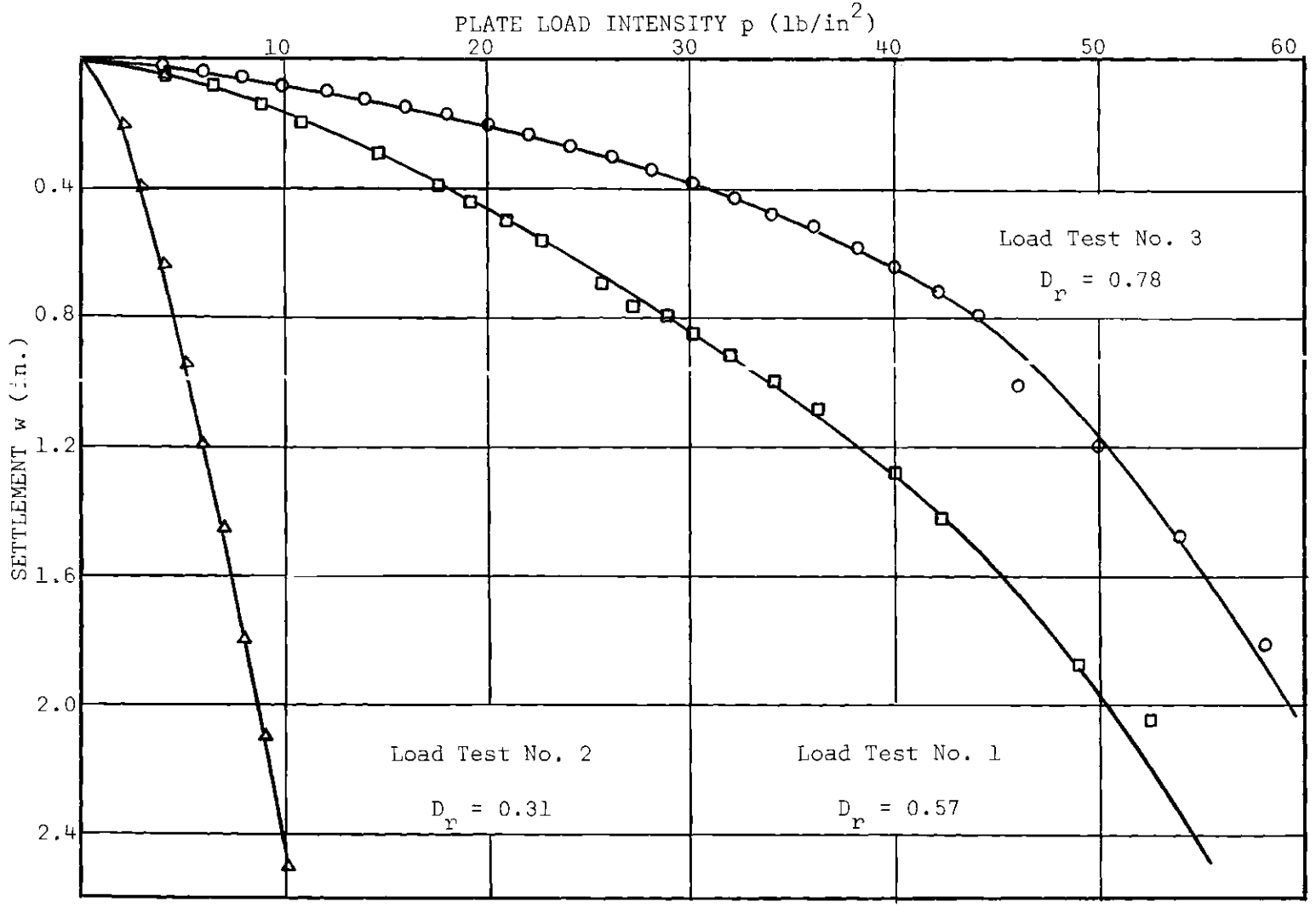

Figure 46. Load-Deflection Data for 17.5 in. Diameter Rigid Plate-Load Tests on Surface of Sand.

and a latter portion in which a small load increase results in a large increase of deflection. The point of transition which is sometimes referred to as failure, is more clearly defined in the case of the denser (Test No. 3) soil.

The load-settlement curve obtained for test No. 2 may be considered to depict failure in its entirety.

In terms of mode of bearing capacity failure, general shear failure occurred in the case of the dense sand, and local or punching shear failure occurred in the mecium and loose sand.

Correlation Between Theoretical and Experimental Load-Settlement Curves

Before discussing the correlation between the theoretical and experimental load-settlement curves it would be instructive to consider the nature of a theoretical curve in terms of the response of the soil at different depths and at different stress intensities acting on the boundary.

Variation in Octahedral Normal and Shear Stresses with Depth

To illustrate the variation in octahedral normal and shear stresses with depth, the stresses corresponding to a uniform pressure of 20 lbs. per sq. in., and a soil unit weight of 91.0 lbs. per cu. foot (Test No. 1), were plotted versus depth along the axis of symmetry. The results are shown in Figure 47.

The octahedral normal stress is seen to decrease very rapidly to a minimum at a depth of approximately 4 radii and then to increase slowly and linearly with depth. To a depth of 4 radii, the boundary load

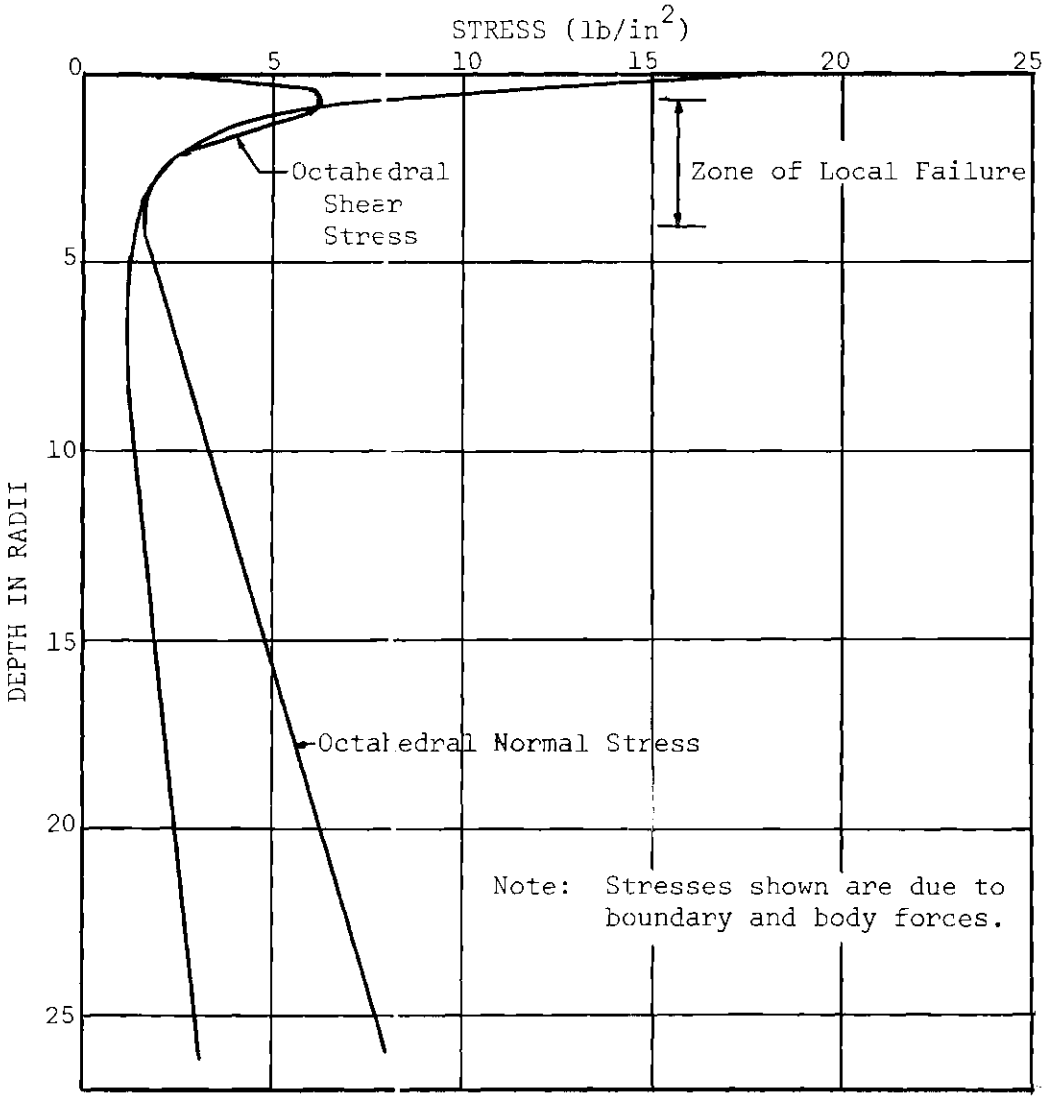

Figure 47. Variation in Octahedral Normal and Shear Stresses with Depth Along the Axis of Symmetry for a Uniform Pressure Distribution of 20 lbs. per sq. in. Acting on the Surface.

predominates while at depths beyond 4 radii, the body forces predominate.

The octahedral shear stress increases to a depth of approximately 0.7 radii, then decreases to a depth of about 6 radii, then increases linearly with depth.

Since for the sand investigated, failure conditions prevailed when the ratio of the octahedral normal stress to the octahedral shear stress was less than approximately 1.5, there was a zone, as indicated in Figure 47, in which failure conditions existed.

Variation in Bulk and Shear Moduli with Depth

For the stresses indicated in Figure 47, the corresponding values of the bulk and shear moduli were presented graphically in Figure 48.

The bulk modulus is a function of the octahedral normal stress only, for a given initial density, and therefore its variation with depth is very similar to that of the octahedral normal stress.

The shear modulus, on the other hand, is a function of the octahedral normal and shear stresses for a given initial density. Consequently its variation with depth differs from that of the bulk modulus. The discontinuity at a depth of 18 radii is a consequence of the fact that a single continuous function was not used to relate the shear modulus to the stress system.

The shear modulus in the zone of failure cannot be defined by previously established relationships and must therefore be assigned some arbitrary value in this zone as discussed previously.

The significance of Figure 48 is that it points out the extreme variations in bulk and shear moduli in the immediate vicinity of the boundary where deflections are the highest. It also implies that there

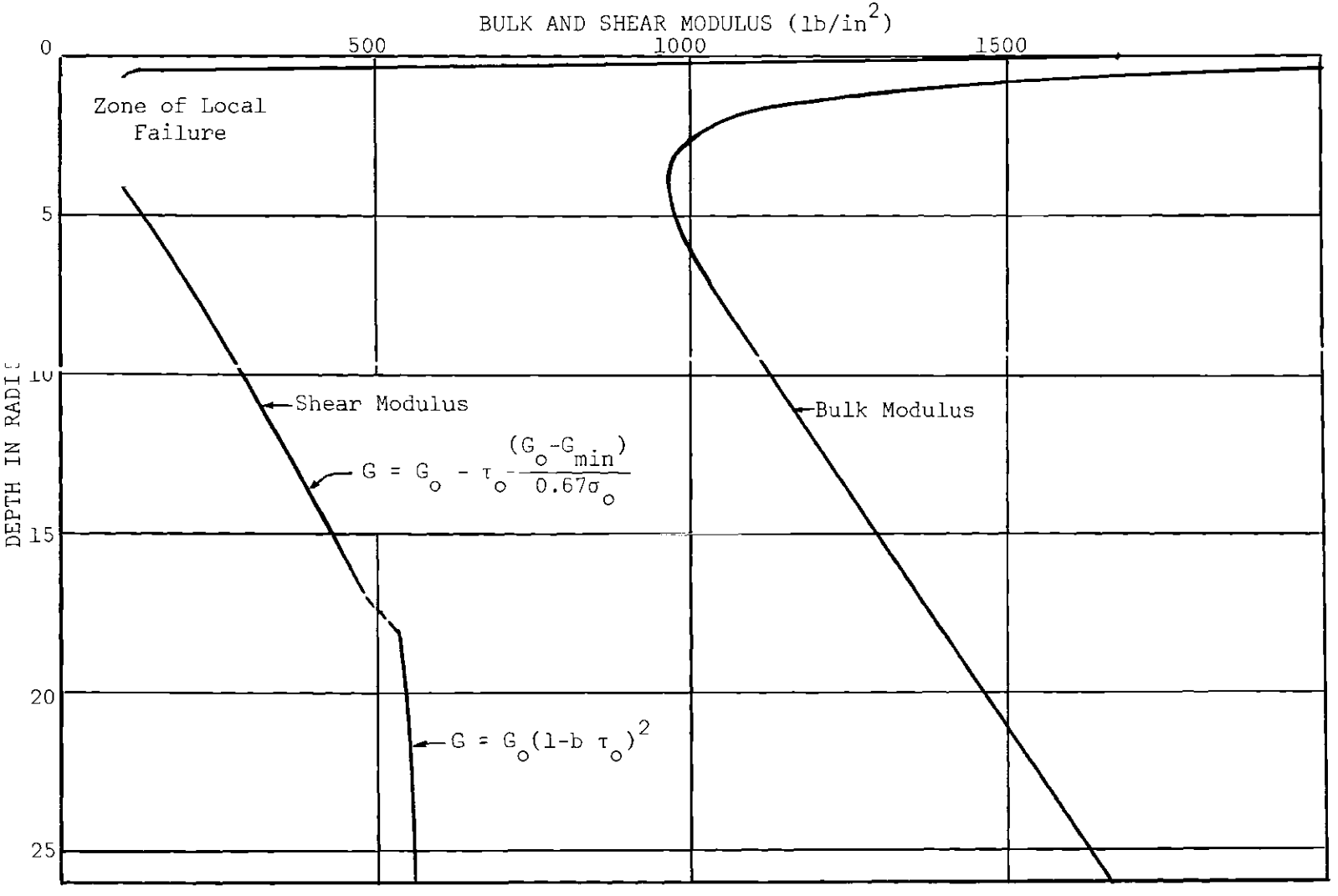

Figure 48. Variation in Bulk and Shear Modulus with Depth along the Axis of Symmetry for a Uniform Pressure Distribution of 20 lbs. per sq. in. Acting on the Surface.

does not exist a single unique relationship between the bulk and shear moduli in terms of elastic constants only.

Variation in Deflection with Depth

To illustrate the variations in the deflection with depth a plot was prepared of the cumulative compression within the layers, expressed as a per cent of the total (Figure 49). The data corresponds to the stresses and moduli depicted in Figures 47 and 48.

As can be seen from Figure 49, the major portion of the deflection is due to compression of the soil within a depth of approximately two diameters.

Nature of the Theoretical Load-Settlement Relationship

To obtain an indication and an understanding of the nature of the theoretical load-settlement curve it is necessary to examine the behavior of a point within the soil mass, to changes in the stress system. To illustrate the behavior, a point immediately below the plate (depth = 0.4a), and a point at a greater depth, 7a, was selected. The variation in bulk and shear moduli with load intensity is given for each point in Figures 50 and 51. The compression of a thin layer containing each point is also presented in each respective figure. The actual magnitude of the compression of each layer should not be compared since the layer thicknesses are not equal. They are merely used to indicate the variation in deflection with load intensity.

Considering first the point at a depth of 0.4a, it is seen that both the bulk and shear moduli increase with load intensity. Consequently the compression of the layer increases with load intensity but at a decreasing rate.

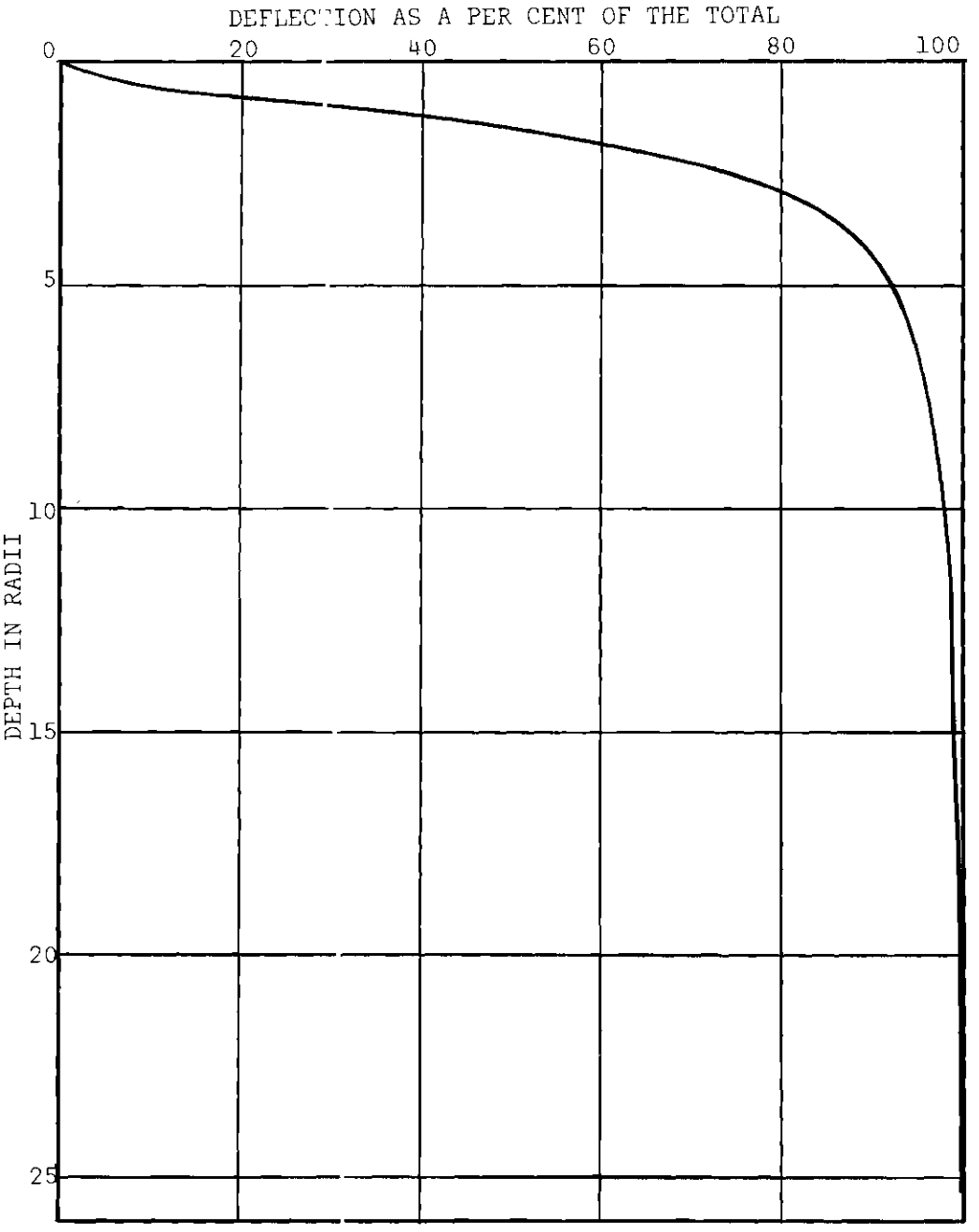

Figure 49. Variation in Deflection with Depth for a Uniform Pressure Distribution of 20 lbs. per sq. in. Acting on the Surface.

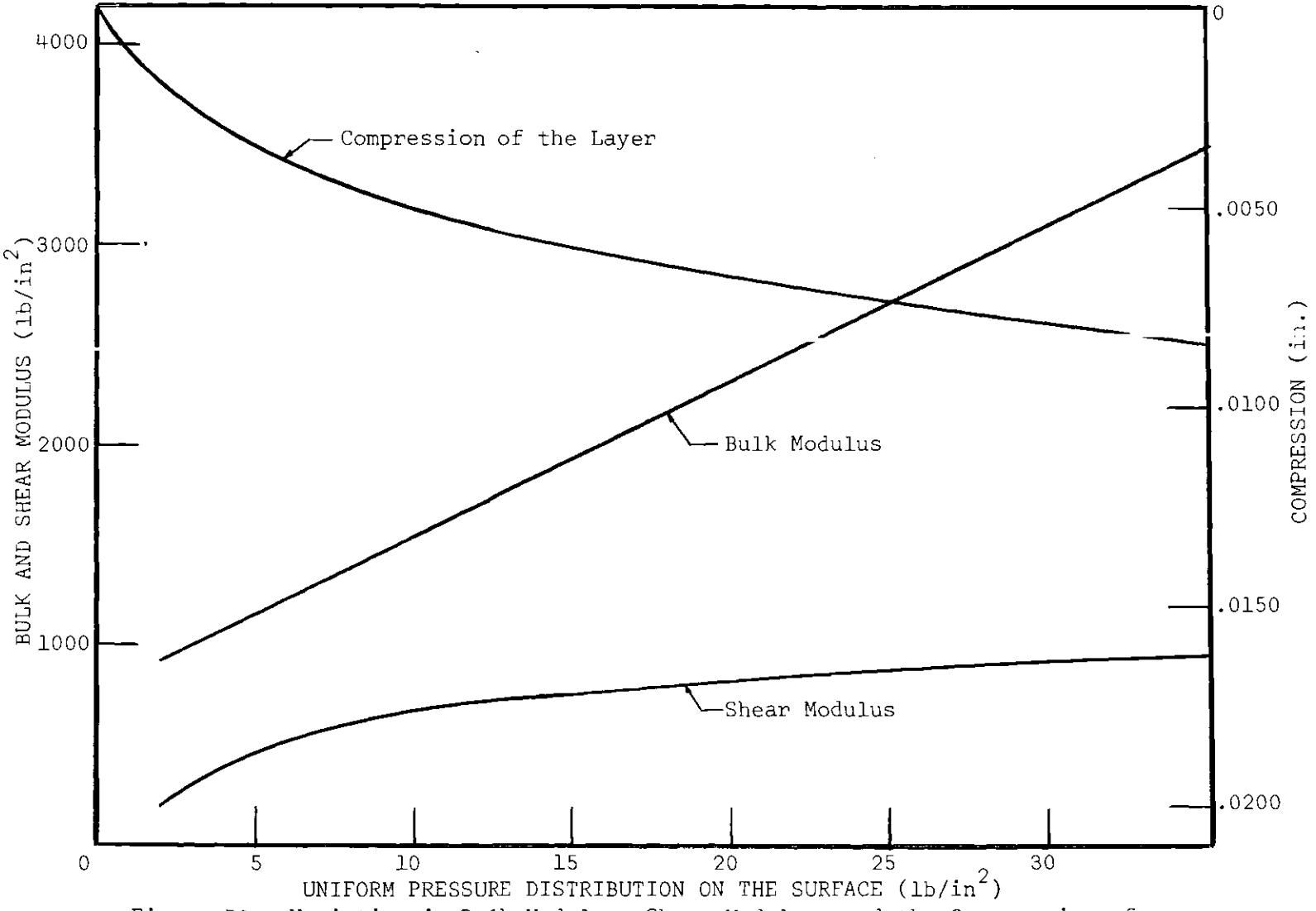

Figure 50. Variation in Bulk Modulus, Shear Modulus, and the Compression of a Thin Layer at a Depth of 0.4 Radii.

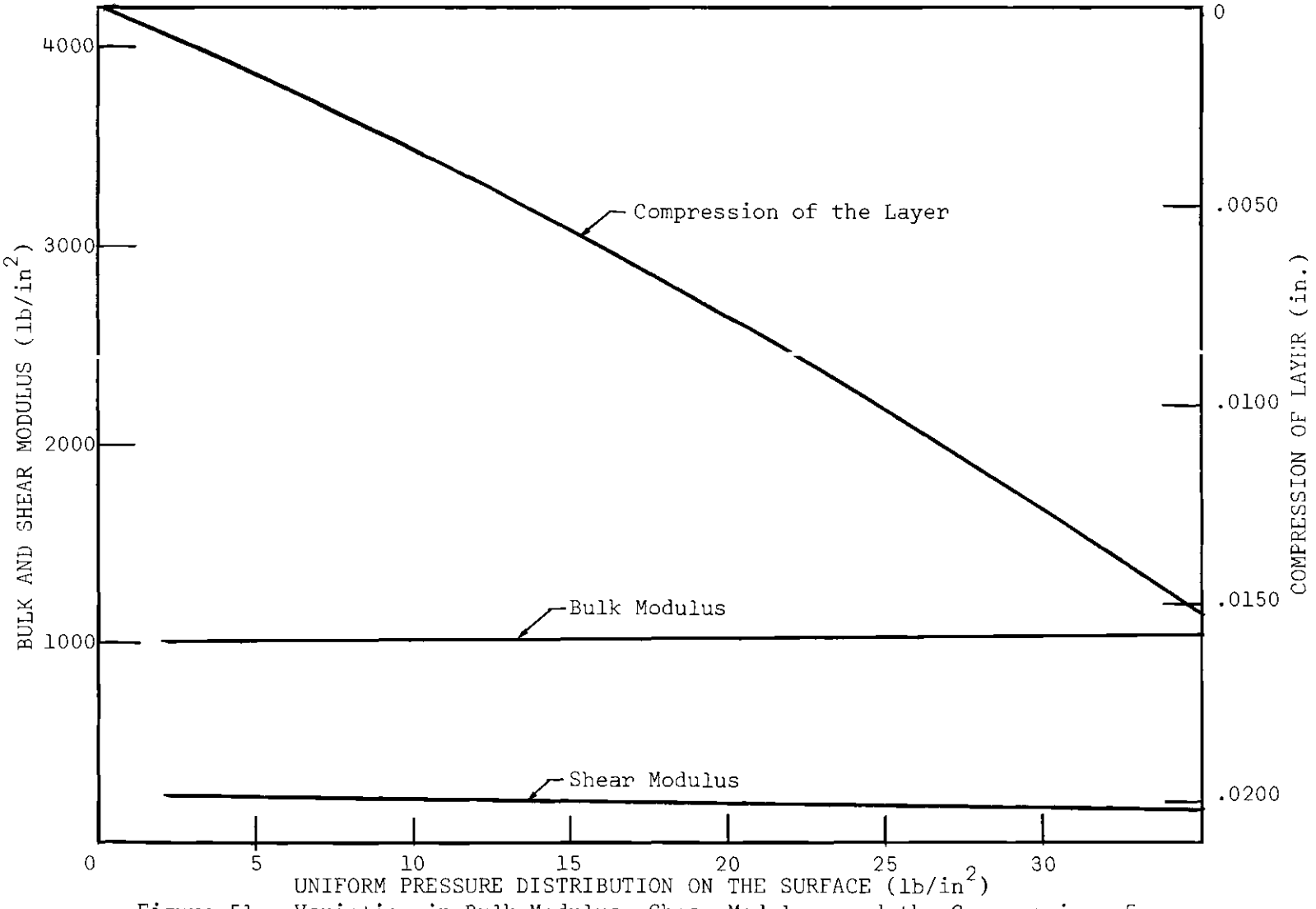

Figure 51. Variation in Bulk Modulus, Shear Modulus, and the Compression of a Thin Layer at a Depth of 7 Radii.

For the point at a depth of 7a, the bulk modulus increases linearly with the load intensity at a very low rate while the shear modulus decreases linearly with load intensity at a low rate. The effect of the increase in bulk modulus is to reduce the rate of increase in deflection, while the effect of the decrease in shear modulus is to increase the rate of increase in deflection. The shear modulus effect is somewhat larger than that of the bulk modulus causing a slight downward trend of the compression curve.

Thus in some layers the load-deflection curve is of the nature depicted by Figure 50, while in others it may be that depicted by Figure 51. The load settlement curve of a point on the surface is the cumulative sum of all layers and hence its nature will depend on the prevalence of the two types illustrated.

From the figure it is evident that the assignment of a constant shear modulus to the zone of local failure will result in a load-compression curve similar to that shown in Figure 50.

It is instructive at this point to recall that in an elastic analysis based on a Young's modulus, the deflection of a point within the soil is directly proportional to the load intensity. Using bulk and shear moduli that are function of the stress system, it has been demonstrated that the relationship is not linear and may deviate in both directions from linearity.

Comparison of Theoretical and Experimental Load-Settlement Curves

For comparative purposes, the experimental and the corresponding theoretical curves are presented on common plots in Figures 52, 53, and 54.

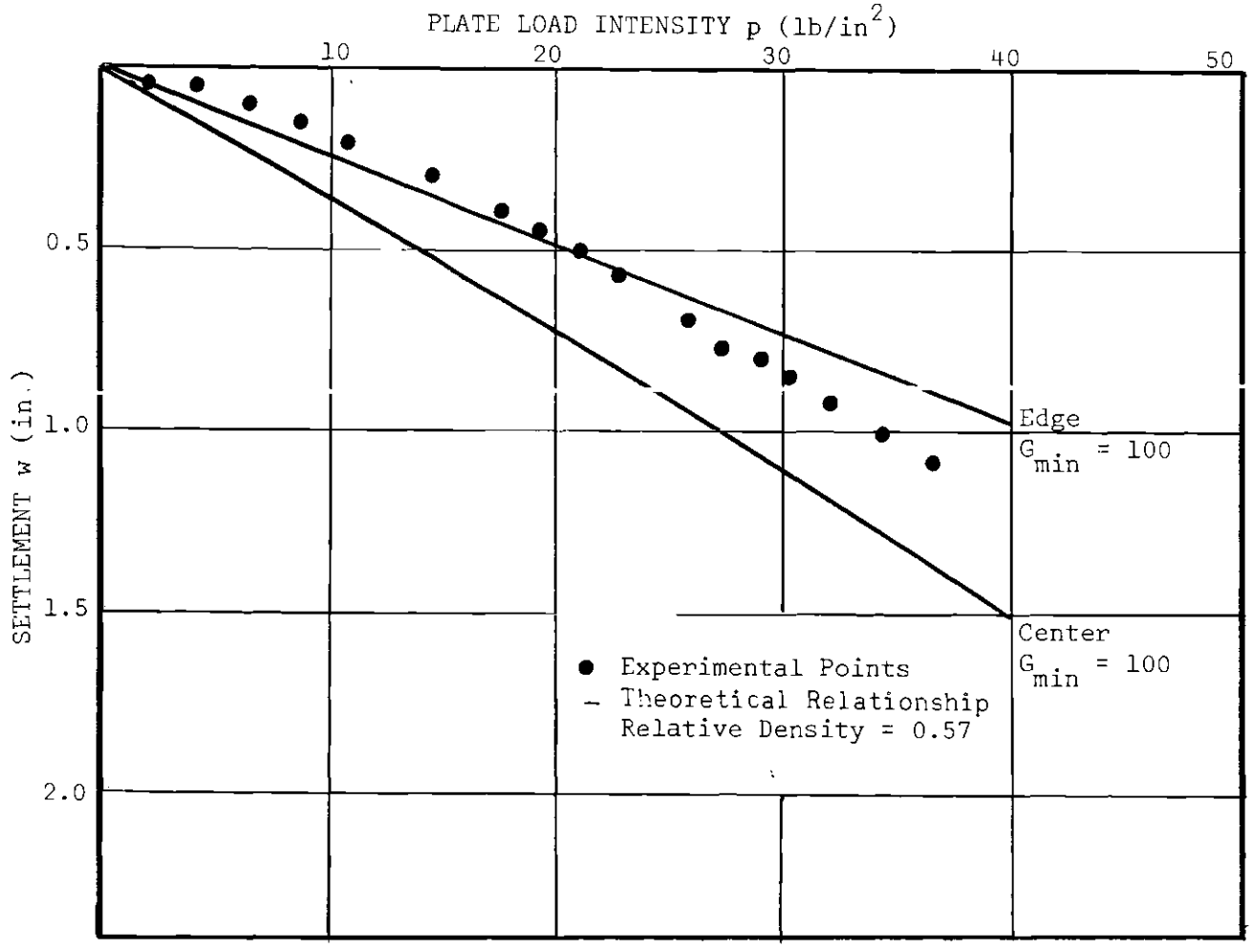

Figure 52. A Comparison of Experimental and Theoretical Load-Settlement Data for Plate Load Test No. 1.

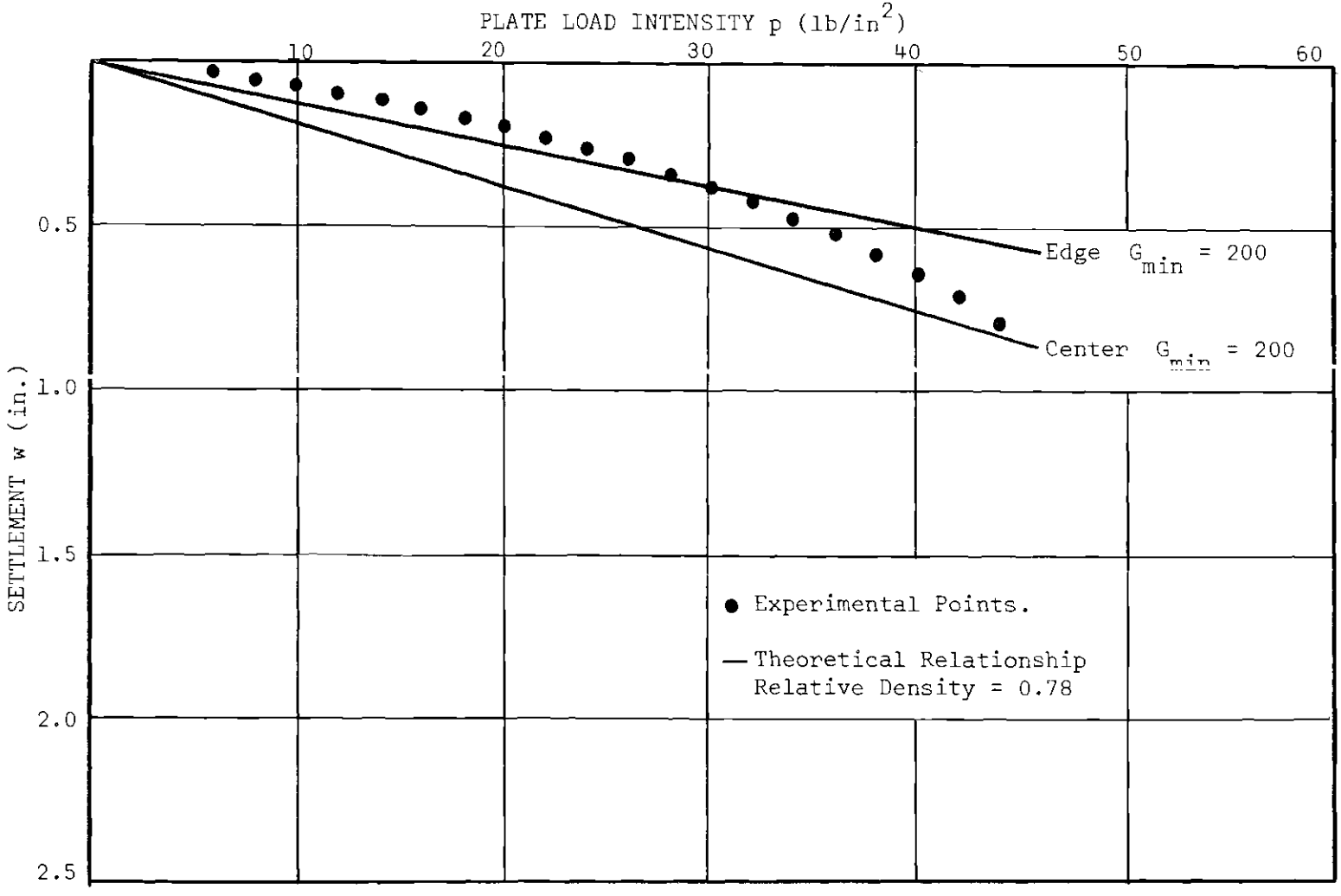

Figure 53. A Comparison of Experimental and Theoretical Load-Settlement Data for Plate Load Test No. 3.

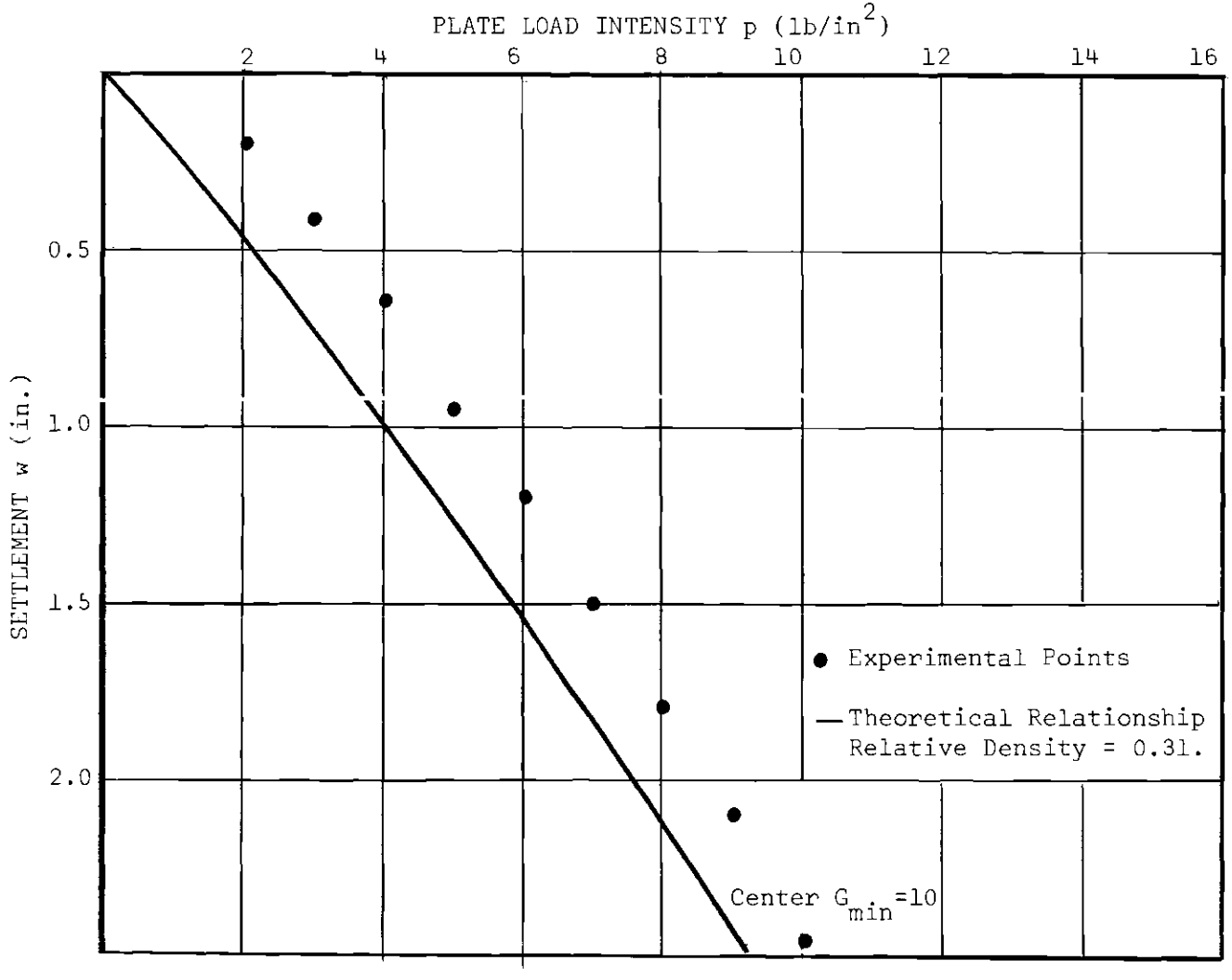

Figure 54. A Comparison of Experimental and Theoretical Load-Settlement Data for Plate Load Test No. 2.

The theoretical curves are based on a uniform pressure distribution on the boundary and therefore the deflection along the boundary is bowl-shaped. For a comparison of theoretical and experimental results, the load-deflection curve was obtained for a point in the center and a point on the edge of the uniformly loaded area. If the pressure distribution under the rigid plate was also uniformly distributed, the load-deflection curve for the plate would be expected to fall approximately mid-way between the two theoretical curves.

As mentioned previously, it was necessary to assign a shear modulus to the soil within the zone where local failure prevailed, as defined by the ratio of octahedral normal to octahedral shear stress. It was felt that the shear modulus based on the triaxial tests, at the stage just prior to complete failure of the sample, would be a good representation of the shear modulus that could be used to characterize local failure. On this basis, the value might range from approximately 100 to 300 lbs. per sq. in. The sand in a dense state would intuitively exhibit a higher value than when in a loose state. The theoretical curves shown in Figures 52 and 53 are based on minimum shear moduli of 200 for the dense sand and 100 for the medium dense sand. In the case of the loose sand (Test No. 3), the load-settlement curve would imply failure at very small loads and the test took on the nature of a resistance to penetration test. It is interesting that by assigning a minimum shear modulus of 10 lbs. per sq. in., a reasonable theoretical proximity of the experimental load-deflection curve is obtained. This would suggest the possibilities of obtaining a complete load settlement curve, by permitting the shear modulus to approach a very small value as overall failure became imminent.

Based on the assigned minimum values of shear moduli, it may be said that there is generally fair agreement between the theoretical and experimental load-settlement curves, insofar as relative magnitudes are concerned. There is considerable deviation in the nature of the respective curves. The theoretical curves are for practical purposes of a linear nature whereas the experimental curves are concave downward.

The reason for the linearity of the theoretical curves arises primarily from the use of a constant minimum shear modulus within the zone of local failure. It will be remembered that this imposition resulted in a load-deflection curve that had a decreasing slope. This had the effect of nullifying any tendency for a load-deflection curve with an increasing slope.

To illustrate the influence of the zone of failure, a load-settlement curve was obtained for a hypothetical case using a surcharge of 10 lbs. per sq. in. in conjunction with the data for the dense sand. The surcharge had the effect of eliminating local failure for an initial portion of the load-deflection relationship. The results are shown in Figure 55.

As can be seen from Figure 55, the load-settlement relationship up to the point of the first occurrence of local failure, is non-linear with an increasing slope. This portion of the curve is important in that it truly illustrates the concept of utilizing variable bulk and shear moduli to characterize the response of the soil.

Beyond the point of initiation of local failure, the theoretical points deviate from a smooth curve and there is a tendency towards linearity as the extent of local failure increases.

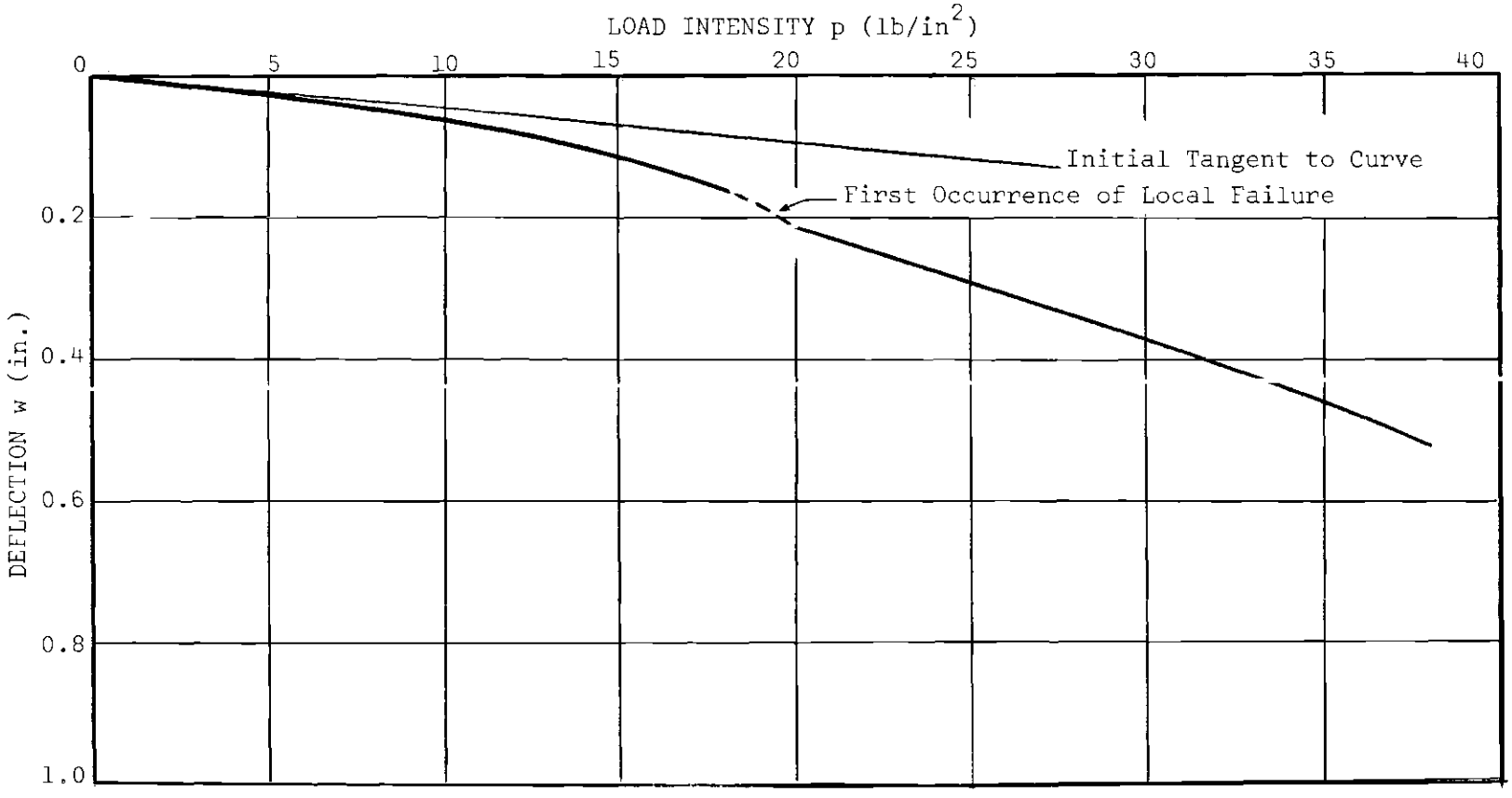

Figure 55. Theoretical Load-Deflection Relationship for Plate Load Test No. 3 Combined with a Surcharge of 10 lbs. per sq. in.

As an alternative to the assignment of a constant shear modulus to the zone of local failure, the following method was used. The shear modulus was expressed as a linear function of the ratio of the octahedral normal stress to the octahedral shear stress and was permitted to approach zero as the ratio approached zero. This method was more consistent with the method of defining the limit of the shear modulus as outlined in the shear modulus study.

From the deflection equation (V-9) it is apparent that permitting the shear modulus to approach zero increases the magnitude of deflection substantially. To obtain good correlation between the magnitude of experimental and theoretical deflection, increased values of the shear modulus at incipient failure had to be used. For the dense sand a value of 300 was used in place of 200 and for the medium dense sand a value of 200 was used in place of 100.

The results are given in Figures 56 and 57. As can be seen from the figures, the method outlined had the effect of making the load-deflection curves non-linear but not to the same degree as the experimental curves.

The merits of this approach to that of using a constant shear modulus in the local failure zone cannot be properly assessed since each method is influenced by an assumed behavior of the soil under conditions of failure.

Other possible reasons for the difference between the theoretical and experimental curves are:

1. The effect of a non-uniform pressure under the rigid plate.

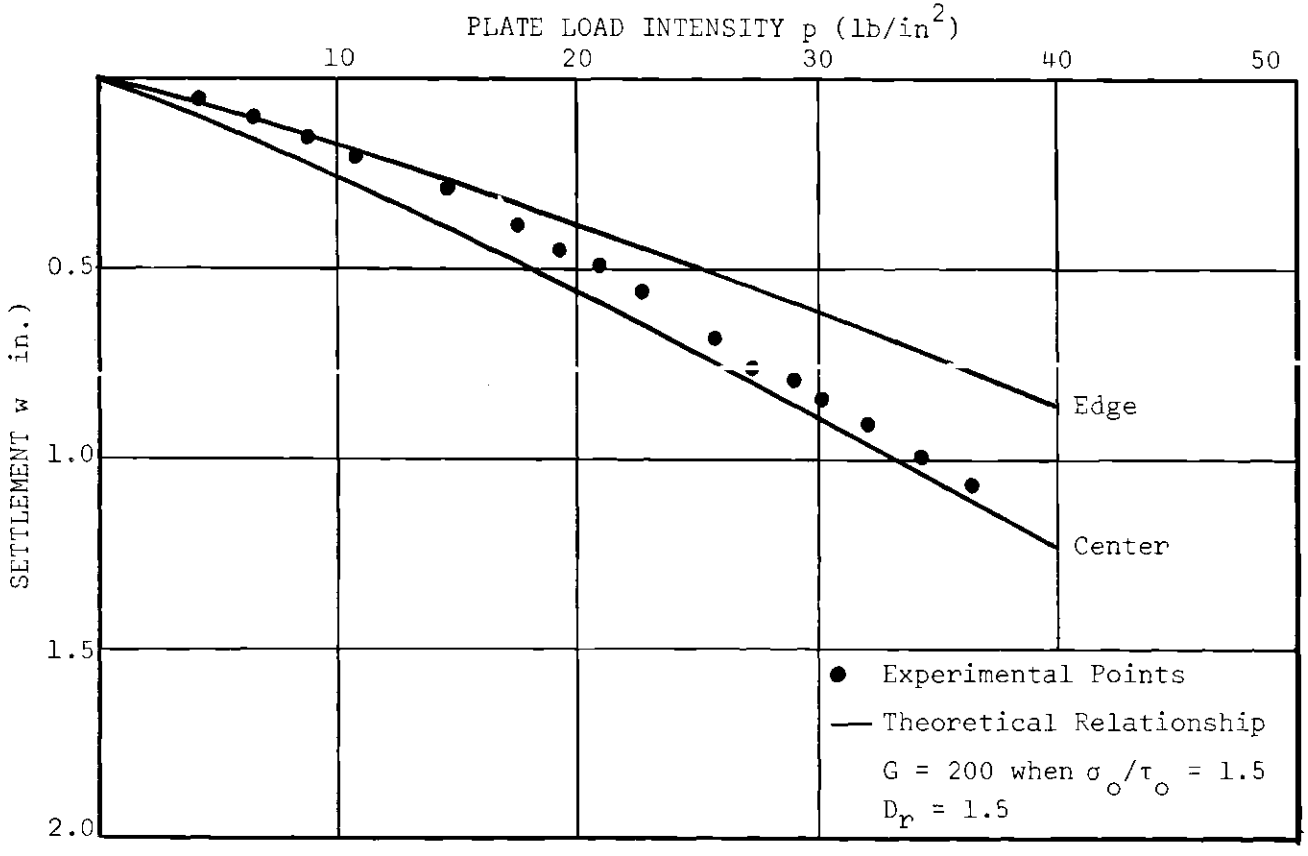

Figure 56. A Comparison of Experimental and Theoretical Load-Settlement Data: Load Test No. 1.

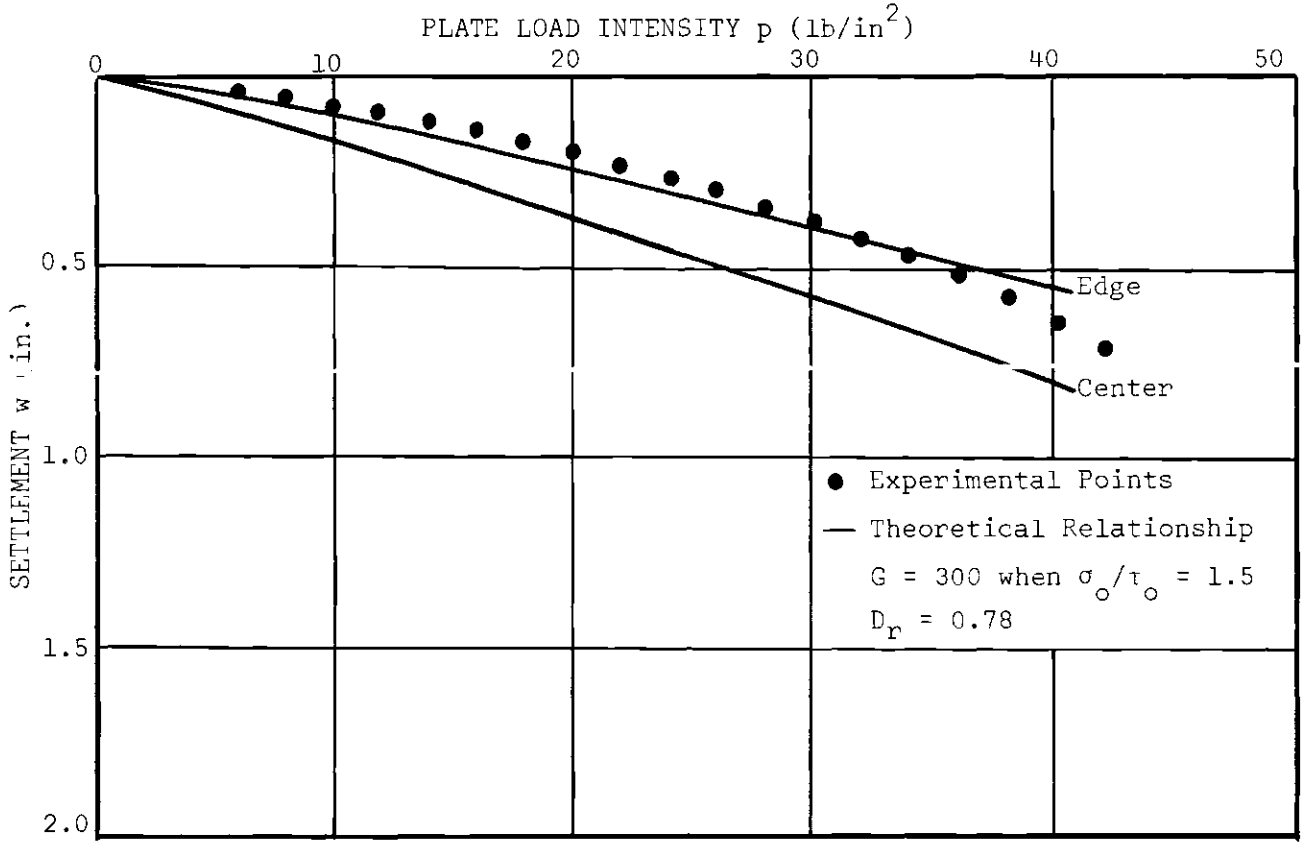

Figure 57. A Comparison of Experimental and Theoretical Load-Settlement Data: Load Test No. 3.

2. The actual stress distribution in the soil mass may be different from that computed according to the Boussinesq theory.

3. Discrepancy between the behavior of a soil mass and that predicted on the basis of laboratory tests.

Conclusions

Based on a uniform pressure distribution acting over a circular area on the surface of a cohesionless soil, the following conclusions may be drawn regarding the behavior of the soil:

1. The bulk and shear moduli defined in terms of octahedral normal and shear stresses, show considerable variance with depth, particularly within the depth of 0 to 2 diameters.

2. The major portion of the deflection is due to the compression of the sand within a depth of 2 diameters.

3. The load-compression relationship of a layer within the mass may be linear, may be non-linear with a decreasing slope, or non-linear with an increasing slope, depending upon the location of the layer with respect to the surface. For layers along the axis of symmetry, as the depth is increased, the relationship changes from non-linear with decreasing slope, to linear, to non-linear with increasing slope.

4. There is a local failure zone within the soil mass as defined by the ratio of the octahedral normal stress to the octahedral shear stress.

5. The existence of local failure necessitates the assigning of a shear modulus to the soil within the failure zone, for which there is neither an empirical nor a theoretical basis.

6. The effect of assigning a constant shear modulus to the failure zone is to render the load-deflection relationship linear, and thus nullify to a large degree the entire concept of non-linear stress-strain response.

7. The theoretical load-deflection curve is sensitive to the method of characterizing the behavior of the soil in the local failure zone.

8. The load-deflection curve for a no local failure condition is non-linear with a continuously increasing slope.

Based on the experimental investigation of the settlement of a rigid plate resting on the surface of a cohesionless soil it may be concluded that:

1. The load-deflection curve is non-linear with an increasing slope.

2. The degree of correlation between theoretical and experimental load-deflection data is influenced by the method used to characterize the behavior of the soil in the local failure zone.

PART C

CONCLUSIONS AND RECOMMENDATIONS FOR THE STUDY

CHAPTER VII

CONCLUSIONS FOR THE STUDY

This chapter is devoted to the compilation and integration of the conclusions of the analytical and experimental studies that were investigated separately. The order in which they are presented is not necessarily the order in which they appeared in previous chapters.

1. The stress-strain behavior of a cohesionless soil may be stated in terms of the volumetric and shearing components, with a bulk modulus and a shear modulus characterizing each component respectively.

2. The bulk modulus is a function of the density of the soil and the octahedral normal stress.

3. For a given initial density, it was found that for the Chattahoochee sand, two straight line segments served to relate the bulk modulus and the octahedral normal stress over an octahedral normal stress range of 0 to 100 lbs. per sq. in.

4. The slopes of the straight line segments may be empirically related to the initial relative density of the soil.

5. The intercept of the first segment is a function of the initial density of the soil, and an empirical linear relationship may be used to relate the two parameters.

6. The octahedral normal stress at the common point of the two line segments, represents the point of maximum change in bulk modulus and may be empirically related to the initial relative density of the soil.

7. The solution for the bulk modulus at a specified octahedral normal stress, and at an initial relative density may be obtained by the use of four empirically determined parameters which define the initial tangent modulus, the rates of change of the modulus, and the octahedral normal stress at which there is a change in the rate of change in modulus.

8. The volumetric strain-octahedral normal stress relationship obtained for isotropic compression tests may be represented by mathematical expressions of the form

$$\varepsilon = \frac{1}{m} \ln (B + m \sigma_o) - C$$

9. For the Chattahoochee sand and an octahedral normal stress range of 0 to 100 lbs. per sq. in., the elastic and permanent volume changes varied linearly (by parts), from (25:75) to (65:35) as the relative density was increased from 0.15 to 0.80.

10. The modulus of shear as defined by the instantaneous slope of the octahedral stress-strain curve obtained for a constant octahedral normal stress triaxial compression test is a function of the density of the soil, the octahedral normal stress, and the octahedral shear stress.

11. The modulus of shear may be expressed by the equation

$$G = G_o (1 - b \tau_o)^2$$

12. The initial tangent shear modulus (G_o) is a function of the octahedral normal stress and the relative density of the soil and may be empirically related to these two parameters.

13. The parameter b is the reciprocal of the octahedral shear

at failure and may be empirically related to the relative density of the soil and the octahedral normal stress.

14. The octahedral stress-strain relationship may be represented by a two parameter hyperbolic function of the form

$$\tau_o = \frac{\gamma_o}{a + b\,\gamma_o}$$

15. For the Chattahoochee sand, there existed a unique relationship between the octahedral normal stress and the octahedral shear stress at failure.

16. The deflection of a point on or within a semi-infinite mass due to a uniformly distributed load acting over a circular area on the boundary may be expressed in terms of the bulk and shear moduli of the mass, assuming the Boussinesq pressure distribution, by the equation:

$$w_z = pa\left[\frac{1}{2G}\sin\alpha + \frac{1 + \frac{3K - 2G}{2(3K+G)}}{3K}\,\frac{1 - \cos\alpha}{\sin\alpha}\right]$$

17. The bulk and shear moduli at any point within the mass may be defined in terms of the octahedral normal and octahedral shear stress at that point.

18. Assuming the Boussinesq stress distribution, the octahedral normal and shear stresses throughout the mass may be obtained from the first and second stress invariants.

19. The variation in bulk and shear moduli throughout the mass may be taken into account in deflection computations by assuming the mass to consist of a multi-layered system, with the response of each layer characterized by an average bulk and shear modulus.

20. The pattern of layers in the multi-layered system is not horizontal but is bulb-shaped reflecting the octahedral stress contours.

21. The major portion of the surface deflection is the result of compression of the soil within a depth of about 2 diameters according to the theory used.

22. The shear strength properties of the Chattahoochee sand are such that there exists a state of local failure at some points within the mass due to a uniformly distributed load acting over a circular area on the boundary.

23. If a constant shear modulus is assigned to the zone of local failure, the effect is to linearize the load-deflection relationship.

24. By the use of a surcharge on the boundary, the local failure condition can be eliminated and the resulting load-settlement relationship is non-linear with an increasing slope, which truly represents the concept of introducing stress dependent bulk and shear moduli in place of a constant Young's modulus and Poisson's ratio.

25. The use of the concept in predicting the settlement of a foundation resting on or near the surface of a cohesionless soil requires the assigning of a shear modulus to the zone of local failure for which there is no experimental basis at present.

26. The concept of separating the volumetric and shearing components of the stress-strain behavior of a cohesionless soil is both sound and practical and it may be used to solve certain soil mechanics problems.

CHAPTER VIII

CRITICAL APPRAISAL OF THE STUDY AND RECOMMENDATIONS FOR FURTHER STUDY

This chapter is devoted to an appraisal of the investigation with the intent of pointing out the limitations, areas of weakness, and to make recommendations for further study.

Appraisal of the Concept

The concept which forms the basis for the study embraces two assertions:

First, that a separation of the stress-strain relationship of a cohesionless soil into volumetric and deviatoric components might better portray the response of the soil in some soil mechanics problems, the solutions of which have the theory of elasticity as their basis. This constitutes the replacement of Young's modulus and Poisson's ratio by the bulk and shear moduli.

Secondly, for cohesionless soils, the moduli are not constant but are functions of the soil properties and the imposed stress system.

This concept can be criticized in that it adds further complexity to the analysis of a material, the behavior of which may be so erratic as to preclude the use of any rational approach. However erraticalness is always measured relative to the method of analysis and hence if the method is inadequate, erraticalness must prevail.

The concept can also be criticized in that the use of two

independent constants, the bulk and shear moduli, is incongruous with the theory of elasticity which implies a unique relationship between the two for a homogeneous isotropic media. The assumption that the moduli are functions of the stress system changes the solution to that for a non-homogeneous soil. However, by treating the soil as a multilayered system, with each layer characterized by an individual set of elastic parameters, and by assuming the law of superposition to be valid, permits the use of solutions based on the theory of elasticity.

In summary it may be said that the present method of applying the theory of elasticity to the solution of soil mechanics problems has proven to be inadequate in the solution of some of these problems. This serves as adequate justification for a search for improved methods.

Bulk Modulus Study

Experimental Investigation

It is felt that more accurate methods might be employed in defining initial conditions. Since initial density was used as the basis of correlation, its accurate determination is essential to the analysis.

The end platens introduce some shearing stress in the sample and affect the volume change characteristics of the soil contained within the "cone." Hence it would be preferable to use a device which does not have any rigid part in contact with the soil.

The magnitude of volume change due to membrane penetration should be ascertained and taken into account if it is found to be significant.

Analytical Study

The use of two straight line segments to define the octahedral

normal stress-bulk modulus relationship is a good approximation as evidenced by a comparison of the experimental stress-strain data and the relationship as given by the mathematical expression. It would be preferable to develop a single continuous relationship. Moreover, there does not appear to be any physical reason for the abrupt change in the rate of change of bulk modulus with octahedral normal stress inherent in the analysis.

Shear Modulus Study

Experimental Investigation

Some problems existed in defining initial conditions accurately. This applied particularly to the axial strain that occurred during the build up of the cell pressure. It might be preferable to use optical methods or a micrometer dial gage directly in contact with the upper platen.

The use of a load cell within the triaxial cell would eliminate any error resulting from induced side friction acting on the piston.

The scope of this investigation should be extended to include a greater number of initial densities and to cover a wider range of octahedral normal stresses, particularly very low octahedral normal stresses. For the low octahedral normal stresses an improved method of applying both the cell pressure and the axial load would be required. The investigation would have to include a study of the effects of utilizing different stress increments since very small increments would be used for low octahedral normal stresses.

Analytical Study

The two parameter hyperbolic function would seem to be a good mathematical representation of the experimental octahedral stress-strain relationship. One drawback lies in the establishment of the parameters at very low octahedral normal stresses. It would be desirable to obtain single continuous mathematical expressions that would relate the parameters (initial shear modulus, and ultimate stress) to the relative density of the soil, and the octahedral normal stress.

Load-Deflection Study

To illustrate the use of a variable bulk and shear modulus for characterizing the behavior of a cohesionless soil, the problem of the deflection under a uniformly distributed load acting over a circular area, provided a good example. However it did present the problem of having to characterize the response of the soil when local failure occurred. Since this is a problem that does exist in practice, the need for a study dealing with this particular aspect is obvious.

The concept should be extended to other forms of boundary pressure distribution, particularly full and partial parabolic, as well as to square and rectangular footings, to obtain a better facsimile of actual building foundations.

The concept should also be extended to other sands and to other soil types. It may well be that it would provide the solution for settlements, both instantaneous and time dependent, of foundations resting directly on clay deposits. It is very likely that the problem of local failure would be non-existent in all but very soft clays.

The experimental study of the load-deflection of a rigid plate resting on the surface presented some difficulties that were not originally anticipated. The primary drawback was the condition of local failure. It should be noted that a similar problem would have existed if a truly uniform pressure distribution could have been achieved. The use of surcharge, only minimizes the problem of local failure but does not completely eliminate it.

The assignment of a shear modulus to the zone of local failure can only serve to approximate load-deflection data. The reliability and accuracy should increase where there is a surcharge effect.

A comprehensive study of the local failure condition should lead to an improved method of predicting load-settlement data for the case of cohesionless soils.

The following is a summary of recommendations for further study.

1. Further investigation on the relationship between the bulk and shear moduli of cohesionless soils and the properties of the soil and the imposed stress system.

2. An extension of the above study to include other cohesionless and cohesive soils.

3. A study to characterize the behavior of a cohesionless soil when localized failure conditions prevail.

4. The application of the concept to the prediction of settlements of foundations exhibiting pressure distributions other than uniform, and having configurations other than circular.

5. The use of a stress distribution theory other than the Boussinesq for defining the bulk and shear moduli within the soil mass.

APPENDIX I

TEST DATA

Table 2. Summary of Isotropic Compression Test Data

Series No. 1					
Test No.	24	37	26	38	49
e_o	1.03	1.0[illegible]	1.02	1.01	1.02
σ_o (lb/in^2)	ε	ε	ε	ε	ε
0.5	.0000	.000[illegible]	.0000	.0000	.0000
0.9	.0014	.000[illegible]	.0005	.0007	.0007
1.3	.0027	.001[illegible]	.0020	.0021	.0020
2.0	.0047	.004[illegible]	.0039	.0042	.0038
3.0	.0075	.006[illegible]	.0057	.0072	.0057
5.0	.0119	.010[illegible]	.0111	.0122	.0097
7.5		.014[illegible]	.0132	.0152	.0131
10.0	.0211	.017[illegible]	.0168	.0180	.0171
15.0		.021[illegible]	.0211	.0230	.0219
20.0	.0256	.025[illegible]	.0243	.0262	.0254
25.0	.0282	.027[illegible]	.0273	.0293	.0274
30.0	.0307	.030[illegible]	.0294	.0320	.0293
40.0	.0346	.035[illegible]	.0335	.0362	.0338
50.0	.0382	.038[illegible]	.0371	.0398	.0370
60.0	.0408	.040[illegible]	.0400	.0428	.0398
70.0	.0433	.043[illegible]	.0428	.0428	.0425
80.0	.0453	.0465	.0453	.0481	.0444
90.0	.0484	.0484	.0476	.0509	.0469
100.0		.0503	.0500	.0530	.0492

Series No. 2					
Test No.	25	31	32	58	59
e_o	0.98	0.97	0.96	0.95	0.96
σ_o (lb/in^2)	ε	ε	ε	ε	ε
0.5	.0000	.0000	.0000	.0000	.0000
0.9	.0005	.0007	.0005	.0007	.0007
1.3	.0012	.0014	.0016	.0014	.0015
2.0	.0026	.0028	.0031	.0030	.0034
3.0	.0035	.0050	.0064	.0049	.0056
5.0	.0053	.0077	.0093	.0093	.0094
7.5	.0083	.0110	.0124	.0123	.0130
10.0	.0114	.0139	.0150	.0162	.0164
15.0	.0154	.0178	.0191	.0200	.0209
20.0	.0184	.0204	.0222	.0232	.0243
25.0	.0209	.0231	.0246	.0260	.0268
30.0	.0230	.0250	.0270	.0283	.0285
40.0	.0272	.0296	.0313	.0327	.0330
50.0	.0302	.0327	.0346	.0361	.0349
60.0	.0330	.0355	.0379	.0389	.0378
70.0	.0358	.0379	.0401	.0415	.0402
80.0	.0384	.0400	.0431	.0445	.0422
90.0		.0419	.0456	.0461	.0451
100.0		.0438	.0472	.0482	.0460

Table 2. (continued)

	Series No. 3				
Test No.	28	34	40	44	60
e_o	0.93	0.91	0.93	0.92	0.90
σ_o (lb/in^2)	ε	ε	ε	ε	ε
0.5	.0000	.0000	.0000	.0000	.0000
0.9	.0005	.0005	.0007	.0005	.0005
1.3	.0010	.0012	.0014	.0012	.0013
2.0	.0021	.0022	.0029	.0021	.0024
3.0	.0037	.0039	.0042	.0035	.0030
5.0	.0059	.0060	.0076	.0062	.0062
7.5	.0084	.0081	.0103	.0085	
10.0	.0105	.0103	.0127	.0107	.0114
15.0	.0137	.0132	.0157	.0140	.0150
20.0	.0162	.0156	.0183	.0164	.0173
25.0	.0181	.0175	.0200	.0185	.0197
30.0	.0199	.0194	.0213	.0206	.0219
40.0	.0231	.0226	.0244	.0239	.0256
50.0	.0255	.0252	.0267	.0266	.0283
60.0	.0279	.0276	.0291	.0292	.0306
70.0	.0300	.0300	.0311	.0317	.0333
80.0	.0319	.0317	.0333	.0339	.0359
90.0	.0336	.0338	.0350	.0360	.0377
100.0	.0353	.0353	.0367	.0377	.0394
	Series No. 4				
Test No.	33	43	53	54	61
e_o	0.88	0.88	0.87	0.89	0.88
σ_o (lb/in^2)	ε	ε	ε	ε	ε
0.5	.0000	.0000	.0000	.0000	.0000
0.9	.0003	.0005	.0005	.0005	.0005
1.3	.0010	.0010	.0015	.0010	.0014
2.0	.0018	.0017	.0027	.0020	.0031
3.0	.0027	.0027	.0040	.0034	.0051
5.0	.0045	.0043	.0069	.0056	.0075
7.5	.0063	.0060	.0087	.0082	.0102
10.0	.0083	.0078	.0112	.0112	.0126
15.0	.0108	.0098	.0142	.0142	.0155
20.0	.0126	.0116	.0165	.0169	.0182
25.0	.0143	.0130	.0189	.0188	.0198
30.0	.0158	.0145	.0209	.0210	.0216
40.0	.0186	.0168	.0241	.0246	.0250
50.0	.208	.0188	.0267	.0272	.0276
60.0	.0228	.0204	.0292	.0295	.0298
70.0	.0245	.0221	.0311	.0318	.0320
80.0	.0263	.0236	.0336	.0343	.0341
90.0	.0278	.0249	.0354	.0359	.0359
100.0	.0294	.0262	.0373	.0374	.0371

Table 2. (continued)

		Series No. 5			
Test No.	20	27	21	45	48
e_o	0.80	0.81	0.82	0.81	0.82
σ_o (lb/in^2)	ε	ε	ε	ε	ε
0.5	.0000	.0000	.0000	.0000	.0000
0.9	.0003	.0003	.0003	.0005	.0005
1.3	.0007	.0007	.0007	.0010	.0010
2.0	.0012	.0014	.0013	.0017	.0016
3.0	.0021	.0019	.0017	.0020	.0024
5.0	.0036	.0038	.0035	.0038	.0036
7.5	.0051	.0053	.0051	.0050	.0052
10.0	.0066	.0068	.0066	.0066	.0067
15.0	.0086	.0090	.0086	.0083	.0088
20.0	.0105	.0107	.0103	.0098	.0104
25.0	.0121	.0115	.0110	.0110	.0121
30.0	.0135	.0135	.0133	.0124	.0135
40.0	.0159	.0157	.0160	.0145	.0159
50.0	.0179	.0177	.0181	.0162	.0180
60.0	.0198	.0196	.0201	.0179	.0197
70.0	.0217	.0211	.0216	.0190	.0215
80.0	.0238	.0227	.0232	.0202	.0230
90.0	.0252	.0244	.0246	.0214	.0246
100.0	0.266	.0256	.0260	.0225	.0260
		Series No. 6			
Test No.	15	55	56	57	62
e_o	0.79	0.78	0.77	0.76	0.77
σ_o (lb/in^2)	ε	ε	ε	ε	ε
0.5	.0000	.0000	.0000	.0000	.0000
0.9	.0003	.0005	.0005	.0007	.0003
1.3	.0007	.0008	.0010	.0014	.0007
2.0	.0010	.0013	.0015	.0020	.0012
3.0	.0018	.0017	.0023	.0032	.0015
5.0	.0030	.0032	.0031	.0044	.0031
7.5	.0040	.0042	.0041	.0058	.0041
10.0	.0051	.0054	.0057	.0075	.0051
15.0	.0067	.0069	.0075	.0093	.0065
20.0	.0082	.0082	.0091	.0107	.0079
25.0	.0094	.0094	.0103	.0119	.0091
30.0	.0108	.0104	.0116	.0131	.0099
40.0	.0126	.0123	.0134	.0145	.0120
50.0	.0141	.0138	.0148	.0165	.0135
60.0	.0158	.0151	.0163	.0178	.0147
70.0	.0174	.0163	.0176	.0190	.0162
80.0	.0186	.0177	.0189	.0202	.0174
90.0	.0200	.0188	.0199	.0212	.0186
100.0	.02.0	.0200	.0209	.0220	.0195

Table 2. (continued)

	Series No. 7				
Test No.	17	22	29	35	47
e_o	0.73	0.72	0.73	0.75	0.75
σ_o (lb/in^2)	ε	ε	ε	ε	ε
0.5	.0000	0000	.0000	.0000	.0000
0.9	.0003	0004	.0003	.0005	.0005
1.3	.0007	0007	.0009	.0010	.0010
2.0	.0010	.0012	.0014	.0016	.0016
3.0	.0016	.0020	.0016	.0021	.0023
5.0	.0024	.0036	.0031	.0035	.0035
7.5	.0034	.0046	.0040	.0049	.0045
10.0	.0044	.0056	.0056	.0059	.0055
15.0	.0058	.0072	.0069	.0075	.0068
20.0	.0069	.0085	.0082	.0089	.0081
25.0	.0081	.0096	.0092	.0101	.0091
30.0	.0090	.0108	.0101	.0112	.0103
40.0	.0107	.0126	.0118	.0129	.0120
50.0	.0120	.0143	.0132	.0141	.0133
60.0	.0134	.0157	.0146	.0153	.0146
70.0	.0146	.0172	.0155	.0164	.0158
80.0	.0156	.0182	.0156	.0174	.0169
90.0	.0164	.0190	.0175	.0185	.0179
100.0	.0170	.0198	.0184	.0193	.0188
	Series No. 8				
Test No.	23	30	50	52	63
e_o	0.70	0.71	0.70	0.69	0.71
σ_o (lb/in^2)	ε	ε	ε	ε	ε
0.5	.0000	.0000	.0000	.0000	.0000
0.9	.0004	.0005	.0003	.0005	.0003
1.3	.0007	.0009	.0006	.0008	.0007
2.0	.0011	.0014	.0011	.0013	.0017
3.0	.0014	.0019	.0016	.0016	.0017
5.0	.0029	.0032	.0028	.0028	.0027
7.5	.0039	.0041	.0034	.0036	.0035
10.0	.0048	.0049	.0046	.0048	.0047
15.0	.0064	.0065	.0059	.0061	.0057
20.0	.0077	.0078	.0069	.0073	.0067
25.0	.0088	.0088	.0077	.0084	.0073
30.0	.0098	.0097	.0087	.0094	.0080
40.0	.0115	.0115	.0102	.0110	.0095
50.0	.0129	.0127	.0115	.0124	.0105
60.0	.0141	.0138	.0126	.0135	.0115
70.0	.0154	.0148	.0136	.0145	.0124
80.0	.0164	.0159	.0147	.0155	.0132
90.0	.0172	.0168	.0159	.0165	.0140
100.0	.0180	.0176	.0165	.0173	.0147

Table 5. Summary of Test Data from Constant Octahedral Normal Stress Triaxial Compression Tests

σ_o = 100 Test No. 66 e_c = 0.86		σ_o = 100 Test No. 67 e_c = 0.89		σ_o = 100 Test No. 68 e_c = 0.86		σ_o = 100 Test No. 69 e_c = 0.78		σ_o = 100 Test No. 70 e_c = 0.80		σ_o = 100 Test No. 71 e_c = 0.78		σ_o = 100 Test No. 72 e_c = 0.74	
τ_o	γ_o	τ_o	γ_o	τ_o	γ_o	τ_o	γ_o	τ_o	γ_o	τ_o	γ_o	τ_o	γ_o
0.0	.0000	0.0	.0000	0.0	.0000	0.0	.0000	0.0	.0000	0.0	.0000	0.0	.0000
2.8	.0002	2.8	.0003	2.8	.0001	2.8	.0005	2.8	.0005	2.8	.0005	2.8	.0005
5.7	.0005	5.7	.0006	5.7	.0009	5.7	.0009	5.7	.0010	5.6	.0009	5.6	.0007
8.5	.0009	8.5	.0010	8.5	.0012	8.5	.0011	8.5	.0014	8.5	.0013	8.5	.0012
11.3	.0013	11.3	.0019	11.3	.0020	11.3	.0016	11.3	.0018	11.3	.0018	11.3	.0016
14.1	.0019	14.1	.0025	14.2	.0026	14.1	.0022	14.1	.0024	14.1	.0022	14.1	.0021
17.0	.0026	16.9	.0039	17.0	.0039	17.0	.0026	17.0	.0030	17.0	.0028	17.0	.0025
18.8	.0034	19.8	.0049	19.8	.0050	19.8	.0032	19.8	.0038	19.8	.0032	19.8	.0029
22.6	.0046	22.6	.0070	22.6	.0066	22.6	.0040	22.6	.0049	22.6	.0039	22.6	.0035
25.5	.0060	25.5	.0086	25.5	.0083	25.5	.0051	25.5	.0058	25.4	.0048	25.5	.0042
28.3	.0077	28.3	.0108	28.3	.0104	28.3	.0060	28.3	.0068	28.3	.0038	28.3	.0051
31.1	.0093	31.1	.0140	31.1	.0132	31.1	.0070	31.1	.0078	31.1	.0068	31.1	.0059
34.0	.0118	33.9	.0175	34.0	.0162	34.0	.0083	33.9	.0097	33.9	.0091	33.9	.0067
36.8	.0144	36.7	.0218	36.8	.0200	36.8	.0095	36.7	.0110	36.8	.0096	36.8	.0089
39.6	.0182	39.6	.0267	39.6	.0238	39.7	.0117	39.6	.0130	39.6	.0111	45.8	.0094
42.5	.0223	42.5	.0330	42.4	.0302	42.5	.0136	42.4	.0152	42.4	.0132	42.4	.0110
45.2	.0278	45.3	.0406	45.2	.0376	45.3	.0165	45.3	.0185	45.3	.0153	45.3	.0132
48.0	.0349	48.0	.0495	48.1	.0462	48.1	.0195	48.0	.0231	48.1	.0193	48.1	.0155
50.8	.0448	50.9	.0632	50.9	.0579	50.9	.0231	51.0	.0271	50.9	.0226	50.9	.0190
53.7	.0593	53.7	.0832	53.7	.0740	53.7	.0279	53.7	.0335	53.8	.0271	53.8	.0230
56.9	.0827	57.6	.1084	56.6	.0986	56.6	.0346	56.5	.0406	56.4	.0324	56.6	.0285
59.7	.1182	58.8	.1503	59.4	.1356	59.6	.0423	59.4	.0510	59.4	.0402	19.4	.0340
		60.3	.2390	60.9	.1661	60.8	.0480	62.1	.649	62.1	.0512	62.2	.0452
				61.7	.2178	62.4	.0529	64.8	.0947	65.3	.0701	64.9	.0640
						63.8	.0578	65.9	.1394	67.2	.0778	67.7	.0964
						64.6	.0706			68.0	.904	69.9	.1084
						66.7	.0861			68.9	.1209		
						68.0	.1121						

Note: Stresses expressed in lbs. per sq. in.

Table 5. (Continued)

σ_o = 100 Test No. 73 e_c = 0.74		σ_o = 100 Test No. 74 e_c = 0.74		σ_o = 80 Test No. 49 e_c = 0.85		σ_o = 80 Test No. 50 e_c = 0.85		σ_o = 80 Test No. 51 e_c = 0.88		σ_o = 80 Test No. 24 e_c = 0.78		σ_o = 80 Test No. 25 e_c = 0.79	
τ_o	γ_o	τ_o	γ_o	τ_o	γ_o	τ_o	γ_o	τ_o	γ_o	τ_o	γ_o	τ_o	γ_o
0.0	.0000	0.0	.0000	0.0	.0000	0.0	.0000	0.0	.0000	0.0	.0000	0.0	.0000
2.8	.0005	2.8	.0005	2.8	.0004	2.8	.0004	2.8	.0005	2.2	.0005	2.2	.0004
5.7	.0010	5.6	.0007	5.7	.0008	5.6	.0007	5.7	.0009	5.0	.0006	5.0	.0008
8.5	.0014	8.5	.0012	8.5	.0012	8.5	.0013	8.5	.0013	7.9	.0011	7.9	.0011
11.3	.0019	11.3	.0016	11.3	.0018	11.3	.0020	11.3	.0021	10.7	.0018	10.7	.0018
14.1	.0023	14.1	.0021	14.1	.0026	14.2	.0030	14.1	.0031	13.6	.0024	13.6	.0023
17.0	.0028	17.0	.0025	17.0	.0038	17.0	.0038	17.0	.0045	16.4	.0032	16.4	.0029
19.8	.0032	19.8	.0029	19.8	.0052	19.8	.0057	19.8	.0061	19.3	.0042	19.3	.0038
22.6	.0036	22.6	.0035	22.6	.0070	22.6	.0075	22.7	.0080	22.1	.0054	22.1	.0048
25.4	.0042	25.4	.0042	25.4	.0101	25.4	.0102	25.5	.0114	25.0	.0066	25.0	.0065
28.3	.0048	28.3	.0051	28.3	.0129	28.3	.0137	28.3	.0147	27.8	.0082	27.8	.0083
31.1	.0057	31.1	.0059	31.2	.0171	31.1	.0177	31.1	.0184	30.6	.0106	30.7	.0107
33.9	.0066	33.9	.0067	33.9	.0227	33.9	.0238	33.9	.0249	33.5	.0130	33.5	.0131
36.7	.0076	36.8	.0080	36.9	.0301	36.7	.0312	36.8	.0328	36.2	.0179	36.3	.0172
39.6	.0087	45.8	.0094	39.5	.0391	39.6	.0426	39.5	.0428	39.3	.0214	39.1	.0221
42.3	.0106	42.4	.0110	42.3	.0550	42.4	.0597	42.3	.0606	42.0	.0281	42.1	.0296
45.3	.0121	45.3	.0132	43.9	.0610	44.0	.0684	43.8	.0684	43.5	.0313	43.6	.0326
48.1	.0142	48.1	.0155	45.2	.0711	45.3	.0776	45.1	.0819	45.0	.0347	44.9	.0379
50.9	.0164	50.9	.0190	46.5	.0882	46.6	.0887	46.6	.1042	46.3	.0403	46.4	.0420
53.7	.0202	53.8	.0230	48.0	.1160	47.6	.1209	48.0	.1312	47.8	.0477	47.8	.0469
56.5	.0245	56.6	.0285	49.4	.1488	49.0	.1756	49.1	.1684	49.2	.0556	48.8	.0604
59.4	.0298	59.4	.0340	51.2	.2099					50.5	.0667	51.0	.0713
62.3	.0398	62.2	.0452							52.0	.0888		
65.2	.0525	64.9	.0640										
66.8	.0576	67.7	.0964										
68.0	.0626	69.9	.1084										
69.0	.0785												
70.8	.1135												

Note: Stresses expressed in lbs. per sq. in.

Table 5. (Continued)

σ_o = 80 Test No. 52 e_c = 0.77		σ_o = 80 Test No. 20 e_c = 0.71		σ_o = 80 Test No. 21 e_c = 0.70		σ_o = 60 Test No. 32 e_c = 0.89		σ_o = 60 Test No. 33 e_c = 0.89		σ_o = 60 Test No. 34 e_c = 0.88		σ_o = 60 Test No. 29 e_c = 0.83	
τ_o	γ_o	τ_o	γ_o	τ_o	γ_o	τ_o	γ_o	τ_o	γ_o	τ_o	γ_o	τ_o	γ_o
0.0	.0000	0.0	.0000	0.0	.0000	0.0	.0000	0.0	.0000	0.0	.0000	0.0	.0000
2.8	.0004	2.2	.0004	2.2	.0004	2.8	.0004	2.8	.0004	2.8	.0004	2.8	.0004
5.6	.0008	5.0	.0007	5.1	.0008	5.7	.0010	5.7	.0010	5.7	.0010	5.7	.0008
8.5	.0012	7.9	.0010	7.9	.0013	8.5	.0017	10.6	.0023	8.5	.0019	8.5	.0014
11.3	.0018	10.7	.0012	10.7	.0015	11.3	.0032	11.3	.0037	11.3	.0032	11.3	.0022
14.1	.0024	13.6	.0016	13.6	.0019	14.1	.0049	14.1	.0060	14.1	.0054	14.1	.0033
17.0	.0032	16.4	.0019	16.5	.0021	17.0	.0076	17.0	.0089	17.0	.0083	17.0	.0050
18.2	.0037	19.3	.0022	19.3	.0025	19.8	.0111	19.8	.0129	19.8	.0117	19.8	.0065
22.7	.0048	22.1	.0025	22.1	.0031	22.6	.0161	22.6	.0183	22.6	.0161	22.6	.0094
25.5	.0063	25.0	.0037	25.0	.0037	25.4	.0235	25.4	.0247	25.4	.0239	25.4	.0130
28.3	.0078	27.8	.0048	27.8	.0044	28.2	.0345	28.2	.0345	28.2	.0348	28.3	.0186
31.1	.0097	30.7	.0061	30.6	.0053	29.7	.0415	29.8	.0405	29.7	.0393	29.7	.020
34.0	.0122	33.6	.0077	33.5	.0064	31.1	.0503	31.1	.0489	31.0	.0489	31.1	.0243
36.3	.0157	36.4	.0102	36.3	.0076	32.5	.0603	33.3	.0591	32.6	.0596	32.5	.0305
39.6	.0193	39.2	.0129	39.0	.0092	33.8	.0797	33.9	.0767	33.9	.0747	33.9	.0373
42.3	.0245	42.0	.0166	42.0	.0120	35.3	.1083	35.6	.0957	35.2	.1051	35.3	.0473
43.8	.0273	43.5	.0192	43.5	.0137	36.7	.0736	36.7	.0736	36.7	.0736	36.7	.0612
45.2	.0306	45.0	.0219	44.9	.0156							38.1	.0851
46.7	.0368	46.3	.0251	46.4	.0180							39.2	.0763
48.3	.0417	47.7	.0297	47.8	.0204								
49.5	.0479	49.2	.0348	49.2	.0240								
51.0	.0559	50.8	.0402	50.5	.0290								
52.1	.0695	51.9	.0503	52.2	.0358								
53.6	.0970	53.3	.0662	53.6	.0488								

Note: Stresses expressed in lbs. per sq. in.

Table 5. (Continued)

σ_o = 60 Test No. 30 e_c = 0.83		σ_o = 60 Test No. 31 e_c = 0.83		σ_o = 60 Test No. 3 e_c = 0.76		σ_o = 60 Test No. 13 e_c = 0.78		σ_o = 60 Test No. 14 e_c = 0.76		σ_o = 60 Test No. 26 e_c = 0.71		σ_o = 60 Test No. 27 e_c = 0.72	
τ_o	γ_o	τ_o	γ_o	τ_o	γ_o	τ_o	γ_o	τ_o	γ_o	τ_o	γ_o	τ_o	γ_o
0.0	.0000	0.0	.0000	0.0	.0000	0.0	.0000	0.0	.0000	0.0	.0000	0.0	.0000
2.8	.0004	2.8	.0005	2.8	.0004	2.4	.0004	2.5	.0003	2.8	.0004	2.8	.0004
5.7	.0010	5.7	.0009	5.2	.0008	5.3	.0008	5.2	.0006	5.6	.0009	5.7	.0006
8.5	.0017	8.5	.0015	8.1	.0012	8.1	.0014	8.1	.0011	8.5	.0013	8.5	.0010
11.3	.0026	11.3	.0026	10.9	.0017	10.9	.0022	10.9	.0016	11.3	.0017	11.3	.0014
14.1	.0040	14.1	.0036	13.7	.0026	13.8	.0030	13.8	.0024	14.1	.0023	14.1	.0018
17.0	.0061	17.0	.0054	16.6	.0033	16.6	.0040	16.6	.0034	17.0	.0028	17.0	.0024
19.8	.0082	19.8	.0079	19.5	.0046	19.4	.0057	19.5	.0047	19.8	.0039	19.8	.0035
22.6	.0124	22.7	.0111	22.3	.0062	22.3	.0078	22.3	.0067	22.6	.0055	22.6	.0049
25.4	.0166	25.2	.0150	25.2	.0082	25.2	.0106	25.2	.0091	25.4	.0073	25.5	.0067
28.3	.0234	28.3	.0209	27.6	.0113	28.0	.0152	28.0	.0123	28.2	.0103	28.2	.0093
29.7	.0272	29.7	.0241	31.0	.0157	29.4	.0168	29.5	.0151	29.7	.0118	29.7	.0109
31.1	.0331	31.1	.0302	33.6	.0221	30.8	.0203	31.0	.0178	31.1	.0139	31.1	.0126
32.5	.0387	32.5	.0349	36.4	.0329	32.3	.0252	32.4	.0209	32.5	.0170	32.6	.0158
33.9	.0472	33.8	.0465	39.0	.0543	33.7	.0312	33.6	.0261	33.9	.0212	33.9	.0188
35.4	.0612	35.5	.0546	41.7	.0970	35.2	.0396	35.1	.0318	35.3	.0262	35.3	.0228
36.9	.0765	36.7	.0736			36.7	.0467	36.6	.0393	36.8	.0318	36.7	.0313
38.1	.1023	38.0	.1044			38.0	.0584	37.8	.0474	38.1	.0399	38.3	.0380
39.2	.1500	38.1	.1891			41.1	.1018	41.0	.0815	41.1	.0765	41.1	.0659

Note: Stresses expressed in lbs. per sq. in.

Table 5. (Continued)

σ_o = 60 Test No. 28 e_c = 0.69		σ_o = 40 Test No. 35 e_c = 0.89		σ_o = 40 Test No. 36 e_c = 0.87		σ_o = 40 Test No. 37 e_c = 0.91		σ_o = 40 Test No. 1 e_c = 0.85		σ_o = 40 Test No. 9 e_c = 0.82		σ_o = 40 Test No. 10 e_c = 0.83	
τ_o	γ_o	τ_o	γ_o	τ_o	γ_o	τ_o	γ_o	τ_o	γ_o	τ_o	γ_o	τ_o	γ_o
0.0	.0000	0.0	.0000	0.0	.0000	0.0	.0000	0.0	.0000	0.0	.0000	0.0	.0000
2.8	.0004	1.4	.0004	1.4	.0005	1.4	.0005	1.1	.0005	1.2	.0005	1.4	.0005
5.7	.0008	2.8	.0008	2.8	.0011	2.8	.0009	2.5	.0008	2.6	.0009	2.8	.0010
8.5	.0012	4.2	.0012	4.2	.0015	4.2	.0013	4.0	.0011	4.0	.0013	4.2	.0014
11.3	.0019	5.7	.0017	5.7	.0021	5.7	.0017	5.4	.0014	5.4	.0015	5.7	.0018
14.1	.0024	7.1	.0025	7.1	.0026	7.1	.0024	6.9	.0018	6.8	.0018	7.1	.0024
17.0	.0033	8.5	.0037	8.5	.0036	8.5	.0032	8.3	.0026	8.3	.0024	8.5	.0032
19.8	.0045	9.9	.0054	9.9	.0048	9.9	.0046	9.7	.0035	9.7	.0031	9.9	.0038
22.6	.0061	11.3	.0074	11.3	.0063	11.3	.0068	11.1	.0047	11.1	.0043	11.3	.0051
25.4	.0079	12.7	.0097	12.7	.0086	12.7	.0114	14.0	.0085	12.6	.0057	12.7	.0064
28.3	.0099	14.1	.0120	14.1	.0113	14.1	.0109	16.8	.0147	14.0	.0076	14.1	.0084
29.7	.0130	15.5	.0157	15.6	.0149	15.5	.0145	19.6	.0263	15.4	.0102	15.5	.0108
31.1	.0152	17.0	.0201	17.0	.0192	16.9	.0195	22.2	.0480	16.8	.0124	17.0	.0142
32.5	.0179	18.4	.0245	18.4	.0257	18.4	.0253	24.3	.1108	18.1	.0181	18.4	.0183
33.9	.0208	20.9	.0451	19.8	.0337	19.7	.0355			19.6	.0258	19.8	.0241
35.3	.0260	21.6	.0560	21.2	.0459	21.3	.0427			21.1	.0358	21.2	.0335
36.8	.0317	22.8	.0770	22.6	.0620	22.5	.0721			22.5	.0475	22.7	.0424
38.2	.0392	23.9	.1141	23.9	.0919	23.9	.1043			23.9	.0684	23.9	.0604
39.6	.0503	25.0	.1820	25.1	.1442					25.4	.0941	25.4	.0881
41.1	.0668									26.6	.1314	27.1	.1160

Note: Stresses expressed in lbs. per sq. in.

Table 5. (Continued)

σ_o = 40 Test No. 39 e_c = 0.78		σ_o = 40 Test No. 40 e_c = 0.76		σ_o = 40 Test No. 78 e_c = 0.71		σ_o = 40 Test No. 79 e_c = 0.73		σ_o = 20 Test No. 46 e_c = 0.92		σ_o = 20 Test No. 47 e_c = 0.96		σ_o = 20 Test No. 48 e_c = 0.92	
τ_o	γ_o	τ_o	γ_o	τ_o	γ_o	τ_o	γ_o	τ_o	γ_o	τ_o	γ_o	τ_o	γ_o
0.0	.0000	0.0	.0000	0.0	.0000	0.0	.0000	0.0	.0000	0.0	.0000	0.0	.0000
2.8	.0005	2.8	.0005	1.4	.0002	1.4	.0002	1.4	.0005	1.4	.0005	1.4	.0005
5.6	.0009	5.7	.0009	2.8	.0003	2.8	.0004	2.8	.0014	2.8	.0009	2.8	.0011
8.5	.0016	8.5	.0015	4.2	.0005	4.2	.0006	4.2	.0029	4.2	.0017	4.2	.0022
9.9	.0020	9.9	.0017	5.7	.0007	5.7	.0009	5.7	.0058	5.7	.0031	5.7	.0042
11.3	.0025	11.3	.0021	7.1	.0009	7.1	.0010	7.1	.0097	7.1	.0059	7.1	.0073
12.7	.0029	12.7	.0026	8.4	.0013	8.5	.0013	8.5	.0172	8.5	.0107	8.5	.0101
14.1	.0037	14.1	.0033	9.9	.0015	9.9	.0018	9.2	.0232	9.2	.0152	9.2	.0201
15.6	.0046	15.6	.0040	11.3	.0017	11.3	.0020	9.9	.0316	9.9	.0211	9.9	.0239
17.0	.0056	17.0	.0048	12.7	.0021	12.7	.0025	10.6	.0420	10.6	.0284	10.6	.0339
18.4	.0069	18.4	.0061	14.1	.0025	14.1	.0029	11.2	.0645	11.2	.0523	11.2	.0518
19.8	.0088	19.8	.0075	15.5	.0029	15.6	.0034	12.0	.0932	12.2	.0640	12.0	.0814
21.2	.0114	21.2	.0098	17.0	.0037	17.0	.0040	12.7	.1455	12.3	.1529	12.4	.1592
22.6	.0152	22.6	.0129	18.4	.0043	18.4	.0050						
24.0	.0202	24.0	.0174	19.8	.0058	19.8	.0062						
25.4	.0298	25.5	.0256	21.2	.0072	21.2	.0082						
26.9	.0437	26.9	.0379	22.6	.0092	22.7	.0109						
28.0	.0717			24.1	.0124	24.0	.0155						
				25.5	.0169	25.4	.0224						
				26.9	.0223	26.0	.0351						
				28.1	.0379	28.3	.0559						
				29.5	.0700								

Note: Stresses expressed in lbs. per sq. in.

Table 5. (Continued)

σ_o = 20 Test No. 6 e_c = 0.81		σ_o = 20 Test No. 11 e_c = 0.81		σ_o = 20 Test No. 12 e_c = 0.83		σ_o = 20 Test No. 42 e_c = 0.76		σ_o = 20 Test No. 43 e_c = 0.78		σ_o = 20 Test No. 44 e_c = 0.77		σ_o = 20 Test No. 17 e_c = 0.70	
τ_o	γ_o	τ_o	γ_o	τ_o	γ_o	τ_o	γ_o	τ_o	γ_o	τ_o	γ_o	τ_o	γ_o
0.0	.0000	0.0	.0000	0.0	.0000	0.0	.0000	0.0	.0000	0.0	.0000	0.0	.0000
1.4	.0005	1.3	.0005	1.3	.0005	1.4	.0005	1.4	.0005	1.4	.0005	1.3	.0005
2.8	.0010	2.8	.0011	2.8	.0009	2.8	.0007	2.8	.0010	2.8	.0007	2.8	.0011
4.2	.0016	4.2	.0018	4.2	.0015	4.2	.0018	4.2	.0014	4.2	.0012	4.2	.0015
5.6	.0024	5.6	.0030	5.6	.0030	5.7	.0025	5.7	.0021	5.7	.0017	5.6	.0023
7.0	.0040	7.0	.0050	7.0	.0056	7.1	.0034	7.1	.0030	7.1	.0024	7.0	.0029
8.4	.0060	8.4	.0083	8.4	.0098	8.5	.0046	8.5	.0042	8.5	.0031	8.5	.0041
9.9	.0097	9.9	.0147	9.9	.0179	9.9	.0070	9.2	.0066	9.2	.0036	9.9	.0058
11.3	.0173	11.3	.0272	11.3	.0032	11.3	.0119	9.9	.0090	9.9	.0043	11.3	.0096
12.7	.0320	12.6	.0522	12.6	.0682	12.7	.0239	10.6	.0128	10.6	.0052	12.7	.0168
13.8	.0941			13.4	.1854	14.0	.0597	11.3	.0194	11.3	.0072	14.1	.0324
13.9	.1229							11.4	.0296	12.0	.0088	14.9	.0982
								12.7	.0494	12.7	.0127		
								13.4	.0798	13.4	.0202		
										14.1	.0361		
										14.5	.0841		

Note: Stresses expressed in lbs. per sq. in.

Table 5. (Continued)

σ_o = 20 Test No. 18 e_c = 0.73		σ_o = 10 Test No. 54 e_c = 0.96		σ_o = 10 Test No. 55 e_c = 0.94		σ_o = 10 Test No. 56 e_c = 0.92		σ_o = 10 Test No. 57 e_c = 0.82		σ_o = 10 Test No. 58 e_c = 0.82		σ_o = 10 Test No. 59 e_c = 0.83	
τ_o	γ_o	τ_o	γ_o	τ_o	γ_o	τ_o	γ_o	τ_o	γ_o	τ_o	γ_o	τ_o	γ_o
0.0	.0000	0.0	.0000	0.0	.0000	0.0	.0000	0.0	.0000	0.0	.0000	0.0	.0000
1.3	.0005	0.7	.0003	0.7	.0005	0.7	.0003	0.7	.0005	0.7	.0005	0.7	.0005
2.8	.0010	1.4	.0006	1.4	.0011	1.4	.0007	1.4	.0014	1.4	.0009	1.4	.0009
4.2	.0014	2.1	.0013	2.1	.0019	2.1	.0016	2.1	.0021	2.1	.0014	2.1	.0012
5.6	.0018	2.8	.0025	2.8	.0035	2.8	.0030	2.8	.0025	2.8	.0019	2.9	.0017
7.0	.0024	3.5	.0046	3.5	.0064	3.5	.0052	3.5	.0036	3.5	.0026	3.5	.0024
8.5	.0031	4.2	.0084	4.2	.0100	4.2	.0087	4.2	.0052	4.2	.0035	4.2	.0035
9.9	.0047	4.9	.0149	4.9	.0172	4.9	.0149	5.0	.0070	5.0	.0054	5.0	.0050
11.3	.0069	5.6	.0308	5.7	.0280	5.6	.0294	5.7	.0103	5.7	.0079	5.7	.0078
12.9	.0114	6.2	.0807	6.2	.0702	6.3	.0704	6.4	.0169	6.3	.0129	6.4	.0129
14.1	.0246	6.6	.2087	6.6	.2234	6.6	.2115	7.4	.1230	7.1	.0237	7.1	.0275
15.1	.0802									7.7	.0625		

Note: Stresses expressed in lbs. per sq. in.

Table 5. (Continued)

σ_o = 10 Test No. 60 e_c = 0.76		σ_o = 10 Test No. 61 e_c = 0.76		σ_o = 10 Test No. 62 e_c = 0.78		σ_o = 10 Test No. 63 e_c = 0.75		σ_o = 10 Test No. 64 e_c = 0.72		σ_o = 10 Test No. 65 e_c = 0.74	
τ_o	γ_o	τ_o	γ_o	τ_o	γ_o	τ_o	γ_o	τ_o	γ_o	τ_o	γ_o
0.0	.0000	0.0	.0000	0.0	.0000	0.0	.0000	0.0	.0000	0.0	.0000
0.7	.0005	0.7	.0005	0.7	.0005	0.7	.0005	0.7	.0005	0.7	.0005
1.4	.0009	1.4	.0007	1.4	.0010	1.4	.0015	1.4	.0007	1.4	.0010
2.1	.0012	2.1	.0012	2.1	.0012	2.1	.0019	2.1	.0010	2.1	.0015
2.8	.0017	2.8	.0017	2.8	.0017	2.8	.0021	2.8	.0014	2.8	.0017
3.5	.0022	3.5	.0019	3.5	.0019	3.5	.0026	3.5	.0017	3.5	.0023
4.2	.0027	4.2	.0024	4.2	.0026	4.2	.0033	4.2	.0022	4.2	.0028
5.0	.0034	5.0	.0034	4.9	.0035	4.9	.0043	5.0	.0026	5.0	.0033
5.7	.0044	5.7	.0049	5.7	.0048	5.7	.0057	5.7	.0033	5.7	.0045
6.4	.0065	6.4	.0070	6.4	.0078	6.4	.0080	6.4	.0051	6.4	.0065
7.1	.0095	7.0	.0144	7.0	.0144	7.1	.0155	7.1	.0086	7.0	.0134
		7.8	.0458	7.8	.0530	7.8	.0418	7.8	.0194	7.8	.0363
								8.1	.0949		

Note: Stresses expressed in lbs. per sq. in.

Table 6. Summary of Plate Load Test Results

Load Test No. 1 D_r = 0.57 Plate Diam. = 17.5 in.			
$p(lb/in^2)$	w_1(in)	w_2(in)	w(average)
1.0	0.003	0.005	0.004
2.0	0.014	0.019	0.016
4.3	0.045	0.055	0.050
5.4	0.063	0.075	0.069
6.5	0.085	0.099	0.092
7.7	0.108	0.121	0.115
8.7	0.132	0.147	0.140
9.9	0.154	0.172	0.163
10.9	0.181	0.202	0.292
14.5	0.275	0.303	0.289
17.5	0.376	0.412	0.394
19.3	0.424	0.463	0.444
21.0	0.475	0.522	0.499
22.7	0.531	0.583	0.557
25.6	0.659	0.731	0.695
27.2	0.728	0.815	0.770
28.8	0.761	0.854	0.807
30.0	0.798	0.898	0.847
31.0	0.830	0.938	0.883
32.0	0.859	0.972	0.914
34.0	0.937	1.072	1.004
36.0	1.009	1.161	1.085
38.0	1.139	1.309	1.224
40.0	1.208	1.383	1.295
42.0	1.339	1.526	1.432
0.0	1.252	1.421	1.336
49.0	1.747	2.028	1.887
52.4	1.920	2.203	2.062
57.4			2.76
62.8			3.56
67.8			4.66
73.8			5.66

Table 6. (Continued)

Load Test No. 2 D_r = 0.31 Plate Diam. = 17.5 in.			
p(lb/in^2)	w_1(in)	w_2(in)	w(average)
2.0	0.202	0.190	0.196
3.0	0.418	0.400	0.409
4.0	0.654	0.627	0.640
5.0	0.966	0.926	0.946
6.0	1.232	1.165	1.198
7.0	1.535	1.435	1.485
8.0	1.878	1.732	1.805
9.0	2.223	2.042	2.132
10.0	2.653	2.387	2.520
11.0	2.899	2.606	2.753
12.0	3.237	2.927	3.082
13.0	3.713	3.385	3.549
14.0	3.985	3.623	3.804
15.0	4.357	4.003	4.180
16.0	4.710	4.356	4.533
18.0	5.457	5.109	5.283
20.0	6.553	6.154	6.353

Table 6. (Continued)

Load Test No. 3 D_r = 0.78 Plate Diam. = 17.5 in.			
$p(lb/in^2)$	w_1(in)	w_2(in)	w(average)
2.0	0.010	0.013	0.012
4.0	0.021	0.028	0.024
6.0	0.034	0.045	0.039
8.0	0.048	0.062	0.055
10.0	0.064	0.083	0.074
12.0	0.081	0.107	0.094
14.0	0.101	0.132	0.116
16.0	0.124	0.163	0.144
18.0	0.143	0.192	0.167
20.0	0.164	0.224	0.199
22.0	0.193	0.264	0.233
24.0	0.220	0.313	0.266
26.0	0.245	0.341	0.298
28.0	0.275	0.389	0.337
30.0	0.308	0.439	0.378
32.0	0.342	0.501	0.426
34.0	0.377	0.562	0.475
36.0	0.418	0.630	0.524
38.0	0.459	0.702	0.581
40.0	0.507	0.773	0.640
42.0	0.576	0.857	0.716
44.0	0.641	0.933	0.787
46.0	1.031	1.196	1.113
50.0	1.111	1.281	1.196
54.0	1.346	1.616	1.481
58.0	1.683	1.936	1.814
62.0	2.252	2.481	2.366
66.0	3.009	3.061	3.035

Table 7. Variations in Density of the Sand in the Test Pit

Test No.	Average Density (pcf)	% Within ± 2% of Average	% Within ± 5% of Average
1	90.6	45	96
2	85.0	55	90
3	96.4	100	

APPENDIX II

CALIBRATION CHARTS, DERIVATIONS

Derivation of the Equation for the Minor Principal Strain (ε_3)

Considering the soil sample in a triaxial compression test immediately after isotropic compression, the cross-sectional area is given by

$$A_c = \frac{V_c}{L_c}$$

in which A_c, V_c, and L_c are the values of area, volume, and length respectively.

The cross-sectional area at any time during the test is given by

$$A = \frac{V_c - \Delta V}{L_c - \Delta L}$$

where ΔV and ΔL denote reductions in volume and length respectively. Therefore:

$$A - A_c = \frac{V_c - \Delta V}{L_c - \Delta L} - \frac{V_c}{L_c}$$

or

$$\Delta A = \frac{\pi}{4}(d^2 - d_c^2) = \frac{\pi}{4}\frac{d_c^2 L_c}{L_c}\left[\frac{1 - \frac{\Delta V}{V_c}}{1 - \frac{\Delta L}{L_c}} - 1\right]$$

Simplifying

$$\frac{d^2 - d_c^2}{d_c^2} = \frac{1 - \frac{\Delta V}{V_c}}{1 - \frac{\Delta L}{L_c}} - 1$$

$$\text{or} \quad \left[\frac{d_c + \Delta d}{dc}\right]^2 = \frac{1 - \frac{\Delta V}{V_c}}{1 - \frac{\Delta L}{L_c}}$$

$$1 + \frac{\Delta d}{d_c} = \sqrt{\frac{1 - \frac{\Delta V}{V_c}}{1 - \frac{\Delta L}{L_c}}}$$

$$\frac{\Delta d}{d_c} = \sqrt{\frac{1 - \frac{\Delta V}{V_c}}{1 - \frac{\Delta L}{L_c}}} - 1$$

In accordance with the sign convention for stresses for which the compressive stress is taken to be positive, a decrease in dimension is taken to be positive and an increase in dimension is taken to be negative.

Therefore for a triaxial compression test, the major principal strain is positive while the minor principal strain is negative.

$$\varepsilon_3 = -\frac{\Delta d}{d_c} = -\sqrt{\frac{1 - \frac{\Delta V}{V_c}}{1 - \frac{\Delta L}{L_c}}} - 1 \quad .$$

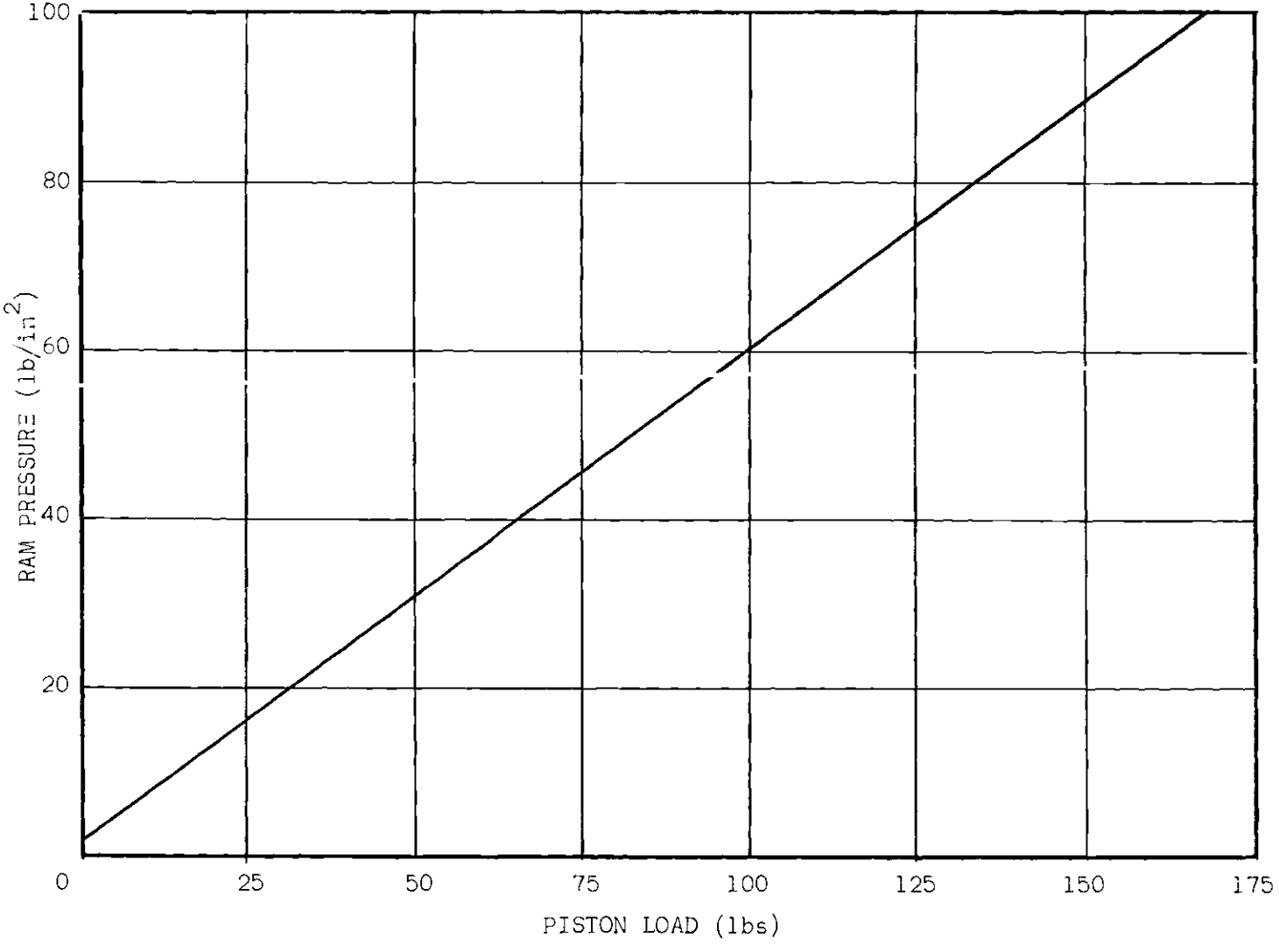

Figure 58. Calibration Chart for 1-1/2 in. Diameter Hydraulic Ram.

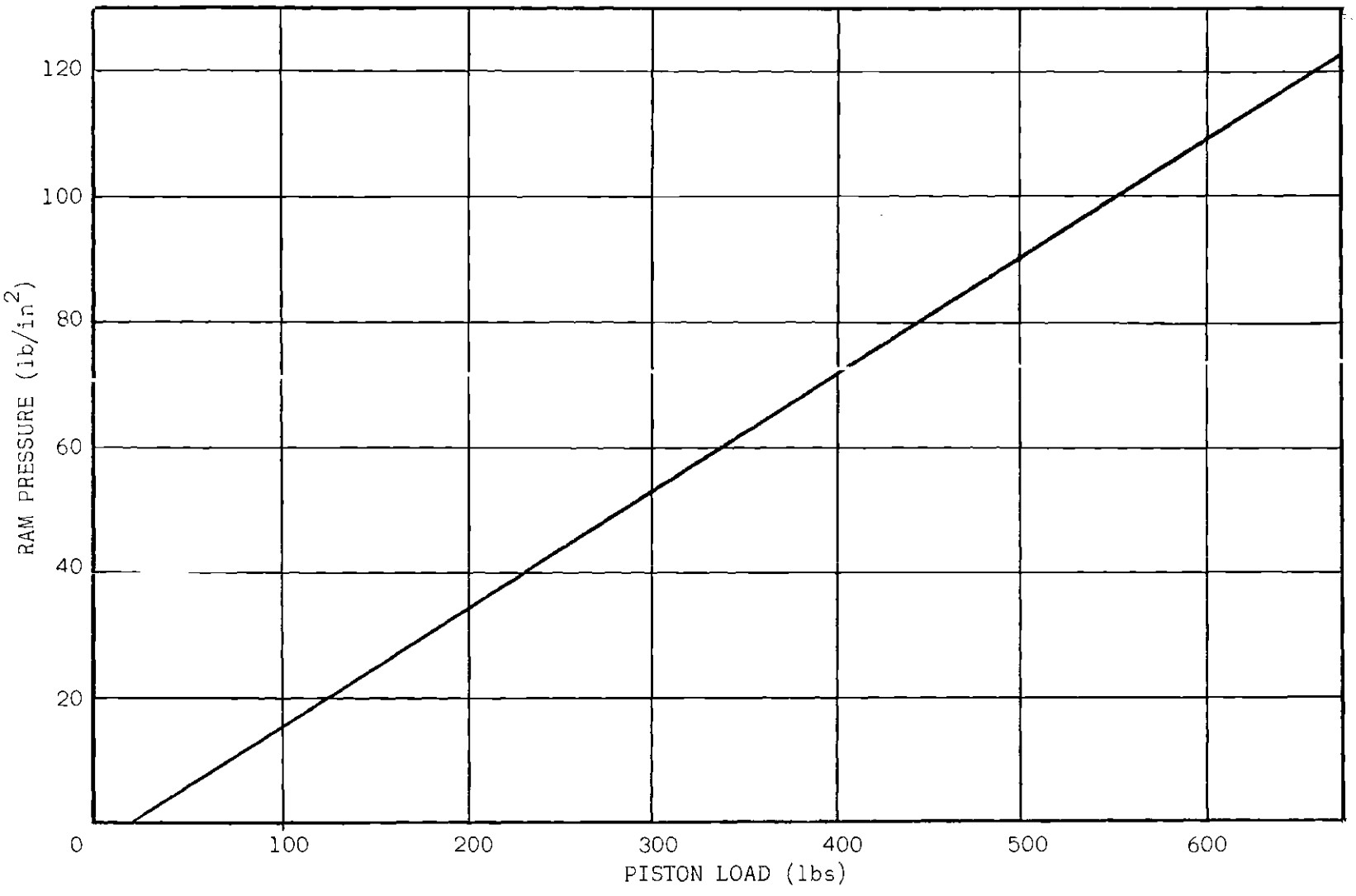

Figure 59. Calibration Chart for 2-5/8 in. Diameter Hydraulic Ram.

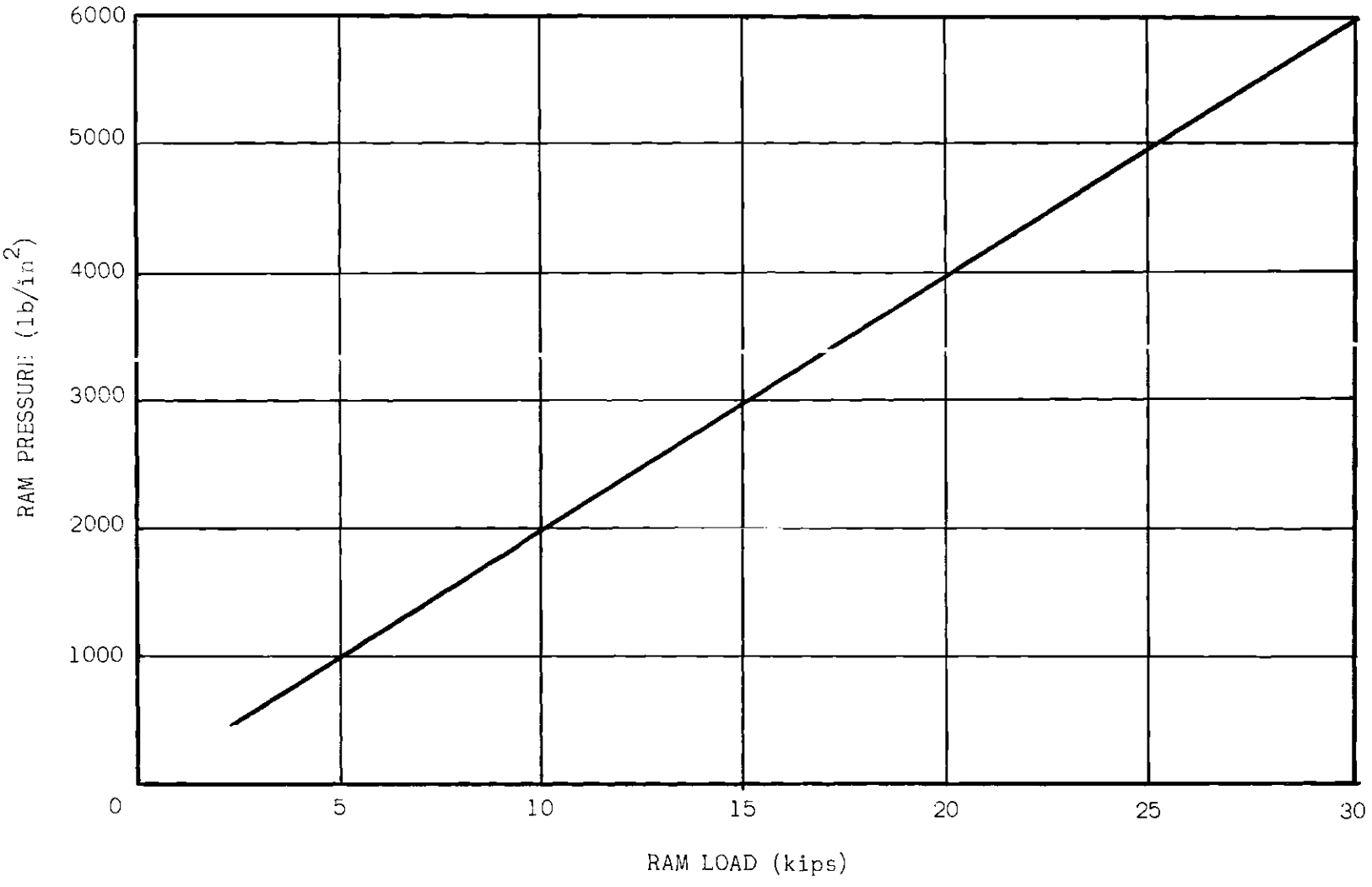

Figure 60. Calibration Chart for Hydraulic Ram Used in Plate Load Tests.

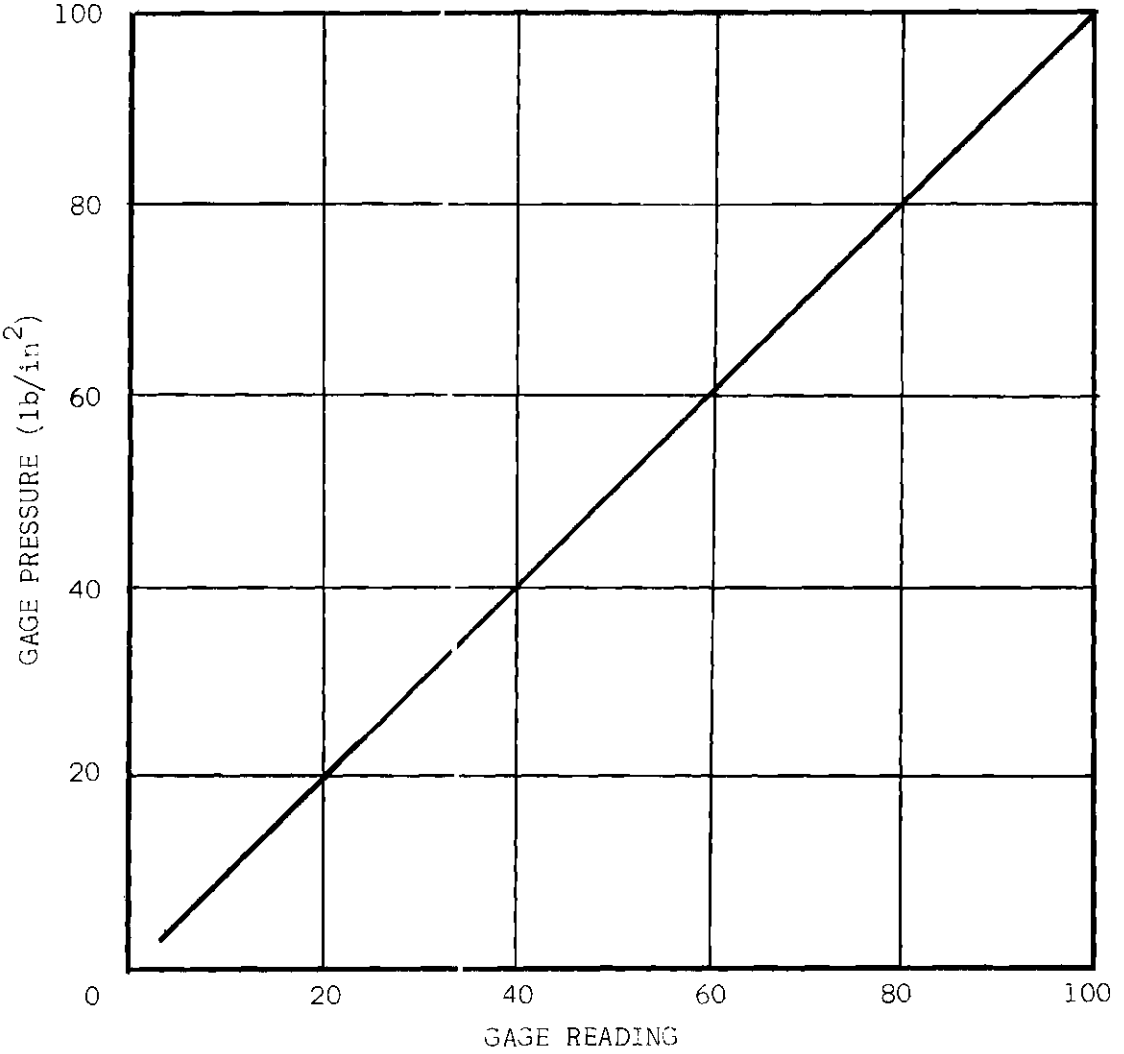

Figure 61. Calibration Chart for Cell Pressure Gage.

BIBLIOGRAPHY

LITERATURE CITED

1. Schiffman, R. W., "The Use of Viscoelastic Stress-Strain Law in Soil Testing," Special Technical Publication No. 254, American Society for Testing Materials, 1954, pp. 131-155.

2. Papazian, H. S., "The Response of Linear Viscoelastic Materials in the Frequency Domain with Emphasis on Asphaltic Concrete," Proceedings, International Conference on the Structural Design of Asphalt Pavements, 1963, pp. 454-463.

3. Secor, K. E. and Monismith, C. L., "Analysis of Triaxial Test Data on Asphalt Concrete Using Viscoelastic Principles," Proceedings, Highway Research Board, vol. 40, 1961, pp. 295-314.

4. Saada, A. S., "A Rheological Analysis of Shear and Consolidation of Saturated Clays," Bulletin 342, Highway Research Board, 1962, pp. 52-89.

5. Pister, K. S. and Monismith, C. L., "Analysis of Viscoelastic Flexible Pavements," Bulletin 269, Highway Research Board, 1960.

6. Pister, K. S., "Viscoelastic Plate on a Viscoelastic Foundation, Proceedings, American Society of Civil Engineers, vol. 87, 1961, pp. 13-22.

7. Pister, K. S. and Williams, M. L., "Bending of Plates on a Viscoelastic Foundation," Proceedings, American Society of Civil Engineers, Jour. Eng. Mech. Div., vol. 86, No. EM5, 1960.

8. Freudenthal, A. M. and Lensch, H. G., "The Infinite Elastic Beam on a Linear Viscoelastic Foundation," Proceedings, American Society of Civil Engineers, Jour. Eng. Mech. Div., vol. 83, No. EM1, 1957.

9. Hoskin, B. C. and Lee, E. H., "Analysis of Flexible Surfaces over Subgrades with Viscoelastic Material Behavior," Proceedings, American Society of Civil Engineers, Jour. Eng. Mech. Div., vol. 85, No. EM4, 1959.

10. Reissner, E., "Stresses in Elastic Plates over Flexible Subgrades," Proceedings, American Society of Civil Engineers, vol. 81, Separate No. 690, 1955.

11. Reissner, E., "A Note on Deflection of Plates on a Viscoelastic Foundation," Transactions, American Society of Mechanical Engineers, Journal Applied Mechanics, vol. 80, 1958, pp. 144-145.

12. Kondner, R. L. and Zelasco, J. S., "A Hyperbolic Stress-Strain Formulation for Sands," Proceedings, 2nd Pan American Conference on Soil Mechanics and Foundation Engineering, vol. I, 1963, pp. 289-334.

13. Kondner, R. L. and Zelasko, J. S., "Void Ratio Effects on the Hyperbolic Stress-Strain Response of a Sand," Special Technical Publication No. 361, American Society for Testing Materials, Symposium on the Laboratory Shear Testing of Soils, 1964, pp. 250-257.

14. Wroth, C. P. and Basset, R. E., "A Stress-Strain Relationship for the Shearing Behavior of a Sand," Geotechnique, vol. xv, No. 1, 1965, pp. 32-56.

15. Rowe, P. W., "A Stress-Strain Theory for Cohesionless Soil with Applications to Earth Pressures at Rest and Moving Walls," Geotechnique, vol. iv, 1954, p. 70.

16. Duffy, J. and Mindlin, R. D., "Stress-Strain Relations of a Granular Medium," Transactions, American Society of Mechanical Engineers, Journal Applied Mechanics, vol. 79, 1957, p. 585.

17. Richart, F. E., Jr, Hall, J. R. and Lysmer, J., "Study of the Propagation and Dissipation of Elastic Wave Energy in Granular Soils," Gainsville, Florida, 1962.

18. Barkan, D. D., "Dynamics of Bases and Foundations," McGraw Hill, 1962.

19. Terzaghi, K., "Theoretical Soil Mechanics," John Wiley and Sons, 1943.

20. Jacobson, B., "Some Fundamental Properties of Sand," Proceedings, 4th International Conference on Soil Mechanics and Foundation Engineering, vol. I, 1957, p. 167.

21. Ladanyi, B., "Etude des Relations Entre Les Contraintres Et Les Deformations Lors Du Cisaillement Des Sols Pulvurulents," Annales Des Travaux Publics de Belgique, 1960, pp. 1 - 30.

22. Clough, G. W., "An Investigation of the Shear Strength of Sand at High Pressures," M. Sc. Thesis, Georgia Institute of Technology, 1964.

23. Wilson, G. and Sutton, J. L. E., "A Contribution to the Study of the Elastic Properties of Sand," Proceedings, 2nd Int. Cont. Soil Mech. Found. Engr., vol. I, 1948, pp. 197-202.

24. Habib, P., "Influence de la Variation de la Contraintre Principale Meyenne sur la Resistance au Cisaillement des Sols," Proceedings, 3rd Int. Conf. Soil Mech. Found. Eng., vol. II, 1953, pp. 131-136.

25. Richart, F. E., Jr., "Foundation Vibrations," Proceedings, American Society of Civil Engineers, Jour. Soil Mech. Found. Eng. Div., vol. 86, No. SM4, 1960.

26. Kerisel, J., "Evaluation de la Mecanique des Sols," as reported in De Beer, E., "Bearing Capacity and Settlements of Shallow Foundations on Sand," Symposium on the Bearing Capacity of Foundations, Duke University, 1965.

27. Kondner, R. L. and Horner, J. M., "Triaxial Compression of a Cohesive Soil with Effective Octahedral Normal Stress Control," Canadian Geotechnical Journal, vol. 2, No. 1, 1965, pp. 40-52.

28. Vesic, A. S. and Barksdale, R. D., "Discussion on Shear Strength of Sand at Very High Pressures," Special Technical Publication No. 361, American Society for Testing Materials, Symposium on the Laboratory Shear Testing of Soils, 1964, pp. 301-305.

29. Vesic, A. B., "Bearing Capacity of Deep Foundations in Sand, 42nd Annual Meeting of the Highway Research Board, Washington, D. C., 1963.

30. Bishop, A. W. and Henkel, D. J., " The Measurement of Soil Properties in the Triaxial Test," Edward Arnold Limited, 1962.

31. Roscoe, K. H. Schofield, A. N., and Thurairajah, A., "An Evaluation of Test Data For Selecting a Yield Criterion for Soils," Special Technical Publication No. 361, American Society for Testing Materials, Symposium on Laboratory Shear Testing of Soils, 1964, pp. 111-133.

32. Boussinesq, J., "Application des Potentials a l'Etude de l'Equilibre et des Movement des Solides Elastiques," Paris, Gauther-Villars, 1885.

33. Love, A. E. H., "The Stress Produced in a Semi-infinite Body by Pressure on Part of the Boundary," Philosophical Transactions of the Royal Society, Series A, vol. 228, 1928, pp. 377-420.

34. Scott, R. F., "Principles of Soil Mechanics," Addison-Wesley Publishing Company Incorporated, 1963.

35. Florin, V. A., "Fundamentals of Soil Mechanics," vol. I, Leningrad, 1959.

36. Jurgenson, L., "The Application of Elasticity and Plasticity to Foundation Problems," Journal of the Boston Society of Civil Engineers, vol. 21, 1934, pp. 206-241.

37. Sowers, G. F. and Vesic, A. B., "The Study of Stresses in a Flexible Pavement System," Annual Report No. 1, Engineering Experiment Station, Georgia Institute of Technology, 1959.

38. Mazanti, B. B., "An Analysis of Foundations in Sand," M. S. Thesis, Georgia Institute of Technology, 1955.

39. Burmister, D. M., "The General Theory of Stresses and Displacements in Layered Systems," Journal of Applied Physics, vol. 16, 1945, pp. 296-302.

40. Acum, W. E. A. and Fox, L., "Computation of Stresses and Displacements in Layered Systems," Geotechnique, vol. 2, No. 4, 1951, p. 293.

41. Moore, C. A., Jr., "A Study of the Effect of Mica on the Compressibility of a Sand and a Silt Under Conditions of K_o Consolidation," M. S. Thesis, Georgia Institute of Technology, 1965.

42. Waterways Experiment Station, "Investigation of Pressures and Deflections for Flexible Pavements, Theoretical Stresses Induced by Uniform Circular Loads," Report No. 3, Vicksburg, Mississippi, 1953.

43. Waterways Experiment Station, "Investigation of Pressures and Deflections for Flexible Pavements, Homogeneous Sand Test Section," Report No. 4, Vicksburg, Mississippi, 1954.

44. Newmark, N. M., "Influence Charts for Computation of Stresses in Elastic Foundations," University of Illinois, Engineering Experiment Station, Bulletin No. 338, Urbana, 1942.

45. Vesic, A. B. and Domaschuk, L., Theoretical Analysis of Structural Behavior of Road Test Flexible Pavements," Research Program Report 10, Highway Research Board, 1964.

46. Kögler, F., and Scheidig, A., "Drackverteijung in Baugrunde," Bautechnik, 1927.

47. Schultze, E., "Distribution of Stress Beneath a Rigid Foundation," Proceedings, 5th Int. Conf. Soil Mech. and Found. Eng., vol. 1, 1961, pp. 807-813.

48. Bub, H., "Beitrag zur Ermittlung der Verteilung der Normal-und Schubspannungen an der Sohle von Streifenfundamenten und zur Bemessung flachgegründeter Streifenfundamente aus Unbewehrten Beton," Degebo, Heft 17, 1963.

49. Schleicher, I. F., "Zur Theorie des Bougrundes," Der Bauingenieur, vol. 7, 1926, pp. 931-935.

OTHER REFERENCES

1. Balla, A., "Stress Conditions in Triaxial Compression," Proceedings, American Society of Civil Engineers, Jour. Soil Mech. Found. Eng. Div., vol. 86, SM 5, 1960, p. 2684.

2. Biot, A. M., "Effect of Certain Discontinuities on the Pressure Distribution in a Loaded Soil," Physics, vol. 6, 1935, pp. 367-375.

3. Bishop, A. W. and Green, G. E., "The Influence of End Restraint on the Compression Strength of a Cohesionless Soil," Geotechnique, vol. XV, 1965, pp. 203-265.

4. Chen, L. S., "An Investigation of Stress-Strain and Strength Characteristics of Cohesionless Soils by Triaxial Compression Tests," Proceedings, 2nd Int. Conf. Soil Mech. Found. Eng., vol. 5, 1948, pp. 35-43.

5. Cornforth, D. H., "Some Experiments on the Influences of Strain Conditions on the Strength of Sand," Geotechnique, vol. XIV, June 1964, pp. 143-167.

6. Davis, E. H. and Taylor, H., "The Surface Displacement of an Elastic Layer Due to Horizontal and Vertical Surface Loading," Proceedings, 6th Int. Conf. Soil Mech. and Found. Eng., vol. 2, 1936, p. 157.

7. De Beer, E., "Bearing Capacity and Settlements of Shallow Foundations on Sand," Symposium on the Bearing Capacity of Foundations, Duke University, 1965.

8. De Beer, E. E., "The Scale Effect on the Phenomenon of Progressive Rupture in Cohesionless Soil," Proceedings, 6th Int. Conf. Soil Mech. Found. Eng., vol. II, 1965, pp. 13-17.

9. De Beer, E. E., "Influence of the Mean Normal Stress on the Shearing Strength of Sand," Proceedings, 6th Int. Conf. Soil Mech. Found. Eng., vol. I, 1965, pp. 165-169.

10. Enger, M. L., "High Unit Pressures Found in Experiments on Distribution of Vertical Loading through Sand," Engineering Record, vol. 73, 1913, p. 106.

11. Foster, C. R. and Ahlvin, R. G., "Stresses and Deflections Induced by a Uniform Circular Load," Proceedings, Highway Research Board, vol. 33, 1954, pp. 467-470.

12. Gorbunov-Possadov, M. I., 'Calculations for the Stability of a Sand Bed by a Solution Combining the Theories of Elasticity and Plasticity," Proceedings, 6th Int. Conf. Soil Mech. Found. Eng., vol. II, 1965, pp. 51-55.

13. Gray, H., "Stress Distribution in Elastic Solids," Proceedings, 1st Int. Conf. Soil Mech. and Found. Eng., vol. 2, 1936, pp. 157-168.

14. Hansen, J. B., "Some Stress-Strain Relationships for Soils," Proceedings, 6th Int. Conf. Soil Mech. and Found. Eng., vol. 1, 1965, pp. 231-234.

15. Haythornthwaite, R. M., "Mechanics of the Triaxial Test for Soils," Proceedings, American Society of Civil Engineers, Jour. Soil Mech. Found. Eng., vol. 86, 1960, p. 2625.

16. Henkel, D. J., Gilbert, G. D., "The Effect of the Rubber Membrane on the Measured Triaxial Compression Strength of Clay Samples," Geotechnique, vol. III, 1965, pp. 20-29.

17. Hirschfeld, R. C., and Poulos, S. J., "High-Pressure Triaxial Tests on a Compacted Sand and an Undisturbed Silt," Special Technical Publication No. 361, American Society for Testing Materials, Symposium on the Laboratory Shear Testing of Soils, 1964, pp. 329-338.

18. Jones, R., "In-Situ Measurement of the Dynamic Properties of Soil by Vibration Methods," Geotechnique, vol. VIII, No. 1, March 1958, pp. 1-21.

19. Karst, H. et al., "Contribution a l'Etude de la Mecanique des Milieux," Proceedings, 6th Int. Conf. Soil Mech. Found. Eng., vol. I, 1965, pp. 259-263.

20. Kondner, R. L. and Zelasko, J. S., "Void Ratio Effects on the Hyperbolic Stress-Strain Response of a Sand," Special Technical Publication No. 361, American Society for Testing Materials, Symposium on the Laboratory Shear Testing of Soils, 1964, pp. 250-257.

21. Koning, H., "Stress Distribution in a Homogeneous Anisotropic Elastic Semi-Infinite Solid," Proceedings, 4th Int. Conf. Soil Mech. Found. Eng., vol. 1, 1957, pp. 335-338.

22. Makhlouf, H. M. and Stewart, J. J., "Factors Influencing the Modulus of Elasticity of Dry Sand," Proceedings, 6th Int. Conf. Soil Mech. Found. Eng., vol. I, 1965, pp. 298-302.

23. Matsukawa, and Hunter, "The Variation of Sound Velocity with Stress in Sand," Proceedings of the Physical Society, Sect. B, vol. 69, Part 8, No. 440B, August 1956, pp. 847-848.

24. McMahon, T. F. and Yoder, E. J., "Design of a Pressure-Sensitive Cell and Model Studies of Pressures and Flexible Pavement Subgrade," Proceedings, Highway Research Board, vol. 39, 1960, pp. 650-682.

25. McLeod, N. W., "Some Basic Problems in Flexible Pavement Design," Proceedings, Highway Research Board, vol. 32, 1953, pp. 90-118.

26. Meese, R. H. and Long, R. W., "Triaxial Compression Tests on Soils using Variable Lateral Pressure," Special Technical Publication No. 254, American Society for Testing Materials, 1954, p. 366.

27. Murayama, S. and Yagi, N., "On the Deformation Properties of Sand," Annuals, Disaster Prevention Research Institute, Kyota University, No. 7, March 1964.

28. Newland, P. J. and Allely, B. H., "Volume Changes in Drained Triaxial Tests on Granular Materials," Geotechnique, vol. VII, 1957, pp. 17-34.

29. Palmer, L. A. and Barber, E. S., "Soil Displacement Under Circular Loaded Area," Proceedings, Highway Research Board, vol. 20, 1940, pp. 279-286.

30. Picketts, G., "Stress Distribution in a Loaded Soil with Some Rigid Boundaries," Proceedings, Highway Research Board, vol. 18, 1938, pp. 35-48.

31. Poorooshasb, H. B., and Roscoe, K. H., "The Correlation of the Results of Shear Tests with Varying Degrees of Dilation," Proceedings, 5th Int. Conf. on Soil Mech. and Found. Eng., vol. 1, 1961, pp. 297-304.

32. Rowe, P. W., "The Stress-Dilatency, Relation for Static Equilibrium of an Assembly of Particles in Contact," Proceedings, Royal Society, Series A, vol. 269, 1962, pp. 500-527.

33. Rowe, P. W. and Barden, L., "Importance of Free Ends in Triaxial Testing," Proceedings, American Society of Civil Engineers, Jour. Soil Mech. Found. Eng. Div., vol. 90, January 1964.

34. Shannon, W. L., Yamone, G. and Dietrich, R. J., "Dynamic Triaxial Tests on Sand," Proceedings, 1st Pan American Conf. on Soil Mech. and Found. Eng., Mexico City, September 1959.

35. Smoltczyk, H. V., "Discussion on Some Fundamental Properties of Sand," Proceedings, 4th Int. Conf. Soil Mech. Found. Eng., vol. III, 1965, pp. 20-29.

36. Sovinc, J., "Stresses and Displacements in a Limited Layer of Uniform Thickness, Resting on a Rigid Base, and Subjected to a Uniformly Distributed Flexible Load of Rectangular Shape," Proceedings, 5th Int. Conf. soil Mech. and Found. Eng., vol. I, 1961, pp. 823-828.

37. Sowers, G. F. and Vesic, A S., "Stress Distribution Under Pavements of Different Rigidities," Proceedings, 5th Int. Conf. Soil Mech. and Found. Eng., vol. II, 1961, pp. 321-332.

38. Sowers, G. F., "Introductory Soil Mechanics and Foundations," 1951, Macmillan, New York.

39. Sowers, G. F., "Laboratory Manual for Soil Testing," 1955, Georgia Institute of Technology, Atlanta.

40. Timoshenko, S. P., "Theory of Elasticity," Ch. III, XI, McGraw Hill, New York, 1934.

41. Vesic, A. S., "Validity of Layered Solid Theories for Flexible Pavements," Proceedings, Int. Conf. on Structural Design of Asphalt Pavements, 1962, pp. 283-290.

42. Vesic, A. S., "Bending of Beams on an Elastic-Isotropic Solid," Proceedings, American Society of Civil Engineers, Jour. Eng. Mech. Div., vol. 87, 1961.

43. Waterways Experiment Station, "Investigations of Pressures and Deflections for Flexible Pavements," Report No. 1, Homogeneous Clayey-Silt Test Section, Vicksburg, Mississippi, 1951.

44. Weiskopf, W. R., "Stresses in Soils Under a Foundation," Jour. Frank. Inst. vol. 239, June 1945, pp. 445-465.

45. Westergaard, H. M., "A Problem of Elasticity Suggested by a Problem in Soil Mechanics, Soft Material Reinforced by Numerous Strong Horizontal Sheets, Contribution to Mechanics of Solids," Stephen Timoshenko 60th Anniversary Volume, Macmillan, New York, 1938.

VITA

Leonard Domaschuk was born in Elphinstone, Manitoba, Canada on July 28, 1933. He obtained his senior matriculation from the Elphinstone Consolidated School in 1951. He spent the following two years teaching elementary school in rural Manitoba. In 1953 he enrolled at the University of Manitoba and in 1957 he received a Bachelor of Science in Civil Engineering degree. For the following year he was employed by the Hydro-Electric Power Commission of Ontario, Soil and Geology Division, Toronto, Ontario. In 1958 Mr. Domaschuk received a Canadian Good Roads Scholarship for post-graduate work and attended the University of Alberta, majoring in soil mechanics and highway engineering. He obtained a Master of Science degree in June of 1960 and joined the civil engineering staff at the University of Saskatchewan. In the summer of 1962 he was the recipient of an Asphalt Institute Grant-In-Aid and attended a short course in asphalt technology and pavement design at the Georgia Institute of Technology.

In September of 1963 Mr. Domaschuk resigned his position at the University of Saskatchewan to attend the Georgia Institute of Technology in pursuit of a Doctor of Philosophy degree. At this school he was employed as a graduate research and teaching assistant and was also the recipient of a Ford Foundation Fellowship-Assistantship for prospective engineering teachers.

Mr. Domaschuk is a member of the following societies: Sigma Xi (associate), Chi Epsilon, International Society of Soil and Snow Mechanics

(Canadian Division), Saskatchewan Association of Professional Engineers, and the Engineering Institute of Canada.

Mr. Domaschuk is the co-author of two technical publications in the field of soil mechanics and highway engineering.

He is married to the former Margaret Louise Hudson and they have one daughter, Kira Anne.